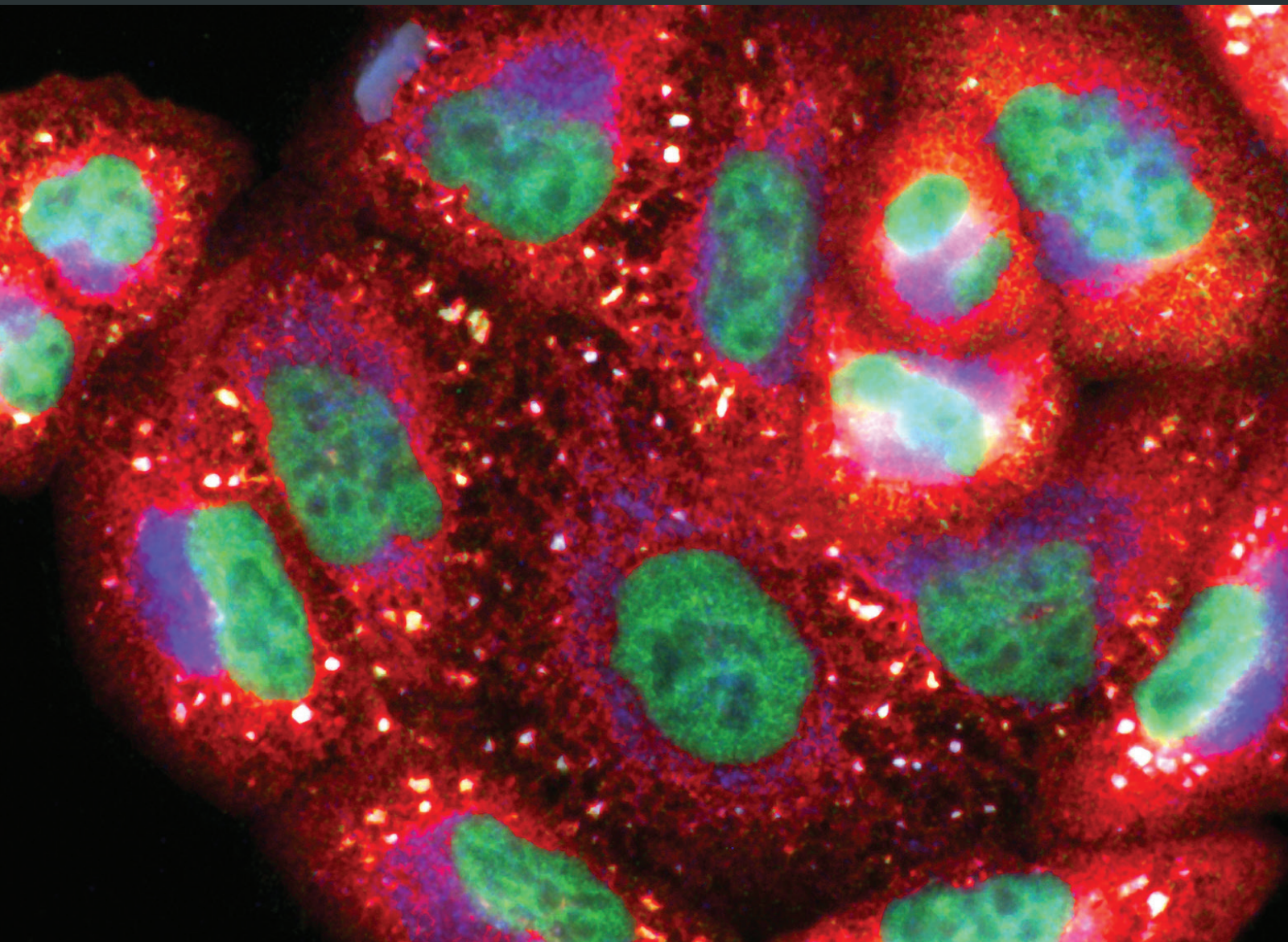


Interplay between Redox Signaling, Oxidative Stress, and Unfolded Protein Response (UPR) in Pathogenesis of Human Diseases

Lead Guest Editor: Ireneusz Majsterek

Guest Editors: Dariusz Pytel, Jaroslaw Dziadek, and Tomasz Poplawski






**Interplay between Redox Signaling,
Oxidative Stress, and Unfolded Protein Response
(UPR) in Pathogenesis of Human Diseases**

Oxidative Medicine and Cellular Longevity

**Interplay between Redox Signaling,
Oxidative Stress, and Unfolded Protein Response
(UPR) in Pathogenesis of Human Diseases**

Lead Guest Editor: Ireneusz Majsterek

Guest Editors: Dariusz Pytel, Jaroslaw Dziadek,
and Tomasz Poplawski




Copyright © 2019 Hindawi. All rights reserved.

This is a special issue published in “Oxidative Medicine and Cellular Longevity.” All articles are open access articles distributed under the Creative Commons Attribution License, which permits unrestricted use, distribution, and reproduction in any medium, provided the original work is properly cited.

Editorial Board



- Fabio Altieri, Italy
Fernanda Amicarelli, Italy
José P. Andrade, Portugal
Cristina Angeloni, Italy
Antonio Ayala, Spain
Elena Azzini, Italy
Peter Backx, Canada
Damian Bailey, UK
Sander Bekeschus, Germany
Ji C. Bihl, USA
Consuelo Borrás, Spain
Nady Braidy, Australia
Ralf Braun, Germany
Laura Bravo, Spain
Amadou Camara, USA
Gianluca Carnevale, Italy
Roberto Carnevale, Italy
Angel Catalá, Argentina
Giulio Ceolotto, Italy
Shao-Yu Chen, USA
Ferdinando Chiaradonna, Italy
Zhao Zhong Chong, USA
Alin Ciobica, Romania
Ana Cipak Gasparovic, Croatia
Giuseppe Cirillo, Italy
Maria R. Ciriolo, Italy
Massimo Collino, Italy
Graziamaria Corbi, Italy
Manuela Corte-Real, Portugal
Mark Crabtree, UK
Manuela Curcio, Italy
Andreas Daiber, Germany
Felipe Dal Pizzol, Brazil
Francesca Danesi, Italy
Domenico D'Arca, Italy
Sergio Davinelli, USA
Claudio De Lucia, Italy
Yolanda de Pablo, Sweden
Sonia de Pascual-Teresa, Spain
Cinzia Domenicotti, Italy
Joël R. Drevet, France
Grégory Durand, France
Javier Egea, Spain
Ersin Fadillioglu, Turkey
- Ioannis G. Fatouros, Greece
Qingping Feng, Canada
Gianna Ferretti, Italy
Giuseppe Filomeni, Italy
Swaran J. S. Flora, India
Teresa I. Fortoul, Mexico
Jeferson L. Franco, Brazil
Rodrigo Franco, USA
Joaquin Gadea, Spain
Juan Gambini, Spain
José Luís García-Giménez, Spain
Gerardo García-Rivas, Mexico
Janusz Gebicki, Australia
Alexandros Georgakilas, Greece
Husam Ghanim, USA
Rajeshwary Ghosh, USA
Eloisa Gitto, Italy
Daniela Giustarini, Italy
Saeid Golbidi, Canada
Aldrin V. Gomes, USA
Tilman Grune, Germany
Nicoletta Guaragnella, Italy
Solomon Habtemariam, UK
Eva-Maria Hanschmann, Germany
Tim Hofer, Norway
John D. Horowitz, Australia
Silvana Hrelia, Italy
Stephan Immenschuh, Germany
Maria Isagulians, Latvia
Luigi Iuliano, Italy
Vladimir Jakovljevic, Serbia
Marianna Jung, USA
Peeter Karihtala, Finland
Eric E. Kelley, USA
Kum Kum Khanna, Australia
Neelam Khaper, Canada
Thomas Kietzmann, Finland
Demetrios Kouretas, Greece
Andrey V. Kozlov, Austria
Jean-Claude Lavoie, Canada
Simon Lees, Canada
Christopher Horst Lillig, Germany
Paloma B. Liton, USA
Ana Lloret, Spain
- Lorenzo Loffredo, Italy
Daniel Lopez-Malo, Spain
Antonello Lorenzini, Italy
Nageswara Madamanchi, USA
Kenneth Maiese, USA
Marco Malaguti, Italy
Tullia Maraldi, Italy
Reiko Matsui, USA
Juan C. Mayo, Spain
Steven McAnulty, USA
Antonio Desmond McCarthy, Argentina
Bruno Meloni, Australia
Pedro Mena, Italy
Víctor M. Mendoza-Núñez, Mexico
Maria U. Moreno, Spain
Trevor A. Mori, Australia
Ryuichi Morishita, Japan
Fabiana Morroni, Italy
Luciana Mosca, Italy
Ange Mouithys-Mickalad, Belgium
Iordanis Mourouzis, Greece
Danina Muntean, Romania
Colin Murdoch, UK
Pablo Muriel, Mexico
Ryoji Nagai, Japan
David Nieman, USA
Hassan Obied, Australia
Julio J. Ochoa, Spain
Pál Pacher, USA
Pasquale Pagliaro, Italy
Valentina Pallottini, Italy
Rosalba Parenti, Italy
Vassilis Paschalis, Greece
Visweswara Rao Pasupuleti, Malaysia
Daniela Pellegrino, Italy
Iliaria Peluso, Italy
Claudia Penna, Italy
Serafina Perrone, Italy
Tiziana Persichini, Italy
Shazib Pervaiz, Singapore
Vincent PIALoux, France
Ada Popolo, Italy
José L. Quiles, Spain
Walid Rachidi, France













Zsolt Radak, Hungary	Sebastiano Sciarretta, Italy	Jeannette Vasquez-Vivar, USA
N. Soorappan Rajasekaran, USA	Ratanesh K. Seth, USA	Daniele Vergara, Italy
Kota V. Ramana, USA	Honglian Shi, USA	Victor M. Victor, Spain
Sid D. Ray, USA	Cinzia Signorini, Italy	László Virág, Hungary
Hamid Reza Rezvani, France	Mithun Sinha, USA	Natalie Ward, Australia
Alessandra Ricelli, Italy	Carla Tatone, Italy	Philip Wenzel, Germany
Paola Rizzo, Italy	Frank Thévenod, Germany	Anthony R. White, Australia
Francisco J. Romero, Spain	Shane Thomas, Australia	Georg T. Wondrak, USA
Joan Roselló-Catafau, Spain	Carlo Tocchetti, Italy	Michal Wozniak, Poland
H. P. Vasantha Rupasinghe, Canada	Angela Trovato Salinaro, Jamaica	Sho-ichi Yamagishi, Japan
Gabriele Saretzki, UK	Paolo Tucci, Italy	Liang-Jun Yan, USA
Luciano Saso, Italy	Rosa Tundis, Italy	Guillermo Zalba, Spain
Nadja Schroder, Brazil	Giuseppe Valacchi, Italy	Mario Zoratti, Italy

Contents




Interplay between Redox Signaling, Oxidative Stress, and Unfolded Protein Response (UPR) in Pathogenesis of Human Diseases

Tomasz Poplawski , Dariusz Pytel, Jaroslaw Dziadek , and Ireneusz Majsterek 
Editorial (2 pages), Article ID 6949347, Volume 2019 (2019)

Hydrogen and Oxygen Mixture to Improve Cardiac Dysfunction and Myocardial Pathological Changes Induced by Intermittent Hypoxia in Rats

Ya-Shuo Zhao , Ji-Ren An , Shengchang Yang , Peng Guan , Fu-Yang Yu , Wenya Li ,
Jie-Ru Li , Yajing Guo , Zhi-Min Sun , and En-Sheng Ji 
Research Article (12 pages), Article ID 7415212, Volume 2019 (2019)

The Role of the ER-Induced UPR Pathway and the Efficacy of Its Inhibitors and Inducers in the Inhibition of Tumor Progression

Anna Walczak , Kinga Gradzik, Jacek Kabzinski , Karolina Przybylowska-Sygut,
and Ireneusz Majsterek 
Review Article (15 pages), Article ID 5729710, Volume 2019 (2019)





Excessive Oxidative Stress Contributes to Increased Acute ER Stress Kidney Injury in Aged Mice

Xiaoyan Liu , Ruihua Zhang, Lianghu Huang, Zihan Zheng, Helen Vlassara, Gary Striker, Xiaoyan Zhang,
Youfei Guan, and Feng Zheng 
Research Article (15 pages), Article ID 2746521, Volume 2019 (2019)

Different Forms of ER Stress in Chondrocytes Result in Short Stature Disorders and Degenerative Cartilage Diseases: New Insights by Cartilage-Specific ERp57 Knockout Mice

Yvonne Rellmann , and Rita Dreier 
Review Article (14 pages), Article ID 8421394, Volume 2018 (2019)

Methane-Rich Saline Ameliorates Sepsis-Induced Acute Kidney Injury through Anti-Inflammation, Antioxidative, and Antiapoptosis Effects by Regulating Endoplasmic Reticulum Stress

Yifan Jia, Zeyu Li, Yang Feng, Ruixia Cui , Yanyan Dong, Xing Zhang, Xiaohong Xiang, Kai Qu ,
Chang Liu , and Jingyao Zhang 
Research Article (10 pages), Article ID 4756846, Volume 2018 (2019)

Editorial

Interplay between Redox Signaling, Oxidative Stress, and Unfolded Protein Response (UPR) in Pathogenesis of Human Diseases

Tomasz Poplawski ¹, Dariusz Pytel,² Jaroslaw Dziadek ³, and Ireneusz Majsterek ⁴

¹Department of Molecular Biology, Faculty of Biology and Environmental Protection, University of Lodz, Lodz, Poland

²Department of Biochemistry and Molecular Biology, Hollings Cancer Center, Medical University of South Carolina, Charleston, South Carolina, USA

³Institute for Medical Biology, Polish Academy of Sciences, Lodz, Poland

⁴Department of Clinical Chemistry and Biochemistry, Medical University of Lodz, Poland

Correspondence should be addressed to Ireneusz Majsterek; ireneusz.majsterek@umed.lodz.pl

Received 5 March 2019; Accepted 6 March 2019; Published 7 April 2019

Copyright © 2019 Tomasz Poplawski et al. This is an open access article distributed under the Creative Commons Attribution License, which permits unrestricted use, distribution, and reproduction in any medium, provided the original work is properly cited.

Endoplasmic reticulum (ER) stress triggers complex adaptive or proapoptotic signaling defined as the unfolded protein response (UPR), involved in several pathophysiological processes. Protein misfolding in the ER triggers the activation of three homologous transmembrane protein kinases, Ire1, the PKR-like ER kinase (PERK), and the transmembrane transcription factor ATF6. Protein folding is highly redox-dependent; the relations between the generation of oxidative stress and ER stress have become very interesting fields for investigation. Evidence suggests that ROS production and oxidative stress are not only coincidental to ER stress but also integral UPR components. These components are triggered by distinct types of ER stressors and facilitate either proapoptotic or proadaptive UPR signaling. Thus, ROS generation can be upstream or downstream UPR targets. Pathways involved in unfolded protein response are important for normal cellular homeostasis and organismal development and may also play key roles in the pathogenesis of many diseases. This special issue intends to address the different aspects relating interaction between oxidative stress, UPR, and cellular redox capacity. We are grateful to the Editorial Board of Oxidative Medicine and Cellular Longevity, who devoted this special issue to UPR, and all authors for their contribution. Many manuscripts were submitted, and after a detailed peer review process, three high-quality research works and two

reviews on topics of novelty were selected to be included in this special issue.

In the review by Y. Rellmann and R. Dreier, mouse models with specific changes in protein folding are described. The authors mainly focus on those mouse models with ER stress-related chondrodysplasia phenotypes. This is particularly important as UPR downregulate essential processes of the endochondral ossification including chondrocyte proliferation and differentiation and ECM protein synthesis. In consequence, autophagy and apoptosis are triggered and lengths of long bones are reduced. However, the detailed description of various mouse models with ER stress is particularly relevant for readers studying different aspects of the UPR. The authors review among others mice with a knock-out of proteins involved in ER folding machinery, UPR signaling, degradation of aggregated proteins, and protein trafficking and secretion. These mouse models could be useful for the study of the molecular pathogenesis of various ER stress-related human diseases as well as to propose novel treatment schemes. One of the ER stress-related diseases is acute kidney injury. The accumulation of unfolded protein in ER in the kidney is observed in aging and during sepsis; however, the molecular background of kidney injury is different. The aged kidney has reduced UPR and elevated oxidative stress in comparison with a younger one. Along this line is

the paper by X. Liu et al. The authors report the increased susceptibility of an aged kidney to ER stress with excessive reactive oxygen species level using a mouse model. This phenomenon is connected with the loss of PERK phosphorylation and XBP-1 mRNA splicing. They also compared the level of ER stress in an aged kidney with and without an antioxidant and found that the antioxidant prevented kidney function failure induced by severe ER stress. A similar protective function against ER stress-induced kidney injury showed methane-rich saline as reported by Y. Jia et al. They found that the ER stress in the kidney is a consequence of sepsis and it is connected with oxidative stress and the ER stress-related apoptosis. They measured histopathological damage, the levels of proinflammatory cytokines, and reactive oxygen species in kidney tissues and apoptosis ratio. Methane has anti-inflammatory and antiapoptotic properties and seems to be a good candidate for supportive treatment in sepsis; however, the molecular mechanisms of methane remain to be elucidated. 67% hydrogen and 33% oxygen mixture (H_2-O_2) work in a similar way. S. Zhao et al. reported that H_2-O_2 mixture inhalation could protect against the cardiac dysfunction and structural disorders induced by ER stress in rats with chronic intermittent hypoxia (CIH). CIH is a consequence of obstructive sleep apnea—a common breathing disorder in humans. The authors found that H_2-O_2 improved cardiac dysfunction and attenuated CIH-induced ER stress by reduction of oxidative stress and cardiac apoptosis. An ER stress-oriented therapy is also used in cancer treatment. In the review by A. Walczak et al., the role of the ER-induced UPR pathway and the efficacy of its inhibitors and inducers in the inhibition of tumor progression are discussed. Correct protein processing and folding are crucial to maintain tumor homeostasis. Endoplasmic reticulum stress is one of the leading factors that causes disturbances in these processes. It is induced by impaired function of the ER and accumulation of unfolded proteins. Induction of ER stress affects many molecular pathways that cause the unfolded protein response. This is the way in which cells can adapt to the new conditions, but when ER stress cannot be resolved, the UPR induces cell death. The molecular mechanisms of this double-edged sword process are involved in the transition of the UPR either in a cell protection mechanism or in apoptosis. However, this process remains poorly understood but seems to be crucial in the treatment of many diseases that are related to ER stress.

A. Walczak et al. discuss that the UPR involvement in the pathogenesis and progression of various types of cancer is presented. Since it is a very promising target for novel anti-cancer therapy, more and more new molecules are being tested. A significant amount of them is naturally occurring chemicals that are present also in plants. Due to the abundance of the compounds affecting UPR, A. Walczak et al. have summarized the literature review on tested modulators in various cancer cell lines. Thus, the UPR modulators are a promising hope for a personalized therapy for patients in whom chemotherapy or radiotherapy has failed. It can become an innovative way to fight several different types of cancer. The response to a given compound depends on the

phenotype of tumor cells, the severity of the disease, and the chemotherapy used so far.

The understanding of the ER stress response, especially in the aspect of pathological consequences of UPR, has the potential to allow us to develop novel therapies and new diagnostic and prognostic markers for cancer. It is emphasized that further experiments and analyses should be carried out using a variety of compounds that have the ability to inhibit and induce the UPR pathway in different types of cancers. It could also be useful in the treatment of noncancerous diseases including neurodegenerative disorders, i.e., glaucoma and Alzheimer's disease.

Conflicts of Interest

The authors declare that there is no conflict of interest regarding the publication of this paper.

Acknowledgments

This work was supported by NCN through grant no. 2015/19/B/NZ5/01421, grant no. 2016/21/B/NZ5/01411, and grant no. 2016/23/B/NZ5/02630.

*Tomasz Poplawski
Dariusz Pytel
Jaroslaw Dziadek
Ireneusz Majsterek*

Research Article

Hydrogen and Oxygen Mixture to Improve Cardiac Dysfunction and Myocardial Pathological Changes Induced by Intermittent Hypoxia in Rats

Ya-Shuo Zhao ^{1,2}, Ji-Ren An ², Shengchang Yang ², Peng Guan ², Fu-Yang Yu ²,
Wenya Li ², Jie-Ru Li ², Yajing Guo ^{1,2}, Zhi-Min Sun ² and En-Sheng Ji ²

¹Scientific Research Center, Hebei University of Chinese Medicine, Shijiazhuang 050200, China

²Department of Physiology, Institute of Basic Medicine, Hebei University of Chinese Medicine, Shijiazhuang 050200, China

Correspondence should be addressed to En-Sheng Ji; jesphy@126.com

Received 29 September 2018; Revised 11 December 2018; Accepted 23 January 2019; Published 7 March 2019

Guest Editor: Ireneusz Majsterek

Copyright © 2019 Ya-Shuo Zhao et al. This is an open access article distributed under the Creative Commons Attribution License, which permits unrestricted use, distribution, and reproduction in any medium, provided the original work is properly cited.

Obstructive sleep apnea (OSA) can cause intermittent changes in blood oxygen saturation, resulting in the generation of many reactive oxygen species (ROS). To discover new antioxidants and clarify the endoplasmic reticulum (ER) stress involved in cardiac injury in OSA, we established a chronic intermittent hypoxia (CIH) rat model with a fraction of inspired O₂ (FiO₂) ranging from 21% to 9%, 20 times/h for 8 h/day, and the rats were treated with H₂-O₂ mixture (67% hydrogen and 33% oxygen) for 2 h/day for 35 days. Our results showed that H₂-O₂ mixture remarkably improved cardiac dysfunction and myocardial fibrosis. We found that H₂-O₂ mixture inhalation declined ER stress-induced apoptosis via three major response pathways: PERK-eIF2 α -ATF4, IRE 1-XBP1, and ATF 6. Furthermore, we revealed that H₂-O₂ mixture blocked c-Jun N-terminal kinase (JNK-) MAPK activation, increased the ratio of Bcl-2/Bax, and inhibited caspase 3 cleavage to protect against CIH-induced cardiac apoptosis. In addition, H₂-O₂ mixture considerably decreased ROS levels via upregulating superoxide dismutase (SOD) and glutathione (GSH) as well as downregulating NADPH oxidase (NOX 2) expression in the hearts of CIH rats. All the results demonstrated that H₂-O₂ mixture significantly reduced ER stress and apoptosis and that H₂ might be an efficient antioxidant against the oxidative stress injury induced by CIH.

1. Introduction

Obstructive sleep apnea (OSA) is a common breathing disorder and characterized by recurrent episodes of upper airway obstruction during sleep [1]. Clinical data have shown that the incidence of OSA was approximately 15-24% in adults [2] and that OSA was accompanied by multiple cardiovascular disorders, such as hypertension, heart failure, and atherosclerosis [3, 4]. OSA patients showed long-term arterial oxygen saturation fluctuations and frequent sleep apnea, exposing them to a specific internal environment with chronic intermittent hypoxia (CIH) and recurrent hypoxia [5-7].

Sun et al. found that increases in the left ventricular diameter and ventricular mass in OSA patients correlated with the severity of the disease [8]. Clinically, continuous

positive airway pressure (CPAP) is the most widely used treatment for OSA during sleep [9]. Unfortunately, CPAP lacks stability and is not effective in reducing the cardiac damage caused by OSA. How can the cardiac damage caused by CIH be effectively reduced? It is necessary to further study the molecular mechanism of injury that is induced by CIH and seek a more effective treatment method for CIH.

The endoplasmic reticulum (ER) is a crucial organelle for protein synthesis, folding, and secretion. When cells are stimulated by ischemia, hypoxia, or oxidative stress, unfolded protein and incorrect proteins accumulate in the ER, triggering the unfolded protein response (UPR), which is called ER stress [10, 11]. UPR activation is regulated by a molecular chaperone protein 78 KD glucose-regulated protein named Bip/GRP 78 [10, 12]. During ER stress, Bip and GRP 78 are separated first, and protein kinase-like kinase (PERK),

inositol-requiring enzyme 1 (IRE 1), and transcription factor 6 (ATF 6) are activated [10, 11]. However, prolonged or severe ER stress could induce cell apoptosis [13, 14]. The apoptosis caused by ER stress is stimulated through the proapoptotic transcriptional factor C/EBP homologous protein (CHOP) [15]. Activated ATF 6, PERK, and IRE 1 accelerate the activation of the CHOP protein and lead to cell apoptosis [13].

During the process of low oxygen/reoxygenation induced by CIH, a large number of reactive oxygen species (ROS) are generated and trigger oxidative stress damage [12, 14, 16, 17]. Xu et al. found that the ER structure was changed and that the GRP 78, CHOP, and caspase 12 levels were increased in the hippocampus of adult mice exposed to CIH for 21 d [12]. These results suggested that the ER stress response was an early event in cardiac apoptosis caused by CIH [18]. Cai et al. revealed that the PERK-eIF2 α -ATF 4 signaling pathway was involved in apoptosis in growing rats when they were exposed to long-term CIH [19]. The study showed that IRE 1-XBP 1 and ATF 6 expression was dramatically increased in rat cardiac tissues when exposed to CIH for 5 weeks [20]. Tauroursodeoxycholic acid (TUDCA), an ER stress inhibitor, could have inhibited ER stress activation and apoptosis in the hippocampus of the rat CIH model [12, 19]. TUDCA also attenuated the activation of PERK, IRE 1, and ATF 6 in the liver of a mouse CIH model [21]. Therefore, the inhibition of ER stress might be an effective way to reduce cardiac injury when animals are exposed to CIH.

As a “novel” antioxidant, H₂ has received extensive attention and is widely used in the prevention and treatment of various diseases [22, 23]. It has been confirmed that H₂ is very stable and easily penetrates cell membranes and barriers without affecting basic metabolism in cells [24]. A study has shown that H₂-rich saline could have weakened hippocampal ER stress after cardiac arrest in a rat model [25]. H₂-rich saline was also efficiently used to attenuate the permeability of the blood-brain barrier and microvascular endothelial cell apoptosis from cardiopulmonary bypass in a rat model [26]. H₂ inhibited isoproterenol-induced cardiac hypertrophy by blocking excess ROS and mitochondrial damage [27].

Our previous research showed that H₂ inhalation significantly increased the level of total superoxide dismutase (T-SOD) in the serum of a CIH rat model [28]. Whether H₂ can attenuate cardiac ER stress and apoptosis remains unclear. To better understand the cardioprotective mechanism of H₂, we investigated the effect of H₂ on cardiac ER stress and apoptosis in a rat model exposed to CIH.

2. Materials and Methods

2.1. Experimental Animals and the CIH Model. All procedures were carried out in accordance with the National Institutes of Health Guide for the Care and Use of Laboratory Animals and were approved by the Animal Care and Use Committee of Medical Ethics of Hebei University of Chinese Medicine (no. HUCM-20117-010). Adult male Sprague-Dawley rats (190–220 g) were purchased from Beijing Vital River Laboratory Animal Technology Co.

Ltd. (Beijing, China). All rats were housed under a constant temperature (22 ± 2°C) and controlled illumination (12 h light and 12 h dark cycle) and given free access to food and water. All rats were allowed to adapt to their living conditions for at least 7 days before the experiment.

The SD rats ($n = 36$) were randomly divided into four groups ($n = 9$ for each group): normoxia control group (normoxia), normoxia H₂-O₂ mixture-treated group (H₂), CIH model group (CIH), and H₂-O₂ mixture-treated CIH model group (CIH+H₂). During the experiment, all rats were housed in chambers with a controlled gas delivery system. The fraction of inspired oxygen (FiO₂) provided to the chambers for the CIH and the CIH+H₂ groups declined from 21% to 9% within 90 s and then gradually increased to 21% via reoxygenation within 90 s. The exposure cycle was repeated every 3 min from 8:00 to 16:00 everyday for 35 days. The rats in the normoxia and H₂ groups received air containing 21% O₂. In addition, the rats in the CIH+H₂ and H₂ groups were successively given H₂-O₂ mixture gas from 17:00 to 19:00 everyday for 35 days. The H₂-O₂ mixture gas was obtained from water electrolyzation with a hydrogen oxygen nebulizer (AMS-H-01, Asclepius Meditec, Shanghai, China) and consisted of 67% H₂ and 33% O₂. During the experiment, the rats were placed in a transparent chamber, and the mixed gas went through the chamber at a rate of 200 ml/min. The concentration of mixed gas was monitored by a detector (Thermo Fisher, MA, USA).

2.2. Echocardiography. Echocardiographic analysis was performed by a high-resolution ultrasound imaging system (Vevo 2100, VisualSonics Inc., Toronto, Canada) with an MS-250 probe. First, the rat was anesthetized with 2.5% isoflurane in 95% oxygen and 5% carbon dioxide, and the hair was removed with depilatory cream. The QRS and T waves were used as indicators of the systolic and diastolic phases, and the left ventricular diameter was measured by combining the opening and closing of the mitral valve on the image. M-mode recordings detected the left ventricular end-diastolic diameter (LVEDd) and left ventricular end-systolic diameter (LVEDs). The left ventricular end-systolic volume (LVESV) = $7 / (2.4 + LVEDs) \times LVEDs^3 \times 1000$, left ventricular end-diastolic volume (LVEDV) = $7 / (2.4 + LVEDd) \times LVEDd^3 \times 1000$, and ejection fraction (EF) = $(LVEDV - LVESV) / LVEDV \times 100\%$ were also measured. Four-chamber echocardiography showed the maximum flow rate in the early diastole (E), maximum flow rate in the systolic phase (A) of the mitral valve (MV), isovolumic contraction period (IVCT), isovolumic relaxation phase (IVRT), and ejection period (ET). The value of the ratio of MV E/A and Tei index = $(IVCT + IVRT) / ET$ was used as indicators to reflect the changes in cardiac function. The technical parameters of the echocardiograph were the same for all test objects, and the average values were taken for at least 3 continuous cycles. The echocardiographic measurements were taken by a blinded observer.

2.3. Histological Assessment. The hearts were removed, soaked in 4% polyformaldehyde, washed with tap water,

and dehydrated with serial dilutions of alcohol. The heart tissues were transparent in xylene and embedded in paraffin for 24 h. The paraffin-enclosed tissue was sliced into 5 μ m sections by a sliding microtome (CM1950, Leica, Solms, Germany). The sections were dewaxed by xylene and rehydrated by a sequence of 100% to 70% ethanol. Hematoxylin and eosin (H&E) staining was used to detect changes in the basic tissue and structure of the heart. Sections were continuously stained with hematoxylin, differentiated with eosin, and dehydrated. Masson's trichrome (MT) staining was used to identify the collagenous fibrous area of the heart. The sections were stained with Masson's trichrome stain, distilled water, phosphomolybdic, and aniline blue solution and then differentiated in order. Finally, the sections were dehydrated, mounted, and imaged using an electric light microscope (DM3000, Leica, Solms, Germany). Image-Pro Plus 6.0 image analysis software was used to analyze and calculate the myocardial collagen volume fraction = collagen area/the total myocardial area (100%).

2.4. Measurement of Oxidative Stress. T-SOD and glutathione (GSH) were the antioxidant indices, while malonyldialdehyde (MDA) was a lipid peroxide marker. The activities of T-SOD and GSH were measured with the hydroxylamine method, and MDA was measured using the thiobarbituric acid method as previously described [29]. First, the left ventricle tissues were prepared to obtain a 10% (*w/v*) ice-buffered homogenate. After centrifugation at 2500 rpm for 10 min (4°C), the supernatant was collected to detect the protein content with a BCA kit (CW0014S, Cwbiotech, Beijing, China). The measurements were all performed according to the manufacturer's instructions (Nanjing Jiancheng Bioengineering Institute, Nanjing, China). The T-SOD, GSH, and MDA levels were measured with a multimode microplate reader (Varioskan LUX, Thermo Fisher, MA, USA) at wavelengths of 550 nm, 532 nm, and 550 nm, respectively.

2.5. Detection of Apoptosis. Apoptosis in the heart tissue was detected by the terminal deoxynucleotidyl transferase-mediated FITC-dUDP nick-end labeling (TUNEL) method. Heart tissue sections were dewaxed and incubated with 3% H₂O₂ for 20 min at room temperature. The reaction mixture (TUN11684817, Roche, Basel, Switzerland) was dropped onto slides and incubated at 37°C for 60 min. After the sections were rinsed 3 times, they were incubated in DAPI (2 mg/ml, Solarbio, Beijing, China) for 5 min. Finally, the number of TUNEL-positive/-DAPI-stained apoptotic bodies was counted with an electric light microscope (DM3000, Leica, Solms, Germany).

2.6. Western Blotting. The cardiac tissues were homogenized in RIPA lysis buffer with a proteinase inhibitor. The suspension was centrifuged at 12,000 g for 20 min at 4°C, the supernatant was collected, and the protein concentration was measured with a BCA protein assay kit (CW0014S, Cwbiotech, Beijing, China). Thirty micrograms of proteins was separated by SDS-PAGE and transferred onto polyvinylidene

fluoride membranes. After blocking with 5% nonfat milk, the blots were incubated with primary antibodies against CHOP (GTX32616, GeneTex, Irvine, USA), GRP 78 (ARG20531, Arigo Biolaboratories, Taiwan, China), caspase 12 (ARG55177, Arigo Biolaboratories, Taiwan, China), p-PERK (DF7576, Affinity Biosciences, OH, USA), PERK (AF5304, Affinity Biosciences, OH, USA), p-eIF 2 α (AF3087, Affinity Biosciences, OH, USA), eIF2 α (A0764, ABclonal Biotechnology, Boston, USA), p-IRE 1 (AF7150, Affinity Biosciences, OH, USA), IRE 1 (DF7709, Affinity Biosciences, OH, USA), ATF 4 (Ab1371, Abcam, Cambridge, UK), ATF 6 (A2570, ABclonal Biotechnology, Boston, USA), XBP 1 (AF5110, Affinity Biosciences, OH, USA), caspase 3 (9665, Cell Signaling Technology, Danvers, USA), p-JNK (4671, Cell Signaling Technology, Danvers, USA), JNK (ARG51218, Arigo Biolaboratories, Taiwan, China), Bcl-2 (YT0470, Immunoway, Plano, USA), Bax (GB11007, Servicebio, Wuhan, China), NOX 2 (GTX56278, GeneTex, Irvine, USA), and β -tubulin (GB13017-2, Servicebio, Wuhan, China) overnight at 4°C. The blots were washed with TBST and then incubated with the secondary antibody conjugated with horseradish peroxidase (Biosharp, Hefei, China) for 90 min at room temperature. The chemiluminescence method (CW0049S, Cwbiotech, Beijing, China) was used to detect the immunoreactive proteins with a multifunctional laser scanning system (Fusion FX5 Spectra, Vilber, Paris, France). All the analyses were repeated at least three times. The densities of the positive proteins were quantified by Image J and expressed as a ratio to β -tubulin.

2.7. Statistical Analyses. The results are presented as the mean \pm SEM. The statistical analysis was carried out using a two-way ANOVA followed by Tukey's post hoc test. The significance level was $p < 0.05$.

3. Results

3.1. H₂-O₂ Mixture Remarkably Improved Cardiac Dysfunction. Echocardiography was utilized to detect the rat cardiac systolic and diastolic functions. M-mode recordings showed higher values of LVEDd (Figures 1(a) and 1(b)) and lower EF (Figure 1(c)), indicating cardiac systolic dysfunction in the CIH rat model. However, the groups with the H₂-O₂ mixture treatment showed lower LVEDd values and higher EF than did the CIH group (Figures 1(a)–1(c)). Four-chamber echocardiography was used to evaluate the cardiac diastolic function (Figure 1(d)). The ratio of MV E/A showed no significant difference among the four groups (Figure 1(e)). CIH rats exhibited high values of the Tei index, indicating that their cardiac diastolic function was impaired (Figure 1(f)). However, H₂-O₂ mixture treatment decreased the Tei value to the normal level and improved cardiac diastolic function induced by CIH (Figure 1(f)). These results suggested that H₂-O₂ mixture treatment was an effective way to reduce cardiac systolic and diastolic dysfunctions in rats when exposed to CIH.

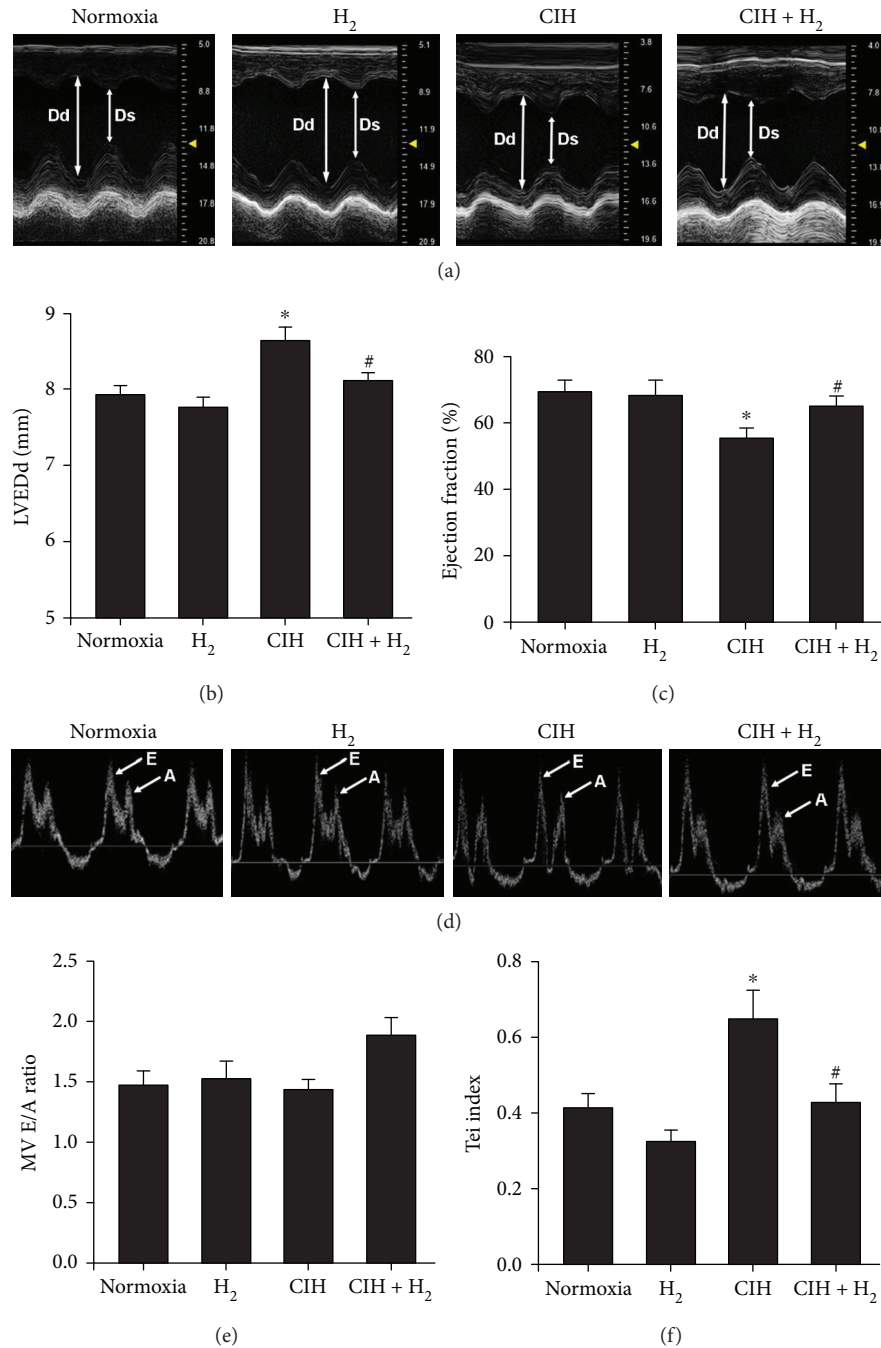


FIGURE 1: The effect of H₂-O₂ mixture on improving cardiac dysfunction in a rat model when exposed to CIH for 35 d. (a) M-mode echocardiography of the short axial section of the thoracic bones in rats. Dd: end-diastolic diameter of the left ventricle; Ds: end-systolic diameter of the left ventricle. (b) The mean value of the left ventricular end-diastolic internal diameter (LVEDd). (c) The ejection fraction (EF) of the left ventricle. (d) Rat four-chamber echocardiograph with atrial contraction waves. (e) The velocity ratio of the E peak to the A peak in the cardiac mitral valve (MV E/A); (f) Tei index = (IVCT + IVRT)/ET. **p* < 0.05 vs. normoxia group; #*p* < 0.05 vs. CIH group; *n* = 5.

3.2. H₂-O₂ Mixture Significantly Reduced Cardiac Histological Changes. Did H₂-O₂ mixture provide protection against pathological changes in the heart of the CIH rat model? H&E and MT staining were used to analyze the left ventricle of the rats. H&E staining showed a clear and complete cardiomyocyte structure and endocardium in normal

rats (Figure 2(a)). H₂-O₂ mixture improved the widespread myocardial structural disorder in the CIH group (Figure 2(a)). In addition, MT staining was used to evaluate myocardial fibrosis in the left ventricle. As shown in Figures 2(b) and 2(c), collagen accumulation shown in blue was increased in the CIH group. However, the groups treated

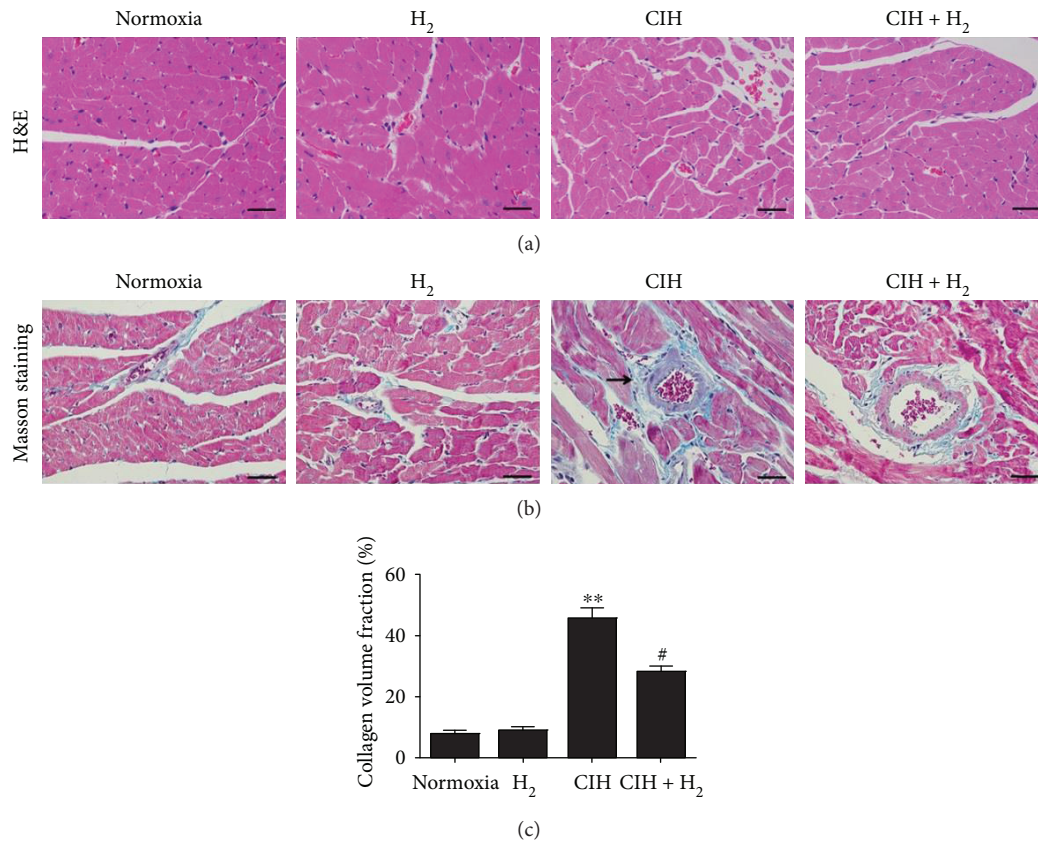


FIGURE 2: The histopathologic changes from H₂-O₂ mixture treatment during CIH for 35 d. (a) H&E staining showed the cardiac architecture in the left ventricle of the four different groups (scale bar = 25 μ m); (b) Masson's trichrome staining showed the collagen deposition in the left ventricle of the heart (scale bar = 25 μ m); (c) the myocardial collagen volume fractions were counted as shown by Masson's trichrome staining. * $p < 0.05$ vs. normoxia group; # $p < 0.05$ vs. CIH group; $n = 3$.

with H₂-O₂ mixture had a significantly lower collagen volume fraction in the left ventricle of the heart than did the CIH group. Altogether, H₂-O₂ mixture improved myocardial structure disorder and collagen deposition when rats were exposed to CIH.

3.3. H₂-O₂ Mixture Remarkably Attenuated CIH-Induced ER Stress. To further study the protective mechanism of H₂-O₂ mixture against cardiac injury induced by CIH, we first evaluated the expression of ER stress markers. GRP 78, CHOP, and caspase 12 were all increased in the cardiac tissue when exposed to CIH (Figure 3(a)). Then, we examined the three major pathways involved in ER stress-induced apoptosis. In the CIH group, the protein levels of p-PERK, p-eIF2 α , and ATF 4 significantly increased compared to those in the normoxia group (Figures 3(b), 3(c), and 3(e)). We found that p-IRE 1, XBP 1, and ATF 6 were also elevated after CIH exposure (Figures 3(d) and 3(e)). However, the activation of p-PERK, p-eIF2 α , and p-IRE 1 was inhibited in the H₂ group compared to that in the CIH group (Figures 3(b)–3(d)). Our results revealed that the protein levels of ATF 4, ATF 6, and XBP 1 (Figure 3(e)) were all decreased when the CIH rat model was treated with H₂-O₂ mixture. These results suggested that H₂-O₂ mixture could reduce ER stress-induced apoptosis via the PERK-eIF2 α -ATF 4, IRE 1-XBP 1, and ATF 6 pathways.

3.4. H₂-O₂ Mixture Greatly Inhibited JNK-MAPK-Induced Apoptosis. Did H₂-O₂ mixture protect against myocardial cell apoptosis via the mitochondrial pathway? First, we detected the occurrence of cardiac apoptosis when rats were exposed to CIH. As shown in Figure 4(a), a large number of apoptotic bodies were observed in the left ventricle when the rat model was exposed to CIH. The total number of apoptotic bodies in the CIH+H₂ group was strikingly lower than that in the CIH group (Figures 4(a) and 4(b)). At the same time, we detected the effect of H₂-O₂ mixture on some apoptotic signaling molecules. Our results indicated that H₂-O₂ mixture significantly increased the decrease in Bcl-2 and reduced the increase in Bax that were induced by CIH (Figure 4(c)). Similarly, the ratio of cleaved-caspase 3/procaspase 3 in the left ventricle was increased in the CIH+H₂ group compared to that in the CIH group (Figure 4(d)). Furthermore, we found that the c-Jun N-terminal kinase- (JNK-) MAPK pathway was activated in the left ventricle when the rats were exposed to CIH (Figure 4(e)). However, H₂-O₂ mixture markedly suppressed the phosphorylation of JNK (Figure 4(e)) in the left ventricle. The results indicated that H₂-O₂ mixture could attenuate myocardial cell apoptosis via the mitochondrial pathway induced by CIH.

3.5. H₂-O₂ Mixture Efficiently Reduced Oxidative Stress in Cardiac Tissue. Oxidative stress might be an inducer of

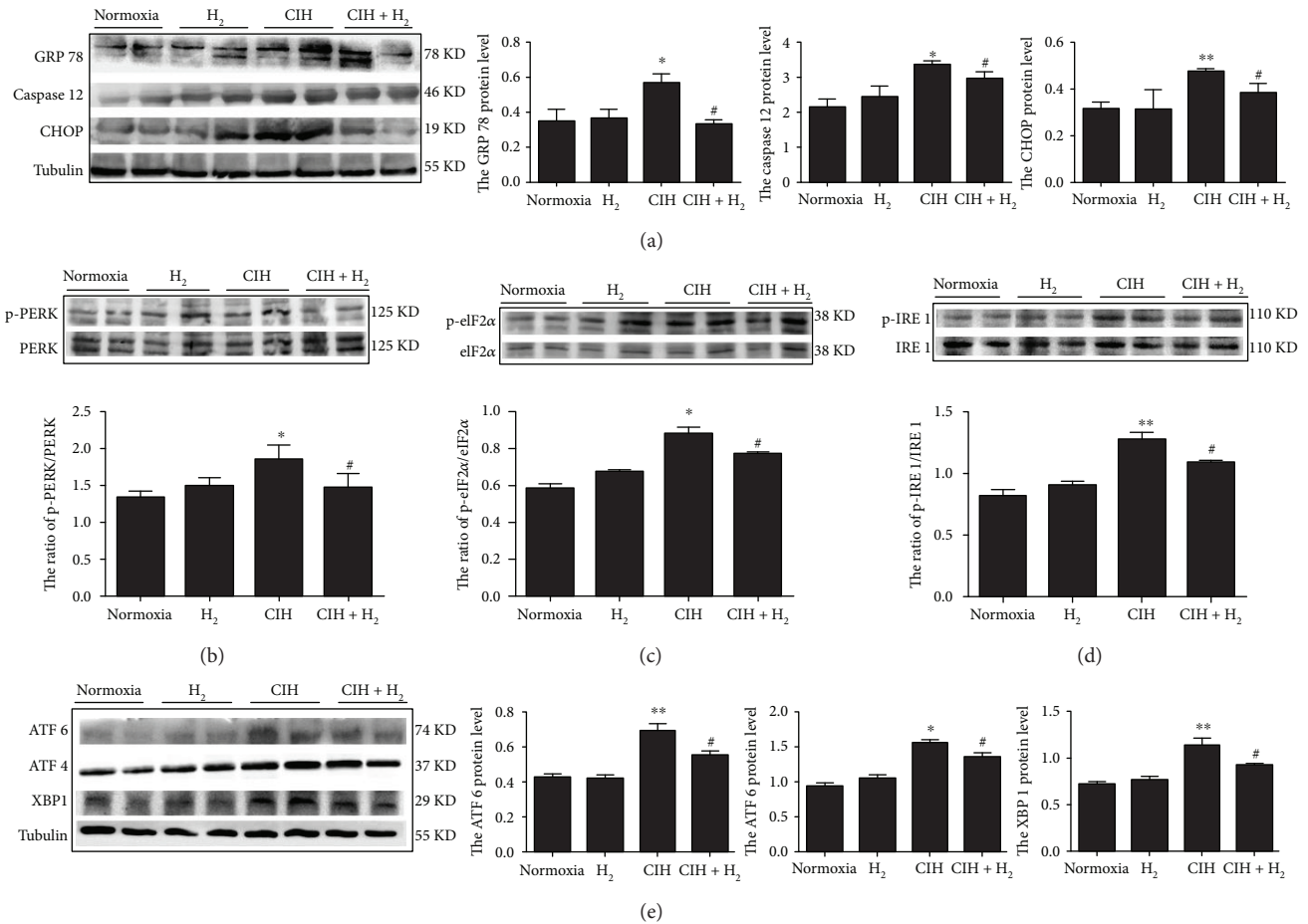


FIGURE 3: The H₂-O₂ mixture-induced inhibition of ER stress caused by CIH for 35 d: (a) the ER stress markers GRP 78, caspase 12, and CHOP protein expressions; (b–d) the ratios of p-PERK, p-eIF2 α /eIF2 α , and p-IRE 1/IRE 1 in the left ventricle; (e) ATF 6, ATF 4, and XBP 1 protein expressions. The results are presented as the mean \pm SEM. * $p < 0.05$; ** $p < 0.01$ vs. normoxia group; # $p < 0.05$ vs. CIH group; $n = 3$.

cardiac apoptosis when animals are exposed to CIH. We investigated whether H₂-O₂ mixture enhanced the antioxidant capacity to protect against CIH-induced oxidative stress injury. SOD and GSH are essentially endogenous antioxidants that scavenge superoxide anion radicals and hydrogen peroxide [30]. T-SOD and GSH activities were substantially elevated in the CIH+H₂ group compared to the CIH group (Figures 5(a) and 5(b)). However, the MDA content declined when the rat model was treated with H₂-O₂ mixture during CIH (Figure 5(c)). NADPH oxidase is an important source of ROS under some pathological conditions [29]. We found that the protein level of NOX 2, which is an important subtype of NADPH oxidase, was decreased when the rats were treated with H₂-O₂ mixture compared to that in the CIH group (Figure 5(d)). The results implied that H₂-O₂ mixture had ability to scavenge ROS in cardiac tissue exposed to CIH.

4. Discussion

OSA leads to CIH and contributes to cardiovascular diseases [31]. In this study, echocardiography revealed that cardiac systolic function declined, as shown by higher values of LVEDd and lower EF in CIH rats than in normoxia rats,

which is consistent with clinical findings [8]. The morphological results showed that the CIH rats showed myocardial fiber fractures and disorders, which might be an important cause of fibrosis in the heart [32]. In our study, we found that H₂-O₂ mixture inhalation could protect against the cardiac dysfunction and structural disorders induced by CIH in vivo. Furthermore, our study demonstrated that the cardioprotective effect of H₂-O₂ mixture was due to decreased ROS accumulation by reducing NADPH oxidase expression and blocking the PERK-eIF2 α -ATF4, IRE-XBP1, ATF 6, and JNK signaling that is involved in ER stress and apoptosis in CIH rats. Similar to other studies [33, 34], there was no significant difference between the normoxia and H₂-O₂ mixture-treated rats. Therefore, we think that H₂ plays the protective effect against CIH-induced cardiac damage.

A study showed that CHOP levels were significantly increased in many cardiac-related diseases [15], and another study showed that a deficiency in the CHOP gene reduced apoptosis in response to ER stress [35]. Our results showed that CHOP proteins were significantly increased in the left ventricle of the CIH rat model, indicating that the heart was undergoing apoptosis. During CIH, a large number of ROS are generated [11, 12], which further accelerates the

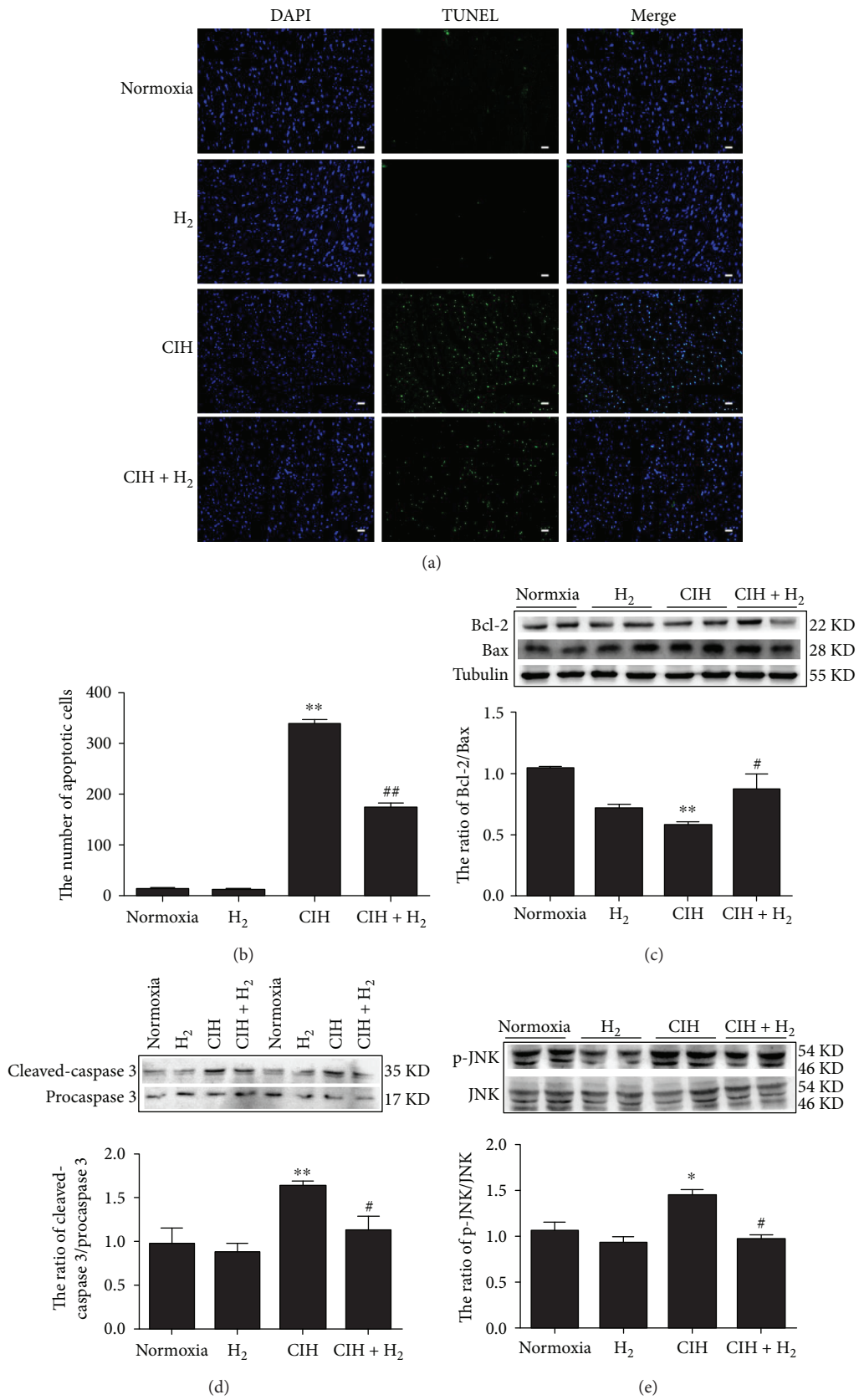


FIGURE 4: The effect of the H₂-O₂ mixture treatment on cardiomyocyte apoptosis in the CIH model: (a) TUNEL staining (scale bar = 25 μm); (b) the number of apoptotic bodies as shown in (a); (c) the ratio of Bcl-2/Bax; (d) the ratio of cleaved-caspase 3/procaspase 3; (e) the ratio of p-JNK and JNK. The results are presented as the mean ± SEM. **p* < 0.05; ***p* < 0.01 vs. normoxia group; #*p* < 0.05 vs. CIH group; *n* = 3.

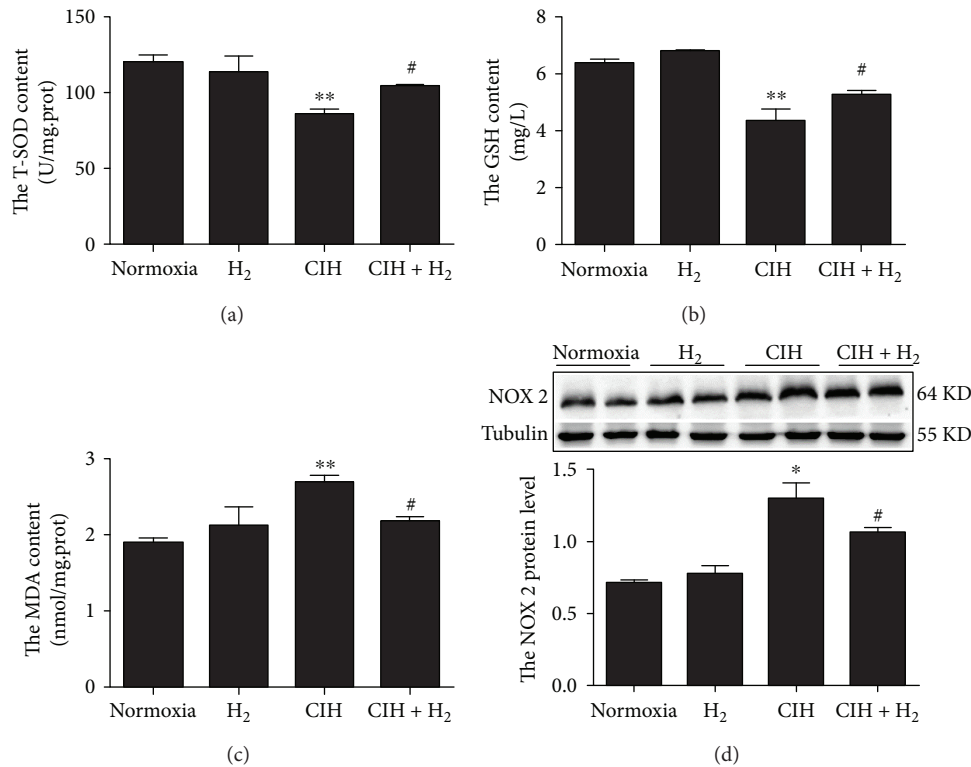


FIGURE 5: The effect of H₂-O₂ mixture on CIH-induced oxidative stress in the heart: (a, b) total superoxide dismutase (T-SOD) and glutathione (GSH) activities; (c) the content of malondialdehyde (MDA); (d) the NOX 2 protein level. The results are presented as the mean \pm SEM. * $p < 0.05$ vs. normoxia group; # $p < 0.05$ vs. CIH group; $n = 3$.

separation of GRP 78 from Bip [20] and activates PERK, IRE 1, and ATF 6 [36, 37]. The activation of PERK, IRE 1, and ATF 6 is all involved in apoptosis via CHOP [15, 38]. Activated PERK can phosphorylate eIF2 α at Ser 51, which selectively induces the translation and protein synthesis of ATF 4 [39]. ATF 4 is a transcription factor and enhances CHOP translation [38]. Additionally, XBP 1 is spliced by the endoribonuclease of IRE 1 under ER stress [40] and becomes a potent transcription factor for CHOP [38]. Our results showed that the PERK-eIF2 α -ATF4, IRE 1-XBP1, and ATF 6 pathways were all inhibited in the CIH+H₂ group compared to the CIH group (Figure 3). These results suggested that ER stress-induced apoptosis was inhibited in cardiac tissues when CIH rats inhaled H₂-O₂ mixture.

Previous studies confirmed that activated JNK-MAPK was involved in cell apoptosis induced by oxidative stress [29, 41]. The high level of ROS directly accelerates JNK-MAPK signaling activation, resulting in apoptosis [20, 29]. Activated JNK promotes Bax translocation from the cytoplasm to the mitochondria and decreases the expression of the antiapoptotic factor Bcl-2, resulting in the release of cytochrome C (Cyto C) into the cytoplasm [42]. Dysfunction in mitochondria would activate caspase 3, degrade the downstream substrate, and eventually lead to apoptosis [43]. Our results showed a lower ratio of Bcl-2/Bax, and the activation of caspase 3 and JNK was induced during CIH (Figure 4). We found that the JNK-MAPK pathway was significantly inhibited when CIH rats were treated with H₂-O₂ mixture. Furthermore, studies have reported that

JNK-MAPK signaling was also related to ER-induced apoptosis [20, 44]. Studies revealed that activated PERK could induce JNK phosphorylation [11] and that phosphorylated IRE 1 was able to recruit TNFR-associated factor-2 (TRAF-2) and activate the downstream target phospho-JNK-MAPK [44]. In addition, activated CHOP is also involved in apoptosis via downregulating Bcl-2 expression [45]. Our results showed that p-PERK, p-IRE, and CHOP were all inhibited when rats were treated with H₂-O₂ mixture (Figure 3). Therefore, JNK-MAPK signaling played multiple roles in the cardioprotective effects of H₂-O₂ mixture (Figure 6).

During the hypoxia/reoxygenation process, ER stress causes calcium ions to continuously drain from the ER and accumulate in mitochondria [10]. The lower calcium ion level induces calcium/calmodulin-dependent protein kinase II (CAMKII) expression, resulting in caspase 12 activation [46]. Furthermore, activated caspase 12 could trigger the caspase cascade in response to ER stress. Caspase 9 activation could be achieved by caspase 12 directly or by an Apaf-1/Cyto C mechanism [43, 46]. The activated caspase 9 catalyzes the cleavage of procaspase 3, resulting in apoptosis [43, 46]. In this study, we also found that caspase 12 protein levels declined when rats were treated with H₂-O₂ mixture (Figure 3(a)). Therefore, H₂-O₂ mixture played an active role in resisting cardiac apoptosis induced by ER stress.

Similar to the injury caused by ischemia-reperfusion, hypoxia and reoxygenation injury caused by CIH is the most important pathophysiological features of OSA [47]. During hypoxia, ATP is decreased, and oxidative phosphorylation

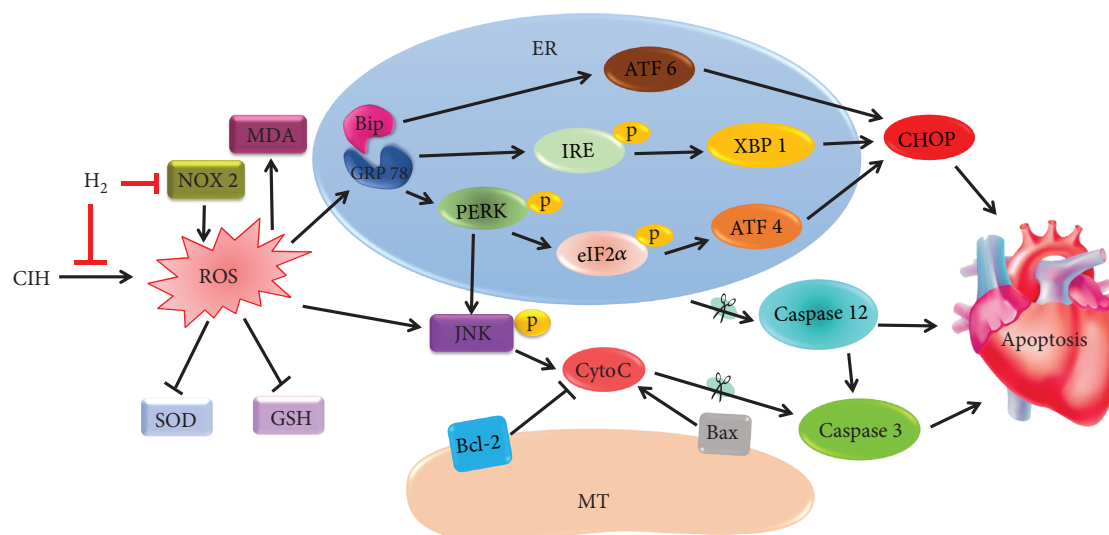


FIGURE 6: A schematic graph of the proposed cardioprotective mechanism of H_2 when rats were exposed to CIH. H_2 reduced the high level of ROS by elevating SOD and GSH activities and decreasing NOX 2 and the MDA content. H_2 inhibited ER stress by downregulating GRP 78, CHOP, and caspase 12 proteins. H_2 decreased CIH-induced apoptosis via three major ER stress response pathways: PERK-eIF2 α -ATF4, IRE 1-XBP1, and ATF 6. H_2 attenuated the JNK-MAPK pathway involved in apoptosis.

of mitochondria is also weakened [48]. When reoxygenation occurs, a large number of oxygen molecules enter mitochondria, and a large number of ROS are generated, including hydroxyl radicals, oxygen radicals, and hydrogen peroxide [48, 49]. Hydroxyl radicals are the most cytotoxic of ROS; H_2 has a strong ability to eliminate hydroxyl radicals and peroxynitrite [22, 24]. Previous researches have demonstrated 67% H_2 and 33% O_2 mixture gas strikingly decreased ROS induced by ischemia-reperfusion in the brain [34, 50], liver [51], and heart [52] in animal models. Clinical studies have reported 67% H_2 and 33% O_2 mixture reduced the inspiratory effort in patients with acute severe tracheal stenosis [53] and restored the exhausted supply of CD4+ T cells in patients with advanced colorectal cancer [54]. Our results showed 67% H_2 and 33% O_2 mixture gas increased T-SOD and GSH activity and decreased MDA content against the elevated ROS level induced by CIH. Other studies also demonstrated H_2 could increase catalase activity [33, 55], induce Nrf 2 transcription [56], and elevate heme oxygenase-1 expression [57] against oxidative stress injury.

During hypoxia and reoxygenation, neutrophils are activated, which triggers NADPH oxidase on the cell membrane and induces the production of free radicals [48, 58]. Heymes et al. first reported that NADPH oxidase was expressed in human myocardium [59] and was an important contributor to oxidative stress [60, 61]. In addition, NOX 2 (a subtype of NADPH oxidase) is specifically expressed in the cytomembrane [59] and plays an integral role in the oxidation-reduction signal pathway [62]. Our results revealed that H_2 - O_2 mixture considerably reduced CIH-induced ROS levels by inhibiting NOX 2 expression (a subtype of NADPH oxidase) (Figure 5). NOX 2 has also been reported to be an inducer of ER stress that mediates apoptosis through a CHOP/CAMKII pathway [63]. Therefore, lower NOX 2 levels suggested decreased ROS levels and CHOP-derived apoptosis when rats were exposed to

CIH (Figure 6). Therefore, we considered H_2 - O_2 mixture to be a safe and effective antioxidant.

5. Conclusion

In conclusion, our results revealed that H_2 - O_2 mixture efficiently improved cardiac dysfunction and structural disorder. The cardioprotective effect of H_2 - O_2 mixture was due to its ability to decrease ROS levels that were induced by CIH. Furthermore, our results revealed that H_2 - O_2 mixture dramatically reduced ER stress and apoptosis when rats were exposed to CIH. The data showed evidence that H_2 - O_2 mixture protected against the cardiac injury induced by CIH.

Data Availability

The data used to support the findings of this study are included within the article.

Conflicts of Interest

The authors declare no conflict of financial interest or benefit.

Authors' Contributions

Ya-Shuo Zhao and Ji-Ren An contributed equally to this work.

Acknowledgments

This work was supported by the Youth Top-notch Project of Hebei Education Department (BJ2017045), Education Department Foundation of Hebei Province (ZD2017057), National Natural Science Foundation of China (81170069), and Science and Technology Department of Hebei Province

(18277786D). We thanked the Shanghai Asclepius Company for providing the hydrogen producer.

References

- [1] C. S. Lam, G. L. Tipoe, K. F. So, and M. L. Fung, "Neuroprotective mechanism of *Lycium barbarum* polysaccharides against hippocampal-dependent spatial memory deficits in a rat model of obstructive sleep apnea," *PLoS One*, vol. 10, no. 2, article e0117990, 2015.
- [2] T. Young, P. E. Peppard, and D. J. Gottlieb, "Epidemiology of obstructive sleep apnea: a population health perspective," *American Journal of Respiratory and Critical Care Medicine*, vol. 165, no. 9, pp. 1217–1239, 2002.
- [3] M. A. Brisco and L. R. Goldberg, "Sleep apnea in congestive heart failure," *Current Heart Failure Reports*, vol. 7, no. 4, pp. 175–184, 2010.
- [4] R. P. Pedrosa, E. M. Krieger, G. Lorenzi-Filho, and L. F. Drager, "Recent advances of the impact of obstructive sleep apnea on systemic hypertension," *Arquivos Brasileiros de Cardiologia*, vol. 97, no. 2, pp. e40–e47, 2011.
- [5] Y. Liu, Z. Yu, D. Hua, Y. Chen, S. Zheng, and L. Wang, "Association of serum hepcidin levels with the presence and severity of obstructive sleep apnea syndrome," *Medical Science Monitor*, vol. 21, pp. 27–31, 2015.
- [6] Q. Luo, H. L. Zhang, X. C. Tao, Z. H. Zhao, Y. J. Yang, and Z. H. Liu, "Impact of untreated sleep apnea on prognosis of patients with congestive heart failure," *International Journal of Cardiology*, vol. 144, no. 3, pp. 420–422, 2010.
- [7] N. T. Huynh, O. Prilipko, C. A. Kushida, and C. Guilleminault, "Volumetric brain morphometry changes in patients with obstructive sleep apnea syndrome: effects of CPAP treatment and literature review," *Frontiers in Neurology*, vol. 5, p. 58, 2014.
- [8] Y. Sun, H. Yuan, M. Q. Zhao, Y. Wang, M. Xia, and Y. Z. Li, "Cardiac structural and functional changes in old elderly patients with obstructive sleep apnoea-hypopnoea syndrome," *The Journal of International Medical Research*, vol. 42, no. 2, pp. 395–404, 2014.
- [9] P. Gordon and M. H. Sanders, "Sleep.7: positive airway pressure therapy for obstructive sleep apnoea/hypopnoea syndrome," *Thorax*, vol. 60, no. 1, pp. 68–75, 2005.
- [10] R. Chen, L. Huo, X. Shi et al., "Endoplasmic reticulum stress induced by zinc oxide nanoparticles is an earlier biomarker for nanotoxicological evaluation," *ACS Nano*, vol. 8, no. 3, pp. 2562–2574, 2014.
- [11] L. Zhou, P. Chen, Y. Peng, and R. Ouyang, "Role of oxidative stress in the neurocognitive dysfunction of obstructive sleep apnea syndrome," *Oxidative Medicine and Cellular Longevity*, vol. 2016, Article ID 9626831, 15 pages, 2016.
- [12] L. H. Xu, H. Xie, Z. H. Shi et al., "Critical role of endoplasmic reticulum stress in chronic intermittent hypoxia-induced deficits in synaptic plasticity and long-term memory," *Antioxidants & Redox Signaling*, vol. 23, no. 9, pp. 695–710, 2015.
- [13] T. Minamino and M. Kitakaze, "ER stress in cardiovascular disease," *Journal of Molecular and Cellular Cardiology*, vol. 48, no. 6, pp. 1105–1110, 2010.
- [14] C. D. Ochoa, R. F. Wu, and L. S. Terada, "ROS signaling and ER stress in cardiovascular disease," *Molecular Aspects of Medicine*, vol. 63, pp. 18–29, 2018.
- [15] Y. Yao, Q. Lu, Z. Hu, Y. Yu, Q. Chen, and Q. K. Wang, "A non-canonical pathway regulates ER stress signaling and blocks ER stress-induced apoptosis and heart failure," *Nature Communications*, vol. 8, no. 1, p. 133, 2017.
- [16] S. Aldosari, M. Awad, E. O. Harrington, F. Sellke, and M. Abid, "Subcellular reactive oxygen species (ROS) in cardiovascular pathophysiology," *Antioxidants*, vol. 7, no. 1, 2018.
- [17] K. Jomova and M. Valko, "Advances in metal-induced oxidative stress and human disease," *Toxicology*, vol. 283, no. 2-3, pp. 65–87, 2011.
- [18] G. Bourdier, P. Flore, H. Sanchez, J. L. Pepin, E. Belaidi, and C. Arnaud, "High-intensity training reduces intermittent hypoxia-induced ER stress and myocardial infarct size," *American Journal of Physiology-Heart and Circulatory Physiology*, vol. 310, no. 2, pp. H279–H289, 2016.
- [19] X. H. Cai, X. C. Li, S. W. Jin et al., "Endoplasmic reticulum stress plays critical role in brain damage after chronic intermittent hypoxia in growing rats," *Experimental Neurology*, vol. 257, pp. 148–156, 2014.
- [20] W. Ding, X. Zhang, H. Huang et al., "Adiponectin protects rat myocardium against chronic intermittent hypoxia-induced injury via inhibition of endoplasmic reticulum stress," *PLoS One*, vol. 9, no. 4, article e94545, 2014.
- [21] Y. Hou, H. Yang, Z. Cui, X. Tai, Y. Chu, and X. Guo, "Tauroursodeoxycholic acid attenuates endoplasmic reticulum stress and protects the liver from chronic intermittent hypoxia induced injury," *Experimental and Therapeutic Medicine*, vol. 14, no. 3, pp. 2461–2468, 2017.
- [22] I. Ohsawa, M. Ishikawa, K. Takahashi et al., "Hydrogen acts as a therapeutic antioxidant by selectively reducing cytotoxic oxygen radicals," *Nature Medicine*, vol. 13, no. 6, pp. 688–694, 2007.
- [23] K. Fukuda, S. Asoh, M. Ishikawa, Y. Yamamoto, I. Ohsawa, and S. Ohta, "Inhalation of hydrogen gas suppresses hepatic injury caused by ischemia/reperfusion through reducing oxidative stress," *Biochemical and Biophysical Research Communications*, vol. 361, no. 3, pp. 670–674, 2007.
- [24] S. Ohta, "Recent progress toward hydrogen medicine: potential of molecular hydrogen for preventive and therapeutic applications," *Current Pharmaceutical Design*, vol. 17, no. 22, pp. 2241–2252, 2011.
- [25] Y. Gao, Q. Gui, L. Jin et al., "Hydrogen-rich saline attenuates hippocampus endoplasmic reticulum stress after cardiac arrest in rats," *Neuroscience Letters*, vol. 640, pp. 29–36, 2017.
- [26] K. Chen, N. Wang, Y. Diao et al., "Hydrogen-rich saline attenuates brain injury induced by cardiopulmonary bypass and inhibits microvascular endothelial cell apoptosis via the PI3K/Akt/GSK3 β signaling pathway in rats," *Cellular Physiology and Biochemistry*, vol. 43, no. 4, pp. 1634–1647, 2017.
- [27] Y. Zhang, J. Xu, Z. Long et al., "Hydrogen (H₂) inhibits isoproterenol-induced cardiac hypertrophy via antioxidative pathways," *Frontiers in Pharmacology*, vol. 7, p. 392, 2016.
- [28] S. C. Yang, L. L. Chen, T. Fu, W. Y. Li, and E. S. Ji, "Improvement of hydrogen on liver oxidative stress injury in chronic intermittent hypoxia rats," *China Journal of Applied Physiology*, vol. 34, no. 1, p. 4, 2018.
- [29] Y. Zhao, Z. Xin, N. Li et al., "Nano-liposomes of lycopene reduces ischemic brain damage in rodents by regulating iron metabolism," *Free Radical Biology & Medicine*, vol. 124, pp. 1–11, 2018.

- [30] Y. S. Zhao, L. H. Zhang, P. P. Yu et al., "Ceruloplasmin, a potential therapeutic agent for Alzheimer's disease," *Antioxidants & Redox Signaling*, vol. 28, no. 14, pp. 1323–1337, 2018.
- [31] M. A. Arias, F. García-Río, A. Alonso-Fernández, O. Mediano, I. Martínez, and J. Villamor, "Obstructive sleep apnea syndrome affects left ventricular diastolic function: effects of nasal continuous positive airway pressure in men," *Circulation*, vol. 112, no. 3, pp. 375–383, 2005.
- [32] M. C. Lai, J. G. Lin, P. Y. Pai et al., "Effects of rhodiola crenulata on mice hearts under severe sleep apnea," *BMC Complementary and Alternative Medicine*, vol. 15, no. 1, p. 198, 2015.
- [33] Z. Peng, W. Chen, L. Wang et al., "Inhalation of hydrogen gas ameliorates glyoxylate-induced calcium oxalate deposition and renal oxidative stress in mice," *International Journal of Clinical and Experimental Pathology*, vol. 8, no. 3, pp. 2680–2689, 2015.
- [34] J. Cui, X. Chen, X. Zhai et al., "Inhalation of water electrolysis-derived hydrogen ameliorates cerebral ischemia-reperfusion injury in rats - a possible new hydrogen resource for clinical use," *Neuroscience*, vol. 335, pp. 232–241, 2016.
- [35] H. Y. Fu, K. Okada, Y. Liao et al., "Ablation of C/EBP homologous protein attenuates endoplasmic reticulum-mediated apoptosis and cardiac dysfunction induced by pressure overload," *Circulation*, vol. 122, no. 4, pp. 361–369, 2010.
- [36] A. D. Friedman, "GADD153/CHOP, a DNA damage-inducible protein, reduced CAAT/enhancer binding protein activities and increased apoptosis in 32D c13 myeloid cells," *Cancer Research*, vol. 56, no. 14, pp. 3250–3256, 1996.
- [37] S. J. Marciniak, C. Y. Yun, S. Oyadomari et al., "CHOP induces death by promoting protein synthesis and oxidation in the stressed endoplasmic reticulum," *Genes & Development*, vol. 18, no. 24, pp. 3066–3077, 2004.
- [38] X. Yang, H. Shao, W. Liu et al., "Endoplasmic reticulum stress and oxidative stress are involved in ZnO nanoparticle-induced hepatotoxicity," *Toxicology Letters*, vol. 234, no. 1, pp. 40–49, 2015.
- [39] P. Zhang, Q. Sun, C. Zhao et al., "HDAC4 protects cells from ER stress induced apoptosis through interaction with ATF4," *Cellular Signalling*, vol. 26, no. 3, pp. 556–563, 2014.
- [40] E. Szegezdi, S. E. Logue, A. M. Gorman, and A. Samali, "Mediators of endoplasmic reticulum stress-induced apoptosis," *EMBO Reports*, vol. 7, no. 9, pp. 880–885, 2006.
- [41] C. Ferrandi, R. Ballerio, P. Gaillard et al., "Inhibition of c-Jun N-terminal kinase decreases cardiomyocyte apoptosis and infarct size after myocardial ischemia and reperfusion in anaesthetized rats," *British Journal of Pharmacology*, vol. 142, no. 6, pp. 953–960, 2004.
- [42] T. Kuwana, M. R. Mackey, G. Perkins et al., "Bid, Bax, and lipids cooperate to form supramolecular openings in the outer mitochondrial membrane," *Cell*, vol. 111, no. 3, pp. 331–342, 2002.
- [43] N. Morishima, K. Nakanishi, H. Takenouchi, T. Shibata, and Y. Yasuhiko, "An endoplasmic reticulum stress-specific caspase cascade in apoptosis. Cytochrome c-independent activation of caspase-9 by caspase-12," *The Journal of Biological Chemistry*, vol. 277, no. 37, pp. 34287–34294, 2002.
- [44] F. Urano, X. Wang, A. Bertolotti et al., "Coupling of stress in the ER to activation of JNK protein kinases by transmembrane protein kinase IRE1," *Science*, vol. 287, no. 5453, pp. 664–666, 2000.
- [45] K. D. McCullough, J. L. Martindale, L. O. Klotz, T.-Y. Aw, and N. J. Holbrook, "Gadd153 sensitizes cells to endoplasmic reticulum stress by down-regulating Bcl2 and perturbing the cellular redox state," *Molecular and Cellular Biology*, vol. 21, no. 4, pp. 1249–1259, 2001.
- [46] Z. G. Xiong, X. M. Zhu, X. P. Chu et al., "Neuroprotection in ischemia: blocking calcium-permeable acid-sensing ion channels," *Cell*, vol. 118, no. 6, pp. 687–698, 2004.
- [47] A. Gabryelska, Z. M. Lukasik, J. S. Makowska, and P. Białasiewicz, "Obstructive sleep apnea: from intermittent hypoxia to cardiovascular complications via blood platelets," *Frontiers in Neurology*, vol. 9, p. 635, 2018.
- [48] T. Kalogeris, C. P. Baines, M. Krenz, and R. J. Korthuis, "Ischemia/reperfusion," *Comprehensive Physiology*, vol. 7, no. 1, pp. 113–170, 2017.
- [49] T. Inagaki, T. Akiyama, C. K. Du, D. Y. Zhan, M. Yoshimoto, and M. Shirai, "Monoamine oxidase-induced hydroxyl radical production and cardiomyocyte injury during myocardial ischemia-reperfusion in rats," *Free Radical Research*, vol. 50, no. 6, pp. 645–653, 2016.
- [50] J. L. Huang, W. W. Liu, and X. J. Sun, "Hydrogen inhalation improves mouse neurological outcomes after cerebral ischemia/reperfusion independent of anti-necroptosis," *Medical Gas Research*, vol. 8, no. 1, pp. 1–5, 2018.
- [51] H. Li, O. Chen, Z. Ye et al., "Inhalation of high concentrations of hydrogen ameliorates liver ischemia/reperfusion injury through A_{2A} receptor mediated PI3K-Akt pathway," *Biochemical Pharmacology*, vol. 130, pp. 83–92, 2017.
- [52] O. Chen, Z. Cao, H. Li et al., "High-concentration hydrogen protects mouse heart against ischemia/reperfusion injury through activation of the PI3K/Akt1 pathway," *Scientific Reports*, vol. 7, no. 1, p. 14871, 2017.
- [53] Z. Q. Zhou, C. H. Zhong, Z. Q. Su et al., "Breathing hydrogen-oxygen mixture decreases inspiratory effort in patients with tracheal stenosis," *Respiration*, vol. 97, no. 1, pp. 42–51, 2019.
- [54] J. Akagi and H. Baba, "Hydrogen gas restores exhausted CD8+ T cells in patients with advanced colorectal cancer to improve prognosis," *Oncology Reports*, vol. 41, no. 1, pp. 301–311, 2018.
- [55] R. Liu, X. Fang, C. Meng et al., "Lung inflation with hydrogen during the cold ischemia phase decreases lung graft injury in rats," *Experimental Biology and Medicine*, vol. 240, no. 9, pp. 1214–1222, 2015.
- [56] W. Fang, G. Wang, L. Tang et al., "Hydrogen gas inhalation protects against cutaneous ischaemia/reperfusion injury in a mouse model of pressure ulcer," *Journal of Cellular and Molecular Medicine*, vol. 22, no. 9, pp. 4243–4252, 2018.
- [57] N. Y. Shen, J. B. Bi, J. Y. Zhang et al., "Hydrogen-rich water protects against inflammatory bowel disease in mice by inhibiting endoplasmic reticulum stress and promoting heme oxygenase-1 expression," *World Journal of Gastroenterology*, vol. 23, no. 8, pp. 1375–1386, 2017.
- [58] G. Vandeplasseche, C. Hermans, F. Thoné, and M. Borgers, "Mitochondrial hydrogen peroxide generation by NADH-oxidase activity following regional myocardial ischemia in the dog," *Journal of Molecular and Cellular Cardiology*, vol. 21, no. 4, pp. 383–392, 1989.
- [59] C. Heymes, J. K. Bendall, P. Ratajczak et al., "Increased myocardial NADPH oxidase activity in human heart failure," *Journal of the American College of Cardiology*, vol. 41, no. 12, pp. 2164–2171, 2003.

- [60] K. Bedard and K. H. Krause, "The NOX family of ROS-generating NADPH oxidases: physiology and pathophysiology," *Physiological Reviews*, vol. 87, no. 1, pp. 245–313, 2007.
- [61] C. Guichard, E. Pedruzzi, M. Fay et al., "The Nox/Duox family of ROS-generating NADPH oxidases," *Medecine Sciences*, vol. 22, no. 11, pp. 953–960, 2006.
- [62] D. I. Brown and K. K. Griendling, "Nox proteins in signal transduction," *Free Radical Biology & Medicine*, vol. 47, no. 9, pp. 1239–1253, 2009.
- [63] F. R. M. Laurindo, T. L. S. Araujo, and T. B. Abrahão, "Nox NADPH oxidases and the endoplasmic reticulum," *Antioxidants & Redox Signaling*, vol. 20, no. 17, pp. 2755–2775, 2014.

Review Article

The Role of the ER-Induced UPR Pathway and the Efficacy of Its Inhibitors and Inducers in the Inhibition of Tumor Progression

Anna Walczak , **Kinga Gradzik**, **Jacek Kabzinski** , **Karolina Przybylowska-Sygut**,
and Ireneusz Majsterek 

Department of Clinical Chemistry and Biochemistry, Medical University of Lodz, Lodz 90-647, Poland

Correspondence should be addressed to Anna Walczak; anna.walczak@umed.lodz.pl

Received 5 October 2018; Revised 8 December 2018; Accepted 18 December 2018; Published 3 February 2019

Academic Editor: Grzegorz Bartosz

Copyright © 2019 Anna Walczak et al. This is an open access article distributed under the Creative Commons Attribution License, which permits unrestricted use, distribution, and reproduction in any medium, provided the original work is properly cited.

Cancer is the second most frequent cause of death worldwide. It is considered to be one of the most dangerous diseases, and there is still no effective treatment for many types of cancer. Since cancerous cells have a high proliferation rate, it is pivotal for their proper functioning to have the well-functioning protein machinery. Correct protein processing and folding are crucial to maintain tumor homeostasis. Endoplasmic reticulum (ER) stress is one of the leading factors that cause disturbances in these processes. It is induced by impaired function of the ER and accumulation of unfolded proteins. Induction of ER stress affects many molecular pathways that cause the unfolded protein response (UPR). This is the way in which cells can adapt to the new conditions, but when ER stress cannot be resolved, the UPR induces cell death. The molecular mechanisms of this double-edged sword process are involved in the transition of the UPR either in a cell protection mechanism or in apoptosis. However, this process remains poorly understood but seems to be crucial in the treatment of many diseases that are related to ER stress. Hence, understanding the ER stress response, especially in the aspect of pathological consequences of UPR, has the potential to allow us to develop novel therapies and new diagnostic and prognostic markers for cancer.

1. Introduction

Cancer refers to any of a large number of diseases characterized by the development of abnormal cells that divide uncontrollably and have the ability to infiltrate and destroy normal body tissue. In the context of rapidly proliferating cells, there is a large demand for protein synthesis [1]. The endoplasmic reticulum (ER) is a cellular organelle responsible for the synthesis and proper folding of transmembrane proteins [2]. Many insults, including hypoxia, nutrient starvation, acidosis, redox imbalance, loss of calcium homeostasis, or exposure to drugs or other compounds, are capable of disturbing ER homeostasis, resulting in diminished capacity for proper protein folding.

These factors can result in unfolded and improperly folded proteins, termed ER stress. Upon ER stress conditions, the activated master regulators of the unfolded protein response (UPR) communicate to the nucleus to regulate the

transcription of genes involved in protein folding and processing to increase the ER protein folding capacity, ERAD, and autophagy components. This further leads to reduction in ER workload and cell survival and death factors to determine the fate of the cell depending on the ER stress condition [3]. Cancerous cells rely on these UPR pathways to adapt to perturbations in ER folding capacity due to the hostile tumor microenvironment as well as the increase in unfolded and misfolded proteins [4]. When the UPR fails to restore ER homeostasis and attenuate ER stress, the UPR activation induces apoptosis [5]. Therefore, UPR can be therapeutically exploited to reduce the survivability of malignant cells or tip the balance towards apoptosis.

In this review, we have discussed the studies on ER stress-induced UPR signaling in cancer as well as other various diseases and applications of ER stress-modulating molecules in therapy. The use of PERK kinase inhibitors appears to be a chance for a modern personalized therapy for people

for whom other therapies have failed. This article is a short analysis of publications published so far in this field.

2. ER Stress, UPR, and Their Role in the Disease Development

The stress of the endoplasmic reticulum (ER) can be induced by various factors. In response to it, the UPR pathway is activated. It is responsible for preservation of cell homeostasis. This ER balance can be perturbed by physiological and pathological insults such as high protein demand, infections, environmental toxins, inflammatory cytokines, and mutant protein expression resulting in the accumulation of misfolded and unfolded proteins in the ER lumen, a condition termed as ER stress.

The stress of the endoplasmic reticulum is associated with the activation of three factors: PKR-like ER kinase (PERK), activating transcription factor 6 (ATF6), and inositol-requiring enzyme 1 (IRE1 α). Studies on the role of this pathway and the effects of its inhibition show different results depending on the activated factor and the type of cancer.

The regulation of the protein synthesis process in response to stress conditions is based on the phosphorylation of the eIF2 α factor by PERK kinase [6]. Interestingly, higher levels of the phosphorylated eIF2 α protein have been discovered in the course of neoplastic diseases, e.g., breast cancer [7]. Activation of the UPR pathway results in the restoration of cellular homeostasis by increasing the translation of ATF4 mRNA which is responsible for the expression of proadaptive genes needed to transmit a signal that allows the cell to survive during stressful conditions [8]. The prolonged stress of the endoplasmic reticulum results in an increased transcription of the CCAAT-enhancer-binding protein homologous (CHOP) protein [9]. It is a factor that can both direct the cell to the pathway of programmed death (by weakening the expression of antiapoptotic Bcl-2 proteins and activation of BIM proteins that bring cells to the apoptosis pathway and enable cell survival by inducing the expression of the GADD34 and ERO1 α genes [6, 10]. On the other hand, it is responsible for the weakening of the UPR associated with PERK kinase and the proapoptotic response induced by the CHOP protein [11, 12].

Other pathway that partially has a crosstalk with the PERK branch of UPR is IRE1 α . IRE1 α is a kinase that undergoes autotransphosphorylation upon ER stress conditions, leading to endoRNase activation. Active IRE1 introduces nicks in X-box-binding protein-1 (XBP1) mRNA, and ligation of the remaining 5' and 3' fragments resulting in the activation of XBP1s (spliced form) Lu et al. [13]. It modulates the expression of several UPR target genes involved in ER folding, glycosylation, and ER-associated degradation (ERAD) [14]. Moreover, the IRE1/endo-RNase activity can affect mRNAs and microRNAs and cause regulated IRE1-dependent decay (RIDD). RIDD has emerged as a novel UPR regulatory component that controls cell fate under ER stress [15].

The last branch of ER stress-induced cellular response via UPR is the activation of ATF6. It was primarily identified

as a cytoprotective factor during ER stress [16]. ATF6 is activated by proteolysis and acts as a transcriptional factor for regulating the downstream expression of genes responsible for stresses [17]. Studies have shown that activated ATF6 signaling is correlated with lower OS of patients with various types of tumors, cancer recurrence, metastatic lesions, tumor growth, and resistance to radio- and chemotherapy [18]. The UPR signaling cascade is shown in Figure 1.

3. Major Inducers of ER Stress

UPR is a factor of known prosurvival factor of tumor cells that can act via adaptive mechanism during cancer progression. In the context of cancer, different extrinsic (hypoxia, nutrient deprivation, and acidosis) and intrinsic (oncogene activation) factors cause endoplasmic reticulum stress and trigger the UPR.

One of the major factors inducing the UPR pathway is hypoxia. The tumor microenvironment is characterized by low oxygen concentration that is related to rapid tumor growth. Cancer cells in this environment show a high proliferative potential and, together with the increase in oxygen concentration, an increasingly aggressive phenotype. Previous studies suggest that hypoxia weakens protein biosynthesis due to the stress of the endoplasmic reticulum, which leads to the activation of the response pathway to UPR. Activation of the UPR in hypoxic tumors leads to increased autophagy [19]. Autophagy liberates amino acids from long-lived proteins and damaged organelles. In multiple cell lines, PERK mediates the upregulation of LC3 and autophagy-related gene 5 via ATF4 and CHOP, respectively, promoting phagophore formation.

Oxidative stress is also one of the main factors causing ER stress. Reactive oxygen species (ROS), i.e., molecules having an unpaired electron, such as hydroxyl (OH) and superoxide (O₂⁻) radicals, are formed endogenously during the processes occurring in the respiratory chain in the mitochondria; hence, their increased amount can be observed in cells with high-energy demand. O₂ may form nitrate (ONOO⁻) together with nitric oxide (NO), which is an extremely overreactive molecule and may interfere with proteins and DNA causing their oxidation or nitration [20]. They arise in large quantities under hypoxia conditions, which stimulate mitochondrial activity. Free radicals can also be delivered to the body exogenously by eating fried and grilled products. Their production is also induced by smoking cigarettes. Free radicals in the human body perform many roles such as signaling, regulation of gene expression, or modulating the level of calcium in the cell [20]. Their excess, however, can be harmful. Oxidative stress interferes with the process of protein folding, leading to the formation of deposits of unfolded proteins, which induces ER stress [21]. Studies carried out on mice may confirm this directly [22]. In transgenic animals that overexpressed the superoxide dismutase (SOD) gene, ATF4 and CHOP levels were observed to be lower than in wild type. It follows that the apoptotic death of hippocampal cells after ischemia associated with ER stress in these mice occurs to a lesser extent if the process of eliminating free radicals is more efficient.

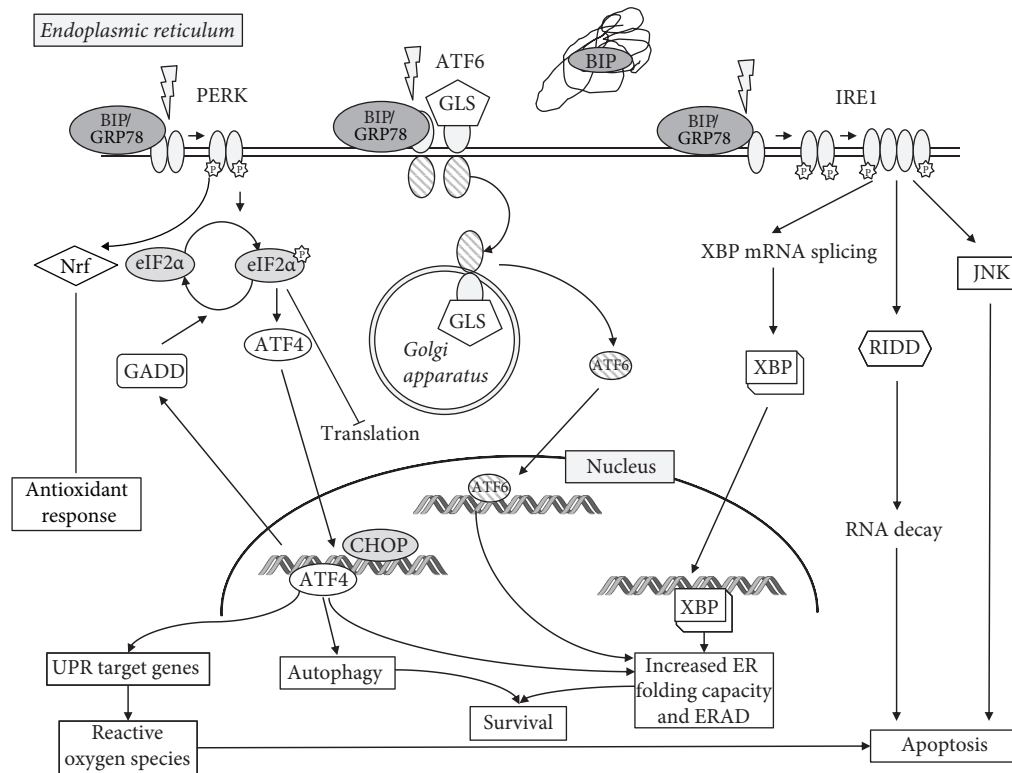


FIGURE 1: The UPR signaling cascade. UPR pathways are activated through competitive binding of the chaperone immunoglobulin heavy-chain-binding protein (BiP) also known as glucose-regulated protein 78 (GRP78) to the receptors. Accumulation of misfolded or unfolded proteins in the endoplasmic reticulum (ER) leads to the dissociation of BiP from 3 transducers: PERK (double-stranded RNA-activated protein kinase-like ER kinase), ATF6 (activating transcription factor 6), and IRE1 (inositol-requiring enzyme). Upon activation, PERK phosphorylates and deactivates the eukaryotic initiation factor (eIF2 α), which results in an increased level of ATF4. This triggers the activation of C/EBP homologous protein (CHOP). Subsequently, DNA damage-inducible protein transcript (GADD) expression is also elevated, what negatively regulates eIF2 α phosphorylation and restores translation. While initially contributing to cellular survival in conditions of ER stress, PERK is considered proapoptotic due to strong induction of CHOP in chronic or terminal ER stress. PERK also regulates several transcription factors including NRF-2 that upregulate the antioxidant response and ATF4 which can lead to both protective and apoptotic signaling. Upon activation, ATF6 is released from BiP that is trafficked to the Golgi apparatus (it consists of two Golgi localization signals, GLS) and cleaved by the proteases into two subunits. Then it translocates to the nucleus where it is the promoter region of UPR target genes termed the endoplasmic reticulum stress element (ERSE), activating genes responsible for the components of the UPR response and leads to the induction of molecular chaperones (e.g., GRP78, Grp94, and calreticulin, as well as CHOP and XBP1). The various ER chaperones are part of a protective adaptive response that regulates protein folding and other components of the UPR. ATF6 is primarily considered prosurvival due to its role in promoting the transcription of chaperones and XBP1. IRE-1 activation is responsible for in the unconventional splicing of XBP-1 mRNA. Spliced XBP-1 encodes a transcription factor that activates the expression of UPR genes, such as chaperones and ER-associated degradation proteins (ERAD). These include the activation of the cell death machinery, degradation of ER-localized mRNAs that encode secreted and membrane proteins through the RIDD (regulated Ire1-dependent decay) pathway, and induction of autophagosomes. This signaling cascade increases the folding capacity of the ER and causes degradation of misfolded proteins. IRE1 is mainly considered as a prosurvival pathway, but it also can contribute to apoptosis through the activation of JNK-dependent pathway.

Induction of oxidative stress is closely related to inflammatory processes. Chronic inflammation can lead to the release of inflammatory factors such as prostaglandins, production of ROS, and secretion of tumor-promoting cytokines. These molecules promote the survival, growth, and metastasis of tumor cells through NFKB/NFkB (nuclear factor kappa B; mediators downstream of the UPR), STAT3 (signal transducer and activator of transcription 3), and AP-1 (AP-1 transcription factor) signaling pathways as well as cytokines such as IL1B/IL1b, IL6, IL11, and IL23A [23]. Experiments performed on pancreatic islet cells and in mice with type

2 diabetes mellitus showed that cytokines such as IL-1B, IL-23, and IL-24 can induce ER stress [21]. By administering serum with antibodies against this particular interleukin, an improved glycemic control and a reduction in ER stress were achieved. The experiments carried out in 2010 by scientists from Belgium, Germany, Greece, and USA have also shown that interferons can cause disturbances leading to excessive ER stress [24].

Other factor that can induce ER stress is ionizing radiation (IR). It is proven that IR can evoke the activation of the PERK-eIF2 α pathway and subsequently cell death [25, 26].

During cancer genesis, an acute demand of protein synthesis is also needed to support different cellular functions, such as tumor proliferation, migration, and differentiation, often driven by oncogenic activation [27]. Eukaryotic cells react to the nutrient starvation by activation of the integrated stress response (ISR). It is driven by kinases (including GCN2 and PERK kinase) that induce eIF2 α phosphorylation and translation of ATF4 [28]. ATF4 regulates adaptation to amino acid deprivation (AAD) by regulation of amino acid transporter expression (SLC3A2, SLC7A5, and GLYT1) and enzymes of amino acids metabolism. Additionally, activation of ATF4 is also vital for suppressing oxidative stress through the induction of glutathione biosynthesis [29]. ATF4 is a protein necessary for cancer cells growth proliferation. Data has shown that ATF4-deficient cell cultures have to be supplemented with antioxidants and necessary amino acids to survive [30, 31]. GCN2 activation/overexpression and increased phospho-eIF2 α were observed in human and mouse tumors compared with normal tissues and abrogation of ATF4 or GCN2 expression significantly inhibited tumor growth *in vivo* [31]. Additionally, Wang et al. [32] showed that amino acid deprivation promotes tumor angiogenesis through the GCN2/ATF4 pathway [32].

UPR can also be induced by glucose deprivation and subsequent acidosis. Tumor cells adapt to low glucose levels by switching to a high rate of aerobic glycolysis, which is correlated with the expression of glucose transporter GLUT1 [33]. The resulting lactic acid production reduces the pH and thus causes acidosis. It is an important feature of the tumor microenvironment that can increase tumor survival rate and its progression by the regulation of CHOP and BCL-2 (B-cell leukemia/lymphoma-2) protein family members [34]. The glucose-regulated protein family, which includes the master UPR regulator GRP78, was discovered due to the upregulation of its members in response to glucose deprivation [35]. Also, elevated XBP1 splicing level was observed upon exposure to a nonmetabolizable glucose analog that simulates glucose deprivation [36].

The most potent intrinsic factors that induce UPR are activated oncogenes. We will discuss three of them: RAS, BRAF, and c-MYC.

Data show that oncogenic HRAS induces and activates the IRE1 α RNase in primary epidermal keratinocytes through the MEK-ERK pathway and that IRE1 α and *Xbp1* splicing are elevated in mouse cutaneous squamous tumors [37]. Moreover, HRAS(G12V)-driven senescence was mediated by the activation of all arms the ER-associated unfolded protein response. It was also found that oncogenic forms of HRAS (HRAS(G12V)), but not its downstream target BRAF (BRAF(V600E)), engaged a rapid cell-cycle arrest and were associated with massive vacuolization and expansion of the ER [38]. ATF4-deficient MEFs transformed with SV40 large T antigen and HRAS(G12V) oncogenes displayed a slow growth, failed to form colonies on soft agar, and formed significantly smaller tumors *in vivo* due to suppressing expression of the INK4a/ARF [39]. Transformation of PERK-deficient cells by SV40 large T antigen and K-RAS (G12V) did not affect growth and anchorage-independent growth, suggesting that ATF4

could have some PERK-independent functions during transformation [40]. Increased levels of p-eIF2 α , XBP1s, and GRP78 were observed in Nf1/p53 mutant mouse model of malignant peripheral nerve sheath tumors (MPNSTs), suggesting that the UPR is activated in HRAS-driven tumors *in vivo* [41].

The BRAF(V600E) mutation is present in up to 70% of malignant melanoma and other cancers and results in an increased activation of the kinase, leading to enhanced MEK/ERK signaling in the absence of extracellular signals [42]. It was proven that the presence of this mutation increased protein synthesis and activated XBP1 and GRP78 in human melanocytes. Activation of the UPR was dependent on protein synthesis, as suppression of protein synthesis attenuates the activation of XBP1s and GRP78 as well as induced autophagy via IRE1 and PERK [43–45].

c-Myc drives important biological processes such as cell growth, proliferation, and its metabolism (especially protein synthesis) and regulates apoptosis [46]. Recent studies showed that cell autonomous stress, such as activation of the protooncogene *MYC/c-Myc*, can also trigger the UPR. It was demonstrated that c-Myc and N-Myc activated the PERK/eIF2 α /ATF4 arm of the UPR, leading to an increased cell survival via the induction of cytoprotective autophagy. Inhibition of PERK significantly reduced Myc-induced autophagy, colony formation, and tumor formation. Moreover, pharmacologic or genetic inhibition of autophagy resulted in increased Myc-dependent apoptosis [47]. Dey et al. [48] also observed EIF2AK3/PERK-dependent induction of cytoprotective autophagy in MYC-overexpressing cells. The deregulated expression of Myc drives tumor progression in most human cancers, and UPR and autophagy have been implicated in the survival of Myc-dependent cancer cells. Data obtained in the animal model (*Drosophila melanogaster*) show that UPR, autophagy, and p62/Nrf2 signaling are required for Myc-dependent cell growth [49].

A number of studies confirm the role of the excess of unfolded proteins in the induction of the PERK kinase-dependent pathway. ER stress is induced to restore cell homeostasis by inhibiting translation.

4. Cancer Cell Targeting via Apoptosis Pathway or Promoting Cell Survival

The stress of the endoplasmic reticulum is associated with the activation of three factors: PERK, ATF6, and IRE1a. Studies on the role of this pathway and the effects of its inhibition show different results depending on the activated factor and the type of cancer.

The role of ER stress as an important factor in cancer development has been proposed in 2004, and since then there are more and more evidence confirming this thesis [50]. For instance, increased expression levels of the major components of the UPR such as PERK and ATF6, IRE1 α , both unspliced and spliced XBP1, were observed in tissue sections from a variety of human tumors including brain, breast, gastric, kidney, liver, lung, and pancreatic cancers [51–58]. Moreover, the chaperone GRP78 that is linked to higher

tumor grades dissemination/metastasis of human tumors and reduced overall survival (OS).

Rubio-Patino et al. [59] showed that in mice with colorectal malignancies, activation of the IRE1-associated UPR pathway led to reduced tumor growth and increased survival [59]. This study, through a low-protein diet, induced ER stress in tumor cells. During the experiment, it also turned out that under such conditions the immune response is much more efficient; these mice had an increased number of NK cells and CD3 + CD8 + lymphocytes infiltrating the tumor. Inhibition of this pathway by the inhibitor resulted in a reduction in the beneficial effect of the low-protein diet, which suggests that the UPR-related pathway associated with IRE1a directed the cells to the pathway of apoptosis and increased sensitivity to the immune system.

It should be noted that studies regarding the role of IRE1a activated in the group of patients with breast cancer showed that splicing XBP1 associated with the above-mentioned factor leads to the adaptation of cells to the conditions of hypoxia [60]. Such tumors are characterized by a worse prognosis. This underlines the very important role of accurate determination of the impact of UPR pathway activation on tumor progression.

In patients with chronic B-chronic lymphocytic leukemia (B-CLL), it was shown that the induction of the UPR pathway associated with ER stress (activation of PERK kinase) leads to apoptotic death of tumor cells. This effect was confirmed by the influence of commercially available ER stress inducers (thapsigargin and tunicamycin) on the progression of tumor growth. Researchers have shown that these compounds induce apoptosis of cells in patients with B-CLL [61]. On the other hand, ER stress also triggers survival signals in B-CLL cells by increasing BiP/GRP78 expression.

The branch of the UPR pathway associated with PERK kinase is responsible for the induction of blood vessel formation in tumor cells under hypoxic conditions. Angiogenesis is mediated by ATF4, which induces the expression of vascular endothelial growth factor (VEGF) [62]. Data have shown that ATF4 binds to the regulatory site of VEGF [63]. Moreover, *in vitro* studies revealed that partially blocking UPR signaling by silencing PERK or ATF4 significantly reduced the production of angiogenesis mediators induced by glucose deprivation [63].

In the melanoma patients, the role of the UPR pathway in promoting cell survival has been confirmed [64]. It induces the expression of proadaptive proteins and at the same time lowers proapoptotic proteins. It also increases the process of autophagy, which allows cancer cells to recover the necessary components, such as amino acids, and remove damaged organelles from cells that are older and more damaged.

It has also been confirmed that the UPR pathway associated with PERK promotes the progression of colorectal tumors. It has been shown that PERK plays an important role in tumor cell adaptation to hypoxic stress by regulating the translation of molecules that promotes cellular adhesion, integrin binding, and capillary morphogenesis necessary for the development of functional microvessels [65]. The association of ATF4 factor promoting angiogenesis and proadaptive gene expression is suspected, and GADD34, which

prevents apoptosis induction during prolonged ER stress, by lowering overtranslation of proteins [66].

Pancreatic cancer cells are under permanent high hypoxic state caused by large volume of the tumor, and only a small fraction of cancer cells are at the normal oxygenation levels of the surrounding normal pancreas [67]. Choe et al. (2011) showed that in pancreatic cancer cells, activation of the PERK and IRE1 arms of the UPR are delayed in the presence of ER stressors, compared to normal pancreatic cells. This was attributed to an abundance of protein-folding machinery, such as chaperones. Additionally, once activated, the prosurvival XBP1 was noted to be activated for a longer period of time in cancer cells when compared to normal cells [68]. Moreover, the unfolded protein response seems to play a predominant homeostatic role in response to mitochondrial stress in pancreatic stellate cells. Su et al. evaluated AMPK/mTOR signaling, autophagy, and the UPR to cell fate responses during metabolic stress induced by mitochondrial dysfunction [69]. Rottlerin treatment induced rapid and sustained PERK/CHOP UPR signaling, causing loss of cell viability and cell death. As well as adapting to chronic ER stress, it has been recently postulated that anterior-gradient 2 (AGR2) may contribute to the initiation and development of PDAC [70].

In addition, the experiment conducted by Liu et al. [71] showed that activation of the UPR pathway leads to the change in ATF6 α , PERK, and IRE1 α expression and is associated with progression of prostate cancer, worse prognosis, and more aggressive growth [71].

The summary and additional information of the UPR involvement in the pathogenesis and progression of various types of cancer is presented in Table 1.

5. ER Stress and Cancer Treatment—Novel UPR Modulating Factors

ER stress plays a large role in both progression and moderation of response to cancer chemo- and radiotherapy. Activation of the UPR pathway takes place under the influence of many factors, which are subjected to a cancer cell: unfolded proteins (protein economy is intensified during cancer, which is a very dynamic process), hypoxia (associated with excessively fast nascent tumor mass), pH changes, or chemotherapy [84].

GRP78 as the chaperone protein is an interesting target for the anticancer therapy, especially in cancer stem cells, and was partially effective in head and neck cancer treatment [85]. An immune adjuvant therapy seems to be effective since monoclonal antibody against GRP78 was shown to suppress signaling through the PI3K/Akt/mTOR pathway, which is responsible for radiation resistance in nonsmall cell lung cancer and glioblastoma multiforme (GBM). It was shown that ionizing radiation increased GRP78 expression through the induction of ER stress, and treatment with the monoclonal antibody along with ionizing radiation in mouse xenograph models showed a significant tumor growth delay [86]. Other study reveals that using a phage, displaying a ligand specific to GRP78

TABLE 1: UPR involvement in cancers.

UPR linked to cancer	Cancer type	Branch of the UPR	References
Cancer initiation	CRC	PERK/eIF2 α axis activation is associated with the loss of stemness	[72, 73]
	Colitis-associated cancer model	IRE1 α pathway induces intestinal stem cell expansion XBP1 loss in epithelial cells results in intestinal stem cell hyperproliferation	
	Prostate cancer	Change in ATF6 α , PERK, and IRE1 α expression	
Tumor quiescence and aggressiveness	B-CLL	BiP/GRP78 overexpression triggers survival signals and prevents apoptosis	[60, 61, 71, 74, 75]
	Triple-negative breast cancers	Constitutively active IRE1 α /XBP1s axis confers higher aggressiveness due to XBP1-mediated hypoxia-inducible factor-1 α activation	
	Glioblastoma (GBM)	IRE1 α endoribonuclease activity regulates the extracellular matrix protein SPARC (secreted protein acidic and rich in cysteine) involved in GBM tumor invasion Increased expression of XBP1s in metastatic tumors correlates with the EMT inducer SNAIL (snail-related protein)	
Tumor epithelial-to-mesenchymal transition	Breast tumors thyroid cell glioblastoma (GBM)	LOXL2 (lysyl oxidase-like 2)/GRP78 activates the IRE1-XBP1 signaling induce EMT-linked transcription factors expression: SNAI1 (snail family transcriptional repressor), SNAI2, ZEB2 (zinc-finger E-box-binding homeobox 2), and TCF3 (transcription factor 3) Serpine B3, a serine/cysteine protease inhibitor overexpression, is associated with chronic UPR induction leading to nuclear factor- κ B activation and interleukin-6 production PERK constitutive activation correlates with the overexpression of the TWIST (twist-related protein) transcription factor	[76–78]
	Human head and neck squamous cell carcinoma	Amino acid deprivation promotes tumor angiogenesis through the GCN2/ATF4 pathway	
	Human head and neck squamous cell carcinoma, breast cancer, and glioma cell lines	Glucose deprivation-induced UPR activation promotes upregulation of proangiogenic mediators (VEGF, FGF2, and IL6) and downregulation of several angiogenic inhibitors (THBS1, CXCL14, and CXCL10) through the PERK/ATF4	
	Colorectal cancer	Hypoxic stress-induced PERK overexpression stimulates the creation of microvessels	
Tumor angiogenesis	Glioblastoma (GBM)	IRE1 α signaling induce vascular endothelial growth factor-A (VEGF-A), interleukin-1 β , and interleukin-6 IRE1 α -mediated mRNA cleavage of the circadian gene PERIOD1,92 an important mediator of regulation of the CXCL3 chemokine supports tumor angiogenesis PERK-ATF4 branch upregulates VEGF in hypoxia Chaperone ORP150 (oxygen-regulated protein 150) controls tumor angiogenesis by promoting the secretion of VEGF	[32, 63, 65, 79–82]
	Prostatic and glioma cancer cells		
	Triple-negative breast cancer cells	Hypoxia-inducible factor-1 α activation, XBP1 upregulates glucose transporter 1 expression promotes glucose uptake of IRE1 α , XBP1s downstream activates enzymes of the hexosamine biosynthetic pathway expression	
Tumor metabolic processes	Triple-negative breast cancer cells	PERK/eIF2 α /ATF4 pathway activation protect tumor cells through autophagy induction via LC3B (autophagy protein microtubule-associated protein 1 light chain 3b) and ATG5 (autophagy protein 5) TNF receptor associated factor 2 (TRAF2)/IRE1 α activates c-Jun N-terminal protein kinase induces autophagy	[83]
Tumor autophagy	Triple-negative breast cancer cells		[19, 83]

with the antiviral drug ganciclovir, prostate cancer bone metastasis tumors were reduced by an average of 50% [87].

A group of patients with AML has been studied for molecular changes that allow survival and resistance to treatment. The results clearly indicate the role of the proadaptive pathway associated with ER stress mediated by PERK kinase. In the case of PERK, selective ATP-competitive PERK kinase inhibitors such as GSK2606414 or GSK2656157 were anti-proliferative in multiple cancer models *in vivo* including multiple myeloma [88, 89]. In the AML cells obtained from the mouse model in which GSK2656157, a PERK inhibitor, was used, the response to treatment was better. An 80% greater decrease in tumor colony growth was obtained against the group in which the UPR pathway occurred correctly [90]. In case of human multiple myeloma, other ER stress modulator STF-083010, a small-molecule inhibitor of Ire1, is a promising target for anticancer therapy [91].

It has been demonstrated that tyrosine kinase inhibitors (TKIs) on Hodgkin's lymphoma are correlated to increase in ER stress and ER stress-induced apoptosis. After treatment of L-428, L-1236, and KM-H2 cells with the TKI sorafenib, the elevated level of p-PERK and phosphorylation of eIF2 α were observed. In addition, proapoptotic signaling molecules GADD34 and CHOP were noted to be upregulated after incubation with sorafenib [92].

It has been also proven that PERK regulates glioblastoma sensitivity to ER stress through promoting radiation resistance [25]. By inhibiting PERK, it was determined that ionizing radiation- (IR-) induced PERK activity led to eIF2 α phosphorylation. IR enhanced the prodeath component of PERK signaling in cells treated with Sal003, an inhibitor of phospho-eIF2 α phosphatase. Mechanistically, ATF4 mediated the prosurvival activity during the radiation response. The data support the notion that induction of ER stress signaling by radiation contributes to adaptive survival mechanisms during radiotherapy.

Adaptation to an environment conducive to ER stress is essential for survival and propagation of pancreatic cancer cells. *In vitro* studies of diindolylmethane derivatives have shown similar ER stress induction activity as thapsigargin followed by subsequent apoptosis via death receptor 5 (DR5) through induction by CHOP [93]. Other compound, a proteasome inhibitor called bortezomib, was increasing the levels of GRP78, CHOP, and c-Jun NH2 terminal kinase (JNK) in L3.6pl pancreatic cancer cells, yet interestingly at the same time was blocking PERK autophosphorylation, and thus inhibiting phosphorylation of eIF2 α [94].

ER stress can be a factor supporting the progression of colorectal cancer. It has been proven that in cell lines of colorectal cancer it plays an important role in the loss of the intestinal stem cell (ISC) phenotype. Activation of the PERK eIF2 α branch in response to ER stress leads to the transformation of CRC cells to a more aggressive type [84].

It has been shown that activation of the UPR pathway and adaptation to stress conditions lead to the emergence of a chemotherapy-resistant phenotype HT-29/MDR [95]. This process takes place by activating the PERK/Nrf2/MRP1 axis. MRP1 is a protein belonging to membrane transporters. Its activity is inversely proportional to the concentration of

doxorubicin in the cell. The induction of MRP1 protein expression by PERK kinase under ER stress conditions was associated with a lower concentration of the chemotherapeutic agent in the cell and hence resistance to treatment [95].

Activation of the UPR pathway in response to ER stress involves targeting the cell both to the apoptosis pathway and to enable its survival. The pathways leading to cell survival allow clones to resist both treatment [84] and those more susceptible depending on the type of chemotherapy and tumor phenotype used [96].

The research conducted by Wielenga et al. [96] in colorectal cancer cells showed that the induction of tumor cell differentiation before stress ER leads to the formation of clones that are more susceptible to chemotherapy [96]. Cell lines taken from patients with colorectal cancer were exposed to an ER stress inducer (subtilase cytotoxin AB, SubAB). The results were as follows: *in vitro* activation of the UPR pathway led to the differentiation of tumor cells whose colonies had increased sensitivity to chemotherapy in the form of oxaliplatin. *In vivo*, supportive treatment in the form of SubAB was shown to improve the tumor response to oxaliplatin, but the experiment did not prove in this model that this was directly due to the changes in the phenotype of the derived cells.

The induction of ER stress with various substances, moderating the course, blocking the branches of the UPR pathway is currently used in *in vitro* and *in vivo* models to assess their impact on growth and progression of CRC. Treatment trials are divided into two streams of ER stress use. One of them induces it with compounds that activate the proapoptotic pathway. The other uses the assumption that CRC stem cells, thanks to the PERK/eIF2 α pathway, differentiate into more aggressive phenotypes and the fact that the primary role of the UPR pathway is to restore homeostasis in the cell and allow it to survive under stress conditions through its other branches.

Yang et al. [97] using levistolide A induced the formation of free radicals that caused ER stress [97]. The wild type and p53 $^{-/-}$ CRC colonies treated with this compound were reduced, since the cells were subject to apoptosis. Administration of N-acetylcysteine, which blocked the action of levistolide A, had an effect in the reduction of tumor mass.

The effect of tolfenamic acid, which belongs to the NSAIDs group, was also investigated on the development of CRC [98]. Tolfenamic acid promotes ER stress, resulting in the activation of the unfolded UPR signaling pathway, of which PERK-mediated phosphorylation of eukaryotic translation initiation factor 2 α (eIF2 α) induces the repression of cyclin D1 translation. In mice with FAP syndrome, the apoptosis in CRC cells was induced through the branch associated with ATF4. It also correlated positively with the decrease in the concentration of cyclin D1 and the activity of Rb oncogene. The result of this study may suggest a likely mechanism of beneficial effects of NSAIDs on the risk of CRC.

Other study confirms the positive effect on CRC tumor regression, due to the activation of the branches associated with CHOP, Bax, and caspase 3 in andrographolide therapies [99]. This compound increases the production of free

TABLE 2: UPR-modulating factors inducing ER stress activity in cancer cells.

Agents	Mechanism	Cancer type/cell lines	References
GSK2606414 and GSK2656157	p-PERK↓, p-eIF2α↓	Multiple myeloma	[88, 89]
STF-083010	Ire1 inhibitor	Multiple myeloma	[91]
Sorafenib tyrosine kinase inhibitor (TKI)	CHOP↑ GADD34↑; p-PERK↑; p-eIF2α↑	L-428, L-1236, and KM-H2 cells	[92]
Sal003, inhibitor of phospho-eif2α phosphatase	ATF4; p-eIF2α↑	Glioblastoma cells	[25]
Diindolylmethane derivatives	CHOP↑; DR5↑	Pancreatic cancer cells	[93]
Bortezomib proteasome inhibitor	GRP78↑, CHOP↑, JNK↑, p-eIF2α↓	L3.6pl pancreatic cancer cells	[94]
Levistolide A	ROS↑; CHOP↑	Colorectal cancer cells	[97]
Andrographolide	ROS↑; CHOP↑	Colorectal cancer cells	[99]
Tolfenamic acid	eIF2α↑; ATF4↑	Colorectal cancer cells	[98]
Cantharidin	GRP78/BiP ↑, IRE1α ↑, IRE1β ↑, ATF6α ↑, XBP1 ↑	H460	[100]
Carnosic acid	ROS↑; CHOP↑; ATF4↑	Renal carcinoma Caki cells	[101]
Casticin	CHOP ↑, p-eIF2α ↑, eIF2α ↑, GRP78/BiP ↑	BGC-823	[102]
Cryptotanshinone	p-eIF2α ↑, GRP94 ↑, GRP78 ↑, CHOP ↑, ROS↑	MCF7	[103]
Curcumin	CHOP ↑, GRP78/BiP ↑, ROS ↑	NCI-H460, HT-29, AGS	[104, 105]
Flavokawain B	CHOP ↑, ATF4 ↑	HCT116	[106]
Fucoidan	CHOP ↑, ATF4 ↑, p-eIF2α ↑, GRP78/BiP ↓, p-IRE1 ↓, XBP1 ↓	MDA-MB-231 HCT116	[107]
Furanodiene	CHOP ↑, BIP ↑	A549, 95-D	[108]
2-3,4 Dihydroxyphenylethanol	IRE1 ↑, XBP1 ↑, GRP78/BiP ↑, PERK ↑, eIF2α ↑, CHOP ↑	HT-29	[109]
7-Dimethoxyflavone	CHOP ↑, GPR78/BiP ↑, ATF4 ↑	Hep3B	[110]
SMIP004 (N-(4-butyl-2-methyl-phenyl)acetamide)	ROS↑ IRE1↑; p-38↑; p-eIF2α↑	Prostate cancer cells	[111]
Licochalcone A	ATF6 ↑, eIF2α ↑, IRE1α ↑, CHOP ↑, GRP94 ↑, XBP1 ↑, GRP78/BiP ↑	HepG2	[112]
Neferine	GRP78/BiP ↑	Hep3B	[113]
Paeonol	GRP78 ↑, CHOP ↑	HepG2	[114]
Pardaxin	ROS↑; p-PERK↑; p-eIF2α↑	HeLa cells	[115]
Parthenolide	ATF4 ↑, p-eIF2α ↑, eIF2α ↑	A549, Calu-1, H1299, H1792	[116]
Piperine	IRE1α ↑, CHOP ↑, GPR78/BiP ↑	HT-29	[117]
Polyphenon E	ATF4 ↑, PERK ↑, p-eIF2α ↑, eIF2α ↑, GRP78/BiP ↑, CHOP ↑, XBP1 ↑, ROS ↑	PC3, PNT1a	[118]
Polyphyllin D	CHOP ↑, GRP78/BiP ↑, PDI ↑	NCI-H460	[119]
Resveratrol	GRP78/BiP ↑, CHOP ↑, XBP1 ↑, eIF2α ↑	HT29	[120]
Dehydrocostuslactone	p-PERK ↑, GRP78/BiP ↑, IRE1 ↑, CHOP ↑, XBP-1 ↑, ROS ↑	NCI-H460 A549	[121]
γ-Tocotrienol	CHOP ↑, GRP78/BiP ↑, XBP1 ↑	MDA-MB-231; MCF-7	[122]
Ω-Hydroxyundec-9-enoic Acid (ω-HUA)	ROS↑; CHOP↑	Lung cancer cells (H1299, A549, HCC827)	[123]
Ampelopsin	ROS↑ GRP78↑; p-PERK↑; p-eIF2α↑	Breast cancer cells (MCF-7; MDA-MB-231)	[124]
Ardisianone	GRP78/BiP ↑	PC3	[125]
Genistein	CHOP ↑, GRP78/BiP ↑	Hep3B	[126]
Guttiferone H	ATF4 ↑, XBP1 ↑, CHOP ↑	HCT116	[127]
Guggulsterone	ROS↑; p-eIF2α↑; CHOP↑ DR5↑	Liver cancer cells (Hep3B; HepG2)	[128]

TABLE 2: Continued.

Agents	Mechanism	Cancer type/cell lines	References
Marchantin M	GRP78/BiP, CHOP ↑, XBP1 ↑, p-eIF2α ↑, eIF2α ↑, ATF4 ↑, ATF6 ↑, ERAD ↓	PC3, DU145, LNCaP	[129]
Sarsasapogenin	ROS↑; CHOP↑	HeLa cells	[130]
Saxifragifolin	IRE1α ↑, XBP1 ↑, CHOP ↑, GRP78/BiP ↑, ROS↑	MDA-MB-231, MCF7	[131]
Prodigiosin	ROS↑; CHOP↑; p-eIF2α↑; PERK↑; GRP78↑; ATF6α↑, IRE1 ↑, eIF2a ↑	Pancreatic (8898); breast cancer cells (MCF-7 and MDA-MB-231)	[132, 133]
Quercetin	GRP78/BiP ↑, ATF4 ↑, IRE1α ↑ ATF6 ↑	PC3	[134]
Honokiol (HNK)	ROS↑ p-eIF2α↑; GRP78↑ CHOP↑	Chondrosarcoma (JJ012 and SW1353); gastric (AGS, SCM-1 and MKN-45) cancer cells	[135–139]
Brefeldin A (BFA)	ROS↑, IRE1α ↑, PERK ↑, XBP1↑; GRP78↑ CHOP↑	Ovarian (OVCAR-3); lung (A549); colorectal (colo 205); breast (MDA-MB-231) cancer cells	[140–142]
A-tocopheryl succinate	SGC-7901	GRP78/BiP ↑, CHOP ↑	[143]
Verrucarin A	GRP78/BiP ↑, p-PERK ↑, p-eIF2α ↑, CHOP ↑	Hep3B, HepG2	[144]
Vitamin E succinate	GRP78/BiP ↑, GRP94 ↓, PERK ↑, ATF4 ↑, ATF6 ↑, XBP1 ↑, CHOP ↑	SGC-7901	[145]
Ultrafine	p-eIF2α ↑, GRP78/BiP ↑	SNU-484	[146]
Zerumbone	ATF4 ↑, CHOP ↑, GRP78/BiP ↑, p-PERK ↑, PERK ↑ eIF2α ↑, p-eIF2α ↑	HCT116-p53null, SW480, PC3	[68, 147]

radicals and induces ER stress, which leads cells to the path of apoptosis. In addition, decreased concentrations of cyclins have also been demonstrated, which in turn inhibits the progression of the cell cycle.

Studies are not limited to the UPR modulators mentioned above. Since it is a very promising target for novel anticancer therapy, more and more new molecules are being tested. A significant amount of them are naturally occurring chemicals that are present also in plants. Due to the abundance of the compounds affecting UPR in Table 2, we have summarized the literature review on tested modulators in various cancer cell lines.

6. Conclusion

Stress of the endoplasmic reticulum is a process commonly occurring under the influence of various factors (free radicals, unfolded or misfolded proteins). The UPR pathway is the physiological response of the cell to the stress conditions affecting the cell. ER stress response has been highlighted as a key factor (next to the mutations) occurring at various stages of the disease progression and the individual response to the treatment. Cancers are a very heterogeneous group in which the UPR pathway can lead to adaptation to stress conditions (e.g., hypoxia in rapidly growing tumors), apoptosis (strengthening the immune response in colorectal cancer cells or induction of apoptosis in B-CLL cells). At the same time, depending on the circumstances and cell's condition, it can lead to resistance to treatment and production of clones less sensitive to chemotherapy. UPR activation is a vital step for oncogenic transformation, as UPR signaling molecules interact with well-established oncogene and tumor

suppressor gene networks to modulate their function during cancer development.

UPR modulators are a promising hope for a personalized therapy for patients in whom chemotherapy or radiotherapy have failed. It can become an innovative way to fight several different types of cancer. The response to a given compound depends on the phenotype of tumor cells, the severity of the disease, and the chemotherapy used so far.

It is emphasized that further experiments and analyses should be carried out using a variety of compounds that have the ability to inhibit and induce the UPR pathway in different types of cancers. It could also be useful in the treatment of noncancerous diseases.

Conflicts of Interest

The authors declare no conflict of interests.

Acknowledgments

This work was supported by the National Science Centre (grant number 2016/23/B/NZ5/02630) and the grant of the Medical University of Lodz for Young Researchers (grant number 502-03/5-108-05/502-54-194).

References

- [1] S. C. Dolfi, L. L.-Y. Chan, J. Qiu et al., "The metabolic demands of cancer cells are coupled to their size and protein synthesis rates," *Cancer & metabolism*, vol. 1, no. 1, pp. 20–20, 2013.
- [2] I. Braakman and D. N. Hebert, "Protein folding in the endoplasmic reticulum," *Cold Spring Harbor Perspectives in Biology*, vol. 5, no. 5, article a013201, 2013.

- [3] J. L. Brodsky and W. R. Skach, "Protein folding and quality control in the endoplasmic reticulum: recent lessons from yeast and mammalian cell systems," *Current Opinion in Cell Biology*, vol. 23, no. 4, pp. 464–475, 2011.
- [4] J. H. Van Drie, "Protein folding, protein homeostasis, and cancer," *Chinese Journal of Cancer*, vol. 30, no. 2, pp. 124–137, 2011.
- [5] C. M. Osowski and F. Urano, "Measuring ER stress and the unfolded protein response using mammalian tissue culture system," *Methods in enzymology*, vol. 490, pp. 71–92, 2011.
- [6] W. Cui, J. Li, D. Ron, and B. Sha, "The structure of the PERK kinase domain suggests the mechanism for its activation," *Acta Crystallographica Section D Biological Crystallography*, vol. 67, no. 5, pp. 423–428, 2011.
- [7] L. Guo, Y. Chi, J. Xue, L. Ma, Z. Shao, and J. Wu, "Phosphorylated eIF2 α predicts disease-free survival in triple-negative breast cancer patients," *Scientific Reports*, vol. 7, no. 1, article 44674, 2017, <https://www.nature.com/articles/srep44674#supplementary-information>.
- [8] E. Bobrovnikova-Marjon, C. Grigoriadou, D. Pytel et al., "PERK promotes cancer cell proliferation and tumor growth by limiting oxidative DNA damage," *Oncogene*, vol. 29, no. 27, pp. 3881–3895, 2010.
- [9] J. Han, S. H. Back, J. Hur et al., "ER-stress-induced transcriptional regulation increases protein synthesis leading to cell death," *Nature Cell Biology*, vol. 15, no. 5, pp. 481–490, 2013.
- [10] S. Oyadomari and M. Mori, "Roles of CHOP/GADD153 in endoplasmic reticulum stress," *Cell Death & Differentiation*, vol. 11, no. 4, pp. 381–389, 2004.
- [11] S. J. Marciniak, C. Y. Yun, S. Oyadomari et al., "CHOP induces death by promoting protein synthesis and oxidation in the stressed endoplasmic reticulum," *Genes & Development*, vol. 18, no. 24, pp. 3066–3077, 2004.
- [12] Y. P. Vandewynckel, D. Laukens, A. Geerts et al., "The paradox of the unfolded protein response in cancer," *Anticancer Research*, vol. 33, no. 11, pp. 4683–4694, 2013.
- [13] Y. Lu, F.-X. Liang, and X. Wang, "A synthetic biology approach identifies the mammalian UPR RNA ligase Rtc B," *Molecular Cell*, vol. 55, no. 5, pp. 758–770, 2014.
- [14] P. Walter and D. Ron, "The unfolded protein response: from stress pathway to homeostatic regulation," *Science*, vol. 334, no. 6059, pp. 1081–1086, 2011.
- [15] M. Maurel, E. Chevet, J. Tavernier, and S. Gerlo, "Getting RIDD of RNA: IRE1 in cell fate regulation," *Trends in Biochemical Sciences*, vol. 39, no. 5, pp. 245–254, 2014.
- [16] K. Yamamoto, T. Sato, T. Matsui et al., "Transcriptional induction of mammalian ER quality control proteins is mediated by single or combined action of ATF6 α and XBP1," *Developmental Cell*, vol. 13, no. 3, pp. 365–376, 2007.
- [17] D. Ron and P. Walter, "Signal integration in the endoplasmic reticulum unfolded protein response," *Nature Reviews Molecular Cell Biology*, vol. 8, no. 7, pp. 519–529, 2007.
- [18] D. Y. Dadey, V. Kapoor, A. Khudanyan et al., "The ATF6 pathway of the ER stress response contributes to enhanced viability in glioblastoma," *Oncotarget*, vol. 7, no. 2, pp. 2080–2092, 2016.
- [19] K. M. A. Rouschop, T. van den Beucken, L. Dubois et al., "The unfolded protein response protects human tumor cells during hypoxia through regulation of the autophagy genes *MAP1LC3B* and *ATG5*," *The Journal of Clinical Investigation*, vol. 120, no. 1, pp. 127–141, 2010.
- [20] A. Karpinska and G. Gromadzka, "Oxidative stress and natural antioxidant mechanisms: the role in neurodegeneration. From molecular mechanisms to therapeutic strategies," *Postepy Hig Med Dosw*, vol. 67, pp. 43–53, 2013.
- [21] S. Z. Hasnain, J. B. Prins, and M. A. McGuckin, "Oxidative and endoplasmic reticulum stress in beta-cell dysfunction in diabetes," *Journal of Molecular Endocrinology*, vol. 56, no. 2, pp. R33–R54, 2016.
- [22] T. Hayashi, A. Saito, S. Okuno, M. Ferrand-Drake, R. L. Dodd, and P. H. Chan, "Damage to the endoplasmic reticulum and activation of apoptotic machinery by oxidative stress in ischemic neurons," *Journal of Cerebral Blood Flow & Metabolism*, vol. 25, no. 1, pp. 41–53, 2005.
- [23] A. D. Garg, A. Kaczmarek, O. Krysko, P. Vandenabeele, D. V. Krysko, and P. Agostinis, "ER stress-induced inflammation: does it aid or impede disease progression?," *Trends in Molecular Medicine*, vol. 18, no. 10, pp. 589–598, 2012.
- [24] F. Allagnat, F. Christulia, F. Ortis et al., "Sustained production of spliced X-box binding protein 1 (XBP1) induces pancreatic beta cell dysfunction and apoptosis," *Diabetologia*, vol. 53, no. 6, pp. 1120–1130, 2010.
- [25] D. Y. A. Dadey, V. Kapoor, A. Khudanyan, D. Thotala, and D. E. Hallahan, "PERK regulates glioblastoma sensitivity to ER stress although promoting radiation resistance," *Molecular Cancer Research*, vol. 16, no. 10, pp. 1447–1453, 2018.
- [26] K. W. Kim, L. Moretti, L. R. Mitchell, D. K. Jung, and B. Lu, "Endoplasmic reticulum stress mediates radiation-induced autophagy by perk-eIF2 α in caspase-3/7-deficient cells," *Oncogene*, vol. 29, no. 22, pp. 3241–3251, 2010.
- [27] N. Dejeans, K. Barroso, M. E. Fernandez-Zapico, A. Samali, and E. Chevet, "Novel roles of the unfolded protein response in the control of tumor development and aggressiveness," *Seminars in Cancer Biology*, vol. 33, pp. 67–73, 2015.
- [28] R. C. Wek, H. Y. Jiang, and T. G. Anthony, "Coping with stress: eIF2 kinases and translational control," *Biochemical Society Transactions*, vol. 34, no. 1, pp. 7–11, 2006.
- [29] X. Yu and Y. C. Long, "Crosstalk between cystine and glutathione is critical for the regulation of amino acid signaling pathways and ferroptosis," *Scientific Reports*, vol. 6, no. 1, article 30033, 2016.
- [30] H. P. Harding, Y. Zhang, H. Zeng et al., "An integrated stress response regulates amino acid metabolism and resistance to oxidative stress," *Molecular Cell*, vol. 11, no. 3, pp. 619–633, 2003.
- [31] J. Ye, M. Kumanova, L. S. Hart et al., "The GCN2-ATF4 pathway is critical for tumour cell survival and proliferation in response to nutrient deprivation," *The EMBO Journal*, vol. 29, no. 12, pp. 2082–2096, 2010.
- [32] Y. Wang, Y. Ning, G. N. Alam et al., "Amino acid deprivation promotes tumor angiogenesis through the GCN2/ATF4 pathway," *Neoplasia*, vol. 15, no. 8, pp. 989–997, 2013.
- [33] T. Amann and C. Hellerbrand, "GLUT1 as a therapeutic target in hepatocellular carcinoma," *Expert Opinion on Therapeutic Targets*, vol. 13, no. 12, pp. 1411–1427, 2009.
- [34] C. B. Ryder, K. McColl, and C. W. Distelhorst, "Acidosis blocks CCAAT/enhancer-binding protein homologous protein (CHOP)- and c-Jun-mediated induction of p53-upregulated mediator of apoptosis (PUMA) during amino acid starvation," *Biochemical and Biophysical Research Communications*, vol. 430, no. 4, pp. 1283–1288, 2013.

- [35] R. P. Shiu, J. Pouyssegur, and I. Pastan, "Glucose depletion accounts for the induction of two transformation-sensitive membrane proteins in Rous sarcoma virus-transformed chick embryo fibroblasts," *Proceedings of the National Academy of Sciences of the United States of America*, vol. 74, no. 9, pp. 3840–3844, 1977.
- [36] M. T. Spiotto, A. Banh, I. Papandreou et al., "Imaging the unfolded protein response in primary tumors reveals microenvironments with metabolic variations that predict tumor growth," *Cancer Research*, vol. 70, no. 1, pp. 78–88, 2010.
- [37] N. Blazanin, J. Son, A. B. Craig-Lucas et al., "ER stress and distinct outputs of the IRE1 α RNase control proliferation and senescence in response to oncogenic Ras," *Proceedings of the National Academy of Sciences of the United States of America*, vol. 114, no. 37, pp. 9900–9905, 2017.
- [38] C. Denoyelle, G. Abou-Rjaily, V. Bezroukove et al., "Anti-oncogenic role of the endoplasmic reticulum differentially activated by mutations in the MAPK pathway," *Nature Cell Biology*, vol. 8, no. 10, pp. 1053–1063, 2006.
- [39] M. Horiguchi, S. Koyanagi, A. Okamoto, S. O. Suzuki, N. Matsunaga, and S. Ohdo, "Stress-regulated transcription factor ATF4 promotes neoplastic transformation by suppressing expression of the INK4a/ARF cell senescence factors," *Cancer Research*, vol. 72, no. 2, pp. 395–401, 2012.
- [40] M. Bi, C. Naczki, M. Koritzinsky et al., "ER stress-regulated translation increases tolerance to extreme hypoxia and promotes tumor growth," *The EMBO Journal*, vol. 24, no. 19, pp. 3470–3481, 2005.
- [41] T. De Raedt, Z. Walton, J. L. Yecies et al., "Exploiting cancer cell vulnerabilities to develop a combination therapy for ras-driven tumors," *Cancer Cell*, vol. 20, no. 3, pp. 400–413, 2011.
- [42] H. Davies, G. R. Bignell, C. Cox et al., "Mutations of the *BRAF* gene in human cancer," *Nature*, vol. 417, no. 6892, pp. 949–954, 2002.
- [43] M. Corazzari, F. Rapino, F. Ciccocanti et al., "Oncogenic *BRAF* induces chronic ER stress condition resulting in increased basal autophagy and apoptotic resistance of cutaneous melanoma," *Cell Death and Differentiation*, vol. 22, no. 6, pp. 946–958, 2015.
- [44] A. Croft, K. H. Tay, S. C. Boyd et al., "Oncogenic activation of MEK/ERK primes melanoma cells for adaptation to endoplasmic reticulum stress," *The Journal of Investigative Dermatology*, vol. 134, no. 2, pp. 488–497, 2014.
- [45] X. H. Ma, S. F. Piao, S. Dey et al., "Targeting ER stress-induced autophagy overcomes *BRAF* inhibitor resistance in melanoma," *The Journal of Clinical Investigation*, vol. 124, no. 3, pp. 1406–1417, 2014.
- [46] H. Chen, H. Liu, and G. Qing, "Targeting oncogenic *Myc* as a strategy for cancer treatment," *Signal Transduction and Targeted Therapy*, vol. 3, no. 1, p. 5, 2018.
- [47] L. S. Hart, J. T. Cunningham, T. Datta et al., "ER stress-mediated autophagy promotes *Myc*-dependent transformation and tumor growth," *The Journal of clinical investigation*, vol. 122, no. 12, pp. 4621–4634, 2012.
- [48] S. Dey, F. Tameire, and C. Koumenis, "PERK-ing up autophagy during *MYC*-induced tumorigenesis," *Autophagy*, vol. 9, no. 4, pp. 612–614, 2013.
- [49] P. Nagy, A. Varga, K. Piracs, K. Hegedus, and G. Juhasz, "Myc-driven overgrowth requires unfolded protein response-mediated induction of autophagy and antioxidant responses in *Drosophila melanogaster*," *PLoS Genetics*, vol. 9, no. 8, article e1003664, 2013.
- [50] Y. Ma and L. M. Hendershot, "The role of the unfolded protein response in tumour development: friend or foe?," *Nature Reviews Cancer*, vol. 4, no. 12, pp. 966–977, 2004.
- [51] F. Y. Al-Rawashdeh, P. Scriven, I. C. Cameron, P. V. Vergani, and L. Wyld, "Unfolded protein response activation contributes to chemoresistance in hepatocellular carcinoma," *European Journal of Gastroenterology & Hepatology*, vol. 22, no. 9, pp. 1099–1105, 2010.
- [52] L. M. Epple, R. D. Dodd, A. L. Merz et al., "Induction of the unfolded protein response drives enhanced metabolism and chemoresistance in glioma cells," *PLoS One*, vol. 8, no. 8, article e73267, 2013.
- [53] W. Fu, X. Wu, J. Li et al., "Upregulation of GRP78 in renal cell carcinoma and its significance," *Urology*, vol. 75, no. 3, pp. 603–607, 2010.
- [54] T. Fujimoto, K. Yoshimatsu, K. Watanabe et al., "Overexpression of human X-box binding protein 1 (XBP-1) in colorectal adenomas and adenocarcinomas," *Anticancer Research*, vol. 27, no. 1a, pp. 127–131, 2007.
- [55] G. Genovese, A. Carugo, J. Tepper et al., "Synthetic vulnerabilities of mesenchymal subpopulations in pancreatic cancer," *Nature*, vol. 542, no. 7641, pp. 362–366, 2017.
- [56] B. Kong, W. Wu, N. Valkovska et al., "A common genetic variation of melanoma inhibitory activity-2 labels a subtype of pancreatic adenocarcinoma with high endoplasmic reticulum stress levels," *Scientific Reports*, vol. 5, no. 1, article 8109, 2015, <https://www.nature.com/articles/srep08109#supplementary-information>.
- [57] E. Lee, P. Nichols, D. Spicer, S. Groshen, M. C. Yu, and A. S. Lee, "GRP78 as a novel predictor of responsiveness to chemotherapy in breast cancer," *Cancer Research*, vol. 66, no. 16, pp. 7849–7853, 2006.
- [58] H. Y. Tsai, Y. F. Yang, A. T. Wu et al., "Endoplasmic reticulum ribosome-binding protein 1 (RRBP1) overexpression is frequently found in lung cancer patients and alleviates intracellular stress-induced apoptosis through the enhancement of GRP78," *Oncogene*, vol. 32, no. 41, pp. 4921–4931, 2013.
- [59] C. Rubio-Patino, J. P. Bossowski, G. M. De Donatis et al., "Low-protein diet induces IRE1 α -dependent anticancer immunosurveillance," *Cell Metabolism*, vol. 27, no. 4, pp. 828–842.e7, 2018.
- [60] M. P. Davies, D. L. Barraclough, C. Stewart et al., "Expression and splicing of the unfolded protein response gene XBP-1 are significantly associated with clinical outcome of endocrine-treated breast cancer," *International Journal of Cancer*, vol. 123, no. 1, pp. 85–88, 2008.
- [61] E. Rosati, R. Sabatini, G. Rampino et al., "Novel targets for endoplasmic reticulum stress-induced apoptosis in B-CLL," *Blood*, vol. 116, no. 15, pp. 2713–2723, 2010.
- [62] K. Zhu, H. Jiao, S. Li et al., "ATF4 promotes bone angiogenesis by increasing VEGF expression and release in the bone environment," *Journal of bone and mineral research*, vol. 28, no. 9, pp. 1870–1884, 2013.
- [63] Y. Wang, G. N. Alam, Y. Ning et al., "The unfolded protein response induces the angiogenic switch in human tumor cells through the PERK/ATF4 pathway," *Cancer Research*, vol. 72, no. 20, pp. 5396–5406, 2012.
- [64] P. Hersey and X. D. Zhang, "Adaptation to ER stress as a driver of malignancy and resistance to therapy in human

- melanoma," *Pigment Cell & Melanoma Research*, vol. 21, no. 3, pp. 358–367, 2008.
- [65] J. D. Blais, C. L. Addison, R. Edge et al., "Perk-dependent translational regulation promotes tumor cell adaptation and angiogenesis in response to hypoxic stress," *Molecular and Cellular Biology*, vol. 26, no. 24, pp. 9517–9532, 2006.
- [66] N. Iwasaki, Y. Sugiyama, S. Miyazaki, H. Nakagawa, K. Nishimura, and S. Matsuo, "An ATF4-signal-modulating machine other than GADD34 acts in ATF4-to-CHOP signaling to block CHOP expression in ER-stress-related autophagy," *Journal of Cellular Biochemistry*, vol. 116, no. 7, pp. 1300–1309, 2015.
- [67] A. C. Koong, V. K. Mehta, Q. T. Le et al., "Pancreatic tumors show high levels of hypoxia," *International Journal of Radiation Oncology Biology Physics*, vol. 48, no. 4, pp. 919–922, 2000.
- [68] M. Edagawa, J. Kawauchi, M. Hirata et al., "Role of activating transcription factor 3 (ATF3) in endoplasmic reticulum (ER) stress-induced sensitization of p53-deficient human colon cancer cells to tumor necrosis factor (TNF)-related apoptosis-inducing ligand (TRAIL)-mediated apoptosis through up-regulation of death receptor 5 (DR5) by zerbivone and celecoxib," *Journal of Biological Chemistry*, vol. 289, no. 31, pp. 21544–21561, 2014.
- [69] H. Y. Su, R. T. Waldron, R. Gong, V. K. Ramanujan, S. J. Pandol, and A. Lugea, "The unfolded protein response plays a predominant homeostatic role in response to mitochondrial stress in pancreatic stellate cells," *PLoS One*, vol. 11, no. 2, article e0148999, 2016.
- [70] L. Dumartin, W. Alrawashdeh, S. M. Trabulo et al., "ER stress protein AGR2 precedes and is involved in the regulation of pancreatic cancer initiation," *Oncogene*, vol. 36, no. 22, pp. 3094–3103, 2017.
- [71] J. Liu, M. Xiao, J. Li et al., "Activation of UPR signaling pathway is associated with the malignant progression and poor prognosis in prostate cancer," *Prostate*, vol. 77, no. 3, pp. 274–281, 2017.
- [72] L. Niederreiter, T. M. Fritz, T. E. Adolph et al., "ER stress transcription factor Xbp1 suppresses intestinal tumorigenesis and directs intestinal stem cells," *The Journal of Experimental Medicine*, vol. 210, no. 10, pp. 2041–2056, 2013.
- [73] L. Vermeulen and H. J. Snippert, "Stem cell dynamics in homeostasis and cancer of the intestine," *Nature Reviews Cancer*, vol. 14, no. 7, pp. 468–480, 2014.
- [74] X. Chen, D. Iliopoulos, Q. Zhang et al., "XBP1 promotes triple-negative breast cancer by controlling the HIF1 α pathway," *Nature*, vol. 508, no. 7494, pp. 103–107, 2014.
- [75] N. Dejeans, O. Pluquet, S. Lhomond et al., "Autocrine control of glioma cells adhesion and migration through IRE1 α -mediated cleavage of SPARC mRNA," *Journal of Cell Science*, vol. 125, no. 18, pp. 4278–4287, 2012.
- [76] Y. X. Feng, E. S. Sokol, C. A. Del Vecchio et al., "Epithelial-to-mesenchymal transition activates PERK-eIF2 α and sensitizes cells to endoplasmic reticulum stress," *Cancer Discovery*, vol. 4, no. 6, pp. 702–715, 2014.
- [77] N. Sheshadri, J. M. Catanzaro, A. J. Bott et al., "SCCA1/SERPINB3 promotes oncogenesis and epithelial-mesenchymal transition via the unfolded protein response and IL6 signaling," *Cancer Research*, vol. 74, no. 21, pp. 6318–6329, 2014.
- [78] L. Ulianich, C. Garbi, A. S. Treglia et al., "Retraction: ER stress is associated with dedifferentiation and an epithelial-to-mesenchymal transition-like phenotype in PC Cl3 thyroid cells," *Journal of Cell Science*, vol. 129, no. 18, p. 3518, 2016.
- [79] B. Drogat, P. Auguste, D. T. Nguyen et al., "IRE1 signaling is essential for ischemia-induced vascular endothelial growth factor-A expression and contributes to angiogenesis and tumor growth *in vivo*," *Cancer Research*, vol. 67, no. 14, pp. 6700–6707, 2007.
- [80] T. Miyagi, O. Hori, K. Koshida et al., "Antitumor effect of reduction of 150-kDa oxygen-regulated protein expression on human prostate cancer cells," *International Journal of Urology*, vol. 9, no. 10, pp. 577–585, 2002.
- [81] K. Ozawa, Y. Tsukamoto, O. Hori et al., "Regulation of tumor angiogenesis by oxygen-regulated protein 150, an inducible endoplasmic reticulum chaperone," *Cancer Research*, vol. 61, no. 10, pp. 4206–4213, 2001.
- [82] O. Pluquet, N. Dejeans, M. Boucheccareilh et al., "Posttranscriptional regulation of *PER1* underlies the oncogenic function of IRE α ," *Cancer Research*, vol. 73, no. 15, pp. 4732–4743, 2013.
- [83] C. M. Ferrer, T. P. Lynch, V. L. Sodi et al., "O-GlcNAcylation regulates cancer metabolism and survival stress signaling via regulation of the HIF-1 pathway," *Molecular Cell*, vol. 54, no. 5, pp. 820–831, 2014.
- [84] T. Avril, E. Vauléon, and E. Chevet, "Endoplasmic reticulum stress signaling and chemotherapy resistance in solid cancers," *Oncogene*, vol. 6, no. 8, article e373, 2017.
- [85] M. J. Wu, C. I. Jan, Y. G. Tsay et al., "Elimination of head and neck cancer initiating cells through targeting glucose regulated protein 78 signaling," *Molecular Cancer*, vol. 9, no. 1, p. 283, 2010.
- [86] D. Y. A. Dadey, V. Kapoor, K. Hoye et al., "Antibody targeting GRP78 enhances the efficacy of radiation therapy in human glioblastoma and non-small cell lung cancer cell lines and tumor models," *Clinical Cancer Research*, vol. 23, no. 10, pp. 2556–2564, 2017.
- [87] F. Ferrara, D. I. Staquicini, W. H. P. Driessen et al., "Targeted molecular-genetic imaging and ligand-directed therapy in aggressive variant prostate cancer," *Proceedings of the National Academy of Sciences of the United States of America*, vol. 113, no. 45, pp. 12786–12791, 2016.
- [88] C. Atkins, Q. Liu, E. Minthorn et al., "Characterization of a novel PERK kinase inhibitor with antitumor and antiangiogenic activity," *Cancer Research*, vol. 73, no. 6, pp. 1993–2002, 2013.
- [89] J. M. Axten, J. R. Medina, Y. Feng et al., "Discovery of 7-methyl-5-(1-([3-(trifluoromethyl)phenyl]acetyl)-2,3-dihydro-1H-indol-5-yl)-7H-pyrrolo[2,3-d]pyrimidin-4-amine (GSK2606414), a potent and selective first-in-class inhibitor of protein kinase R (PKR)-like endoplasmic reticulum kinase (PERK)," *Journal of Medicinal Chemistry*, vol. 55, no. 16, pp. 7193–7207, 2012.
- [90] C. Zhou, D. Di Marcantonio, E. Martinez et al., "C-Jun regulates ER stress signaling to promote chemotherapy resistance in acute myeloid leukemia," *Blood*, vol. 126, no. 23, article 2464, 2015.
- [91] I. Papandreou, N. C. Denko, M. Olson et al., "Identification of an Ire1 α endonuclease specific inhibitor with cytotoxic activity against human multiple myeloma," *Blood*, vol. 117, no. 4, pp. 1311–1314, 2011.

- [92] M. S. Holz, A. Janning, C. Renne, S. Gattenlohner, T. Spieker, and A. Brauning, "Induction of endoplasmic reticulum stress by sorafenib and activation of NF- κ B by lestaurtinib as a novel resistance mechanism in Hodgkin lymphoma cell lines," *Molecular Cancer Therapeutics*, vol. 12, no. 2, pp. 173–183, 2013.
- [93] M. Abdelrahim, K. Newman, K. Vanderlaag, I. Samudio, and S. Safe, "3, 3'-Diindolylmethane (DIM) and its derivatives induce apoptosis in pancreatic cancer cells through endoplasmic reticulum stress-dependent upregulation of DR5," *Carcinogenesis*, vol. 27, no. 4, pp. 717–728, 2006.
- [94] S. T. Nawrocki, J. S. Carew, K. Dunner Jr. et al., "Bortezomib inhibits PKR-like endoplasmic reticulum (ER) kinase and induces apoptosis via ER stress in human pancreatic cancer cells," *Cancer Research*, vol. 65, no. 24, pp. 11510–11519, 2005.
- [95] I. C. Salaroglio, E. Panada, E. Moiso et al., "PERK induces resistance to cell death elicited by endoplasmic reticulum stress and chemotherapy," *Molecular Cancer*, vol. 16, no. 1, p. 91, 2017.
- [96] M. C. B. Wielenga, S. Colak, J. Heijmans et al., "ER-stress-induced differentiation sensitizes colon cancer stem cells to chemotherapy," *Cell Reports*, vol. 13, no. 3, pp. 489–494, 2015.
- [97] Y. Yang, Y. Zhang, L. Wang, and S. Lee, "Levistolide A induces apoptosis via ROS-mediated ER stress pathway in colon cancer cells," *Cellular Physiology and Biochemistry*, vol. 42, no. 3, pp. 929–938, 2017.
- [98] X. Zhang, S.-H. Lee, K.-W. Min et al., "The involvement of endoplasmic reticulum stress in the suppression of colorectal tumorigenesis by tolfenamic acid," *Cancer Prevention Research*, vol. 6, no. 12, pp. 1337–1347, 2013.
- [99] A. Banerjee, V. Banerjee, S. Czinn, and T. Blanchard, "Increased reactive oxygen species levels cause ER stress and cytotoxicity in andrographolide treated colon cancer cells," *Oncotarget*, vol. 8, no. 16, pp. 26142–26153, 2017.
- [100] T. C. Hsia, C. C. Yu, S. C. Hsu et al., "Cantharidin induces apoptosis of H460 human lung cancer cells through mitochondria-dependent pathways," *International Journal of Oncology*, vol. 45, no. 1, pp. 245–254, 2014.
- [101] K.-J. Min, K.-J. Jung, and T. K. Kwon, "Carnosic acid induces apoptosis through reactive oxygen species-mediated endoplasmic reticulum stress induction in human renal carcinoma Caki cells," *Journal of cancer prevention*, vol. 19, no. 3, pp. 170–178, 2014.
- [102] Y. Zhou, L. Tian, L. Long, M. Quan, F. Liu, and J. Cao, "Casticin potentiates TRAIL-induced apoptosis of gastric cancer cells through endoplasmic reticulum stress," *PLoS One*, vol. 8, no. 3, article e58855, 2013.
- [103] I. J. Park, M. J. Kim, O. J. Park et al., "Cryptotanshinone induces ER stress-mediated apoptosis in HepG2 and MCF7 cells," *Apoptosis*, vol. 17, no. 3, pp. 248–257, 2012.
- [104] A. Cao, Q. Li, P. Yin et al., "Curcumin induces apoptosis in human gastric carcinoma AGS cells and colon carcinoma HT-29 cells through mitochondrial dysfunction and endoplasmic reticulum stress," *Apoptosis*, vol. 18, no. 11, pp. 1391–1402, 2013.
- [105] S. H. Wu, L. W. Hang, J. S. Yang et al., "Curcumin induces apoptosis in human non-small cell lung cancer NCI-H460 cells through ER stress and caspase cascade- and mitochondria-dependent pathways," *Anticancer Research*, vol. 30, no. 6, pp. 2125–2133, 2010.
- [106] Y. F. Kuo, Y. Z. Su, Y. H. Tseng, S. Y. Wang, H. M. Wang, and P. J. Chueh, "Flavokawain B, a novel chalcone from *Alpinia pricei* Hayata with potent apoptotic activity: involvement of ROS and GADD153 upstream of mitochondria-dependent apoptosis in HCT116 cells," *Free Radical Biology and Medicine*, vol. 49, no. 2, pp. 214–226, 2010.
- [107] S. Chen, Z. Yang, Z. Yu, and D. Zhang, "Fucoic acid induces cancer cell apoptosis by modulating the endoplasmic reticulum stress cascades," *PLoS One*, vol. 9, article e108157, no. 9, 2014.
- [108] W. S. Xu, Y. Y. Dang, J. J. Guo et al., "Furanodiene induces endoplasmic reticulum stress and presents antiproliferative activities in lung cancer cells," *Evidence-Based Complementary and Alternative Medicine*, vol. 2012, Article ID 426521, 8 pages, 2012.
- [109] C. Guichard, E. Pedruzzi, M. Fay et al., "Dihydroxyphenylethanol induces apoptosis by activating serine/threonine protein phosphatase PP2A and promotes the endoplasmic reticulum stress response in human colon carcinoma cells," *Carcinogenesis*, vol. 27, no. 9, pp. 1812–1827, 2006.
- [110] J. F. Yang, J. G. Cao, L. Tian, and F. Liu, "5, 7-Dimethoxyflavone sensitizes TRAIL-induced apoptosis through DR5 upregulation in hepatocellular carcinoma cells," *Cancer Chemotherapy and Pharmacology*, vol. 69, no. 1, pp. 195–206, 2012.
- [111] E. Rico-Bautista, W. Zhu, S. Kitada et al., "Small molecule-induced mitochondrial disruption directs prostate cancer inhibition via UPR signaling," *Oncotarget*, vol. 4, no. 8, pp. 1212–1229, 2013.
- [112] A. Y. Choi, J. H. Choi, K. Y. Hwang et al., "Licochalcone A induces apoptosis through endoplasmic reticulum stress via a phospholipase $\text{C}\gamma 1$ -, Ca^{2+} -, and reactive oxygen species-dependent pathway in HepG2 human hepatocellular carcinoma cells," *Apoptosis*, vol. 19, no. 4, pp. 682–697, 2014.
- [113] J. S. Yoon, H. M. Kim, A. K. Yadunandam et al., "Neferine isolated from *Nelumbo nucifera* enhances anti-cancer activities in Hep3B cells: molecular mechanisms of cell cycle arrest, ER stress induced apoptosis and anti-angiogenic response," *Phytomedicine*, vol. 20, no. 11, pp. 1013–1022, 2013.
- [114] L. Fan, B. Song, G. Sun, T. Ma, F. Zhong, and W. Wei, "Endoplasmic reticulum stress-induced resistance to doxorubicin is reversed by paeonol treatment in human hepatocellular carcinoma cells," *PLoS One*, vol. 8, no. 5, article e62627, 2013.
- [115] T. C. Huang and J. Y. Chen, "Proteomic analysis reveals that pardaxin triggers apoptotic signaling pathways in human cervical carcinoma HeLa cells: cross talk among the UPR, c-Jun and ROS," *Carcinogenesis*, vol. 34, no. 8, pp. 1833–1842, 2013.
- [116] X. Zhao, X. Liu, and S. Ling, "Parthenolide induces apoptosis via TNFRSF10B and PMAIP1 pathways in human lung cancer cells," *Journal of experimental & clinical cancer research*, vol. 33, no. 1, p. 3, 2014.
- [117] P. B. Yaffe, M. R. Power Coombs, C. D. Doucette, M. Walsh, and D. W. Hoskin, "Piperine, an alkaloid from black pepper, inhibits growth of human colon cancer cells via G1 arrest and apoptosis triggered by endoplasmic reticulum stress," *Molecular Carcinogenesis*, vol. 54, no. 10, pp. 1070–1085, 2015.
- [118] F. Rizzi, V. Naponelli, A. Silva et al., "Polyphenon E (R), a standardized green tea extract, induces endoplasmic reticulum stress, leading to death of immortalized PNT1a cells by anoikis and tumorigenic PC3 by necroptosis," *Carcinogenesis*, vol. 35, no. 4, pp. 828–839, 2014.

- [119] F. M. Siu, D. L. Ma, Y. W. Cheung et al., "Proteomic and transcriptomic study on the action of a cytotoxic saponin (polyphyllin D): induction of endoplasmic reticulum stress and mitochondria-mediated apoptotic pathways," *Proteomics*, vol. 8, no. 15, pp. 3105–3117, 2008.
- [120] J. W. Park, K. J. Woo, J. T. Lee et al., "Resveratrol induces pro-apoptotic endoplasmic reticulum stress in human colon cancer cells," *Oncology Reports*, vol. 18, no. 5, pp. 1269–1273, 2007.
- [121] J. Y. Hung, Y. L. Hsu, W. C. Ni et al., "Oxidative and endoplasmic reticulum stress signaling are involved in dehydrocostuslactone-mediated apoptosis in human non-small cell lung cancer cells," *Lung Cancer*, vol. 68, no. 3, pp. 355–365, 2010.
- [122] S. K. Park, B. G. Sanders, and K. Kline, "Tocotrienols induce apoptosis in breast cancer cell lines via an endoplasmic reticulum stress-dependent increase in extrinsic death receptor signaling," *Breast Cancer Research and Treatment*, vol. 124, no. 2, pp. 361–375, 2010.
- [123] K. M. Yang, B. M. Kim, and J. B. Park, " ω -Hydroxyundec-9-enoic acid induces apoptosis through ROS-mediated endoplasmic reticulum stress in non-small cell lung cancer cells," *Biochemical and Biophysical Research Communications*, vol. 448, no. 3, pp. 267–273, 2014.
- [124] Y. Zhou, F. Shu, X. Liang et al., "Ampelopsin induces cell growth inhibition and apoptosis in breast cancer cells through ROS generation and endoplasmic reticulum stress pathway," *PLoS One*, vol. 9, no. 2, article e89021, 2014.
- [125] C. C. Yu, P. J. Wu, J. L. Hsu et al., "Ardisianone, a natural benzoquinone, efficiently induces apoptosis in human hormone-refractory prostate cancers through mitochondrial damage stress and survivin downregulation," *Prostate*, vol. 73, no. 2, pp. 133–145, 2013.
- [126] T. C. Yeh, P. C. Chiang, T. K. Li et al., "Genistein induces apoptosis in human hepatocellular carcinomas via interaction of endoplasmic reticulum stress and mitochondrial insult," *Biochemical Pharmacology*, vol. 73, no. 6, pp. 782–792, 2007.
- [127] P. Protiva, M. E. Hopkins, S. Baggett et al., "Growth inhibition of colon cancer cells by polyisoprenylated benzophenones is associated with induction of the endoplasmic reticulum response," *International Journal of Cancer*, vol. 123, no. 3, pp. 687–694, 2008.
- [128] D. O. Moon, S. Y. Park, Y. H. Choi, J. S. Ahn, and G. Y. Kim, "Guggulsterone sensitizes hepatoma cells to TRAIL-induced apoptosis through the induction of CHOP-dependent DR5: involvement of ROS-dependent ER-stress," *Biochemical Pharmacology*, vol. 82, no. 11, pp. 1641–1650, 2011.
- [129] H. Jiang, J. Sun, Q. Xu et al., "Marchantin M: a novel inhibitor of proteasome induces autophagic cell death in prostate cancer cells," *Cell Death & Disease*, vol. 4, no. 8, article e761, 2013.
- [130] A. A. Farooqi, K.-T. Li, S. Fayyaz et al., "Anticancer drugs for the modulation of endoplasmic reticulum stress and oxidative stress," *Tumour biology*, vol. 36, no. 8, pp. 5743–5752, 2015.
- [131] J. M. Shi, L. L. Bai, D. M. Zhang et al., "Saxifragifolin D induces the interplay between apoptosis and autophagy in breast cancer cells through ROS-dependent endoplasmic reticulum stress," *Biochemical Pharmacology*, vol. 85, no. 7, pp. 913–926, 2013.
- [132] Y. Liu, H. Zhou, X. Ma et al., "Prodigiosin inhibits proliferation, migration, and invasion of nasopharyngeal cancer cells," *Cellular Physiology and Biochemistry*, vol. 48, no. 4, pp. 1556–1562, 2018.
- [133] M. Y. Pan, Y. C. Shen, C. H. Lu et al., "Prodigiosin activates endoplasmic reticulum stress cell death pathway in human breast carcinoma cell lines," *Toxicology and Applied Pharmacology*, vol. 265, no. 3, pp. 325–334, 2012.
- [134] K. C. Liu, C. Y. Yen, R. S. Wu et al., "The roles of endoplasmic reticulum stress and mitochondrial apoptotic signaling pathway in quercetin-mediated cell death of human prostate cancer PC-3 cells," *Environmental Toxicology*, vol. 29, no. 4, pp. 428–439, 2014.
- [135] Y. J. Chen, C. L. Wu, J. F. Liu et al., "Honokiol induces cell apoptosis in human chondrosarcoma cells through mitochondrial dysfunction and endoplasmic reticulum stress," *Cancer Letters*, vol. 291, no. 1, pp. 20–30, 2010.
- [136] E. R. Hahm, K. Sakao, and S. V. Singh, "Honokiol activates reactive oxygen species-mediated cytoprotective autophagy in human prostate cancer cells," *Prostate*, vol. 74, no. 12, pp. 1209–1221, 2014.
- [137] H. C. Pan, D. W. Lai, K. H. Lan et al., "Honokiol thwarts gastric tumor growth and peritoneal dissemination by inhibiting Tpl2 in an orthotopic model," *Carcinogenesis*, vol. 34, no. 11, pp. 2568–2579, 2013.
- [138] M. L. Sheu, S. H. Liu, and K. H. Lan, "Honokiol induces calpain-mediated glucose-regulated protein-94 cleavage and apoptosis in human gastric cancer cells and reduces tumor growth," *PLoS One*, vol. 2, no. 10, article e1096, 2007.
- [139] T. I. Weng, H. Y. Wu, B. L. Chen, and S. H. Liu, "Honokiol attenuates the severity of acute pancreatitis and associated lung injury via acceleration of acinar cell apoptosis," *Shock*, vol. 37, no. 5, pp. 478–484, 2012.
- [140] J. L. Moon, S. Y. Kim, S. W. Shin, and J. W. Park, "Regulation of brefeldin A-induced ER stress and apoptosis by mitochondrial NADP⁺-dependent isocitrate dehydrogenase," *Biochemical and Biophysical Research Communications*, vol. 417, no. 2, pp. 760–764, 2012.
- [141] C. N. Tseng, Y. R. Hong, H. W. Chang et al., "Brefeldin A reduces anchorage-independent survival, cancer stem cell potential and migration of MDA-MB-231 human breast cancer cells," *Molecules*, vol. 19, no. 11, pp. 17464–17477, 2014.
- [142] C. N. Tseng, C. F. Huang, C. L. Cho et al., "Brefeldin A effectively inhibits cancer stem cell-like properties and MMP-9 activity in human colorectal cancer Colo 205 cells," *Molecules*, vol. 18, no. 9, pp. 10242–10253, 2013.
- [143] X. Huang, L. Li, L. Zhang et al., "Crosstalk between endoplasmic reticulum stress and oxidative stress in apoptosis induced by α -tocopheryl succinate in human gastric carcinoma cells," *British Journal of Nutrition*, vol. 109, no. 4, pp. 727–735, 2013.
- [144] D. O. Moon, Y. Asami, H. Long et al., "Verrucaric acid sensitizes TRAIL-induced apoptosis via the upregulation of DR5 in an eIF2 α /CHOP-dependent manner," *Toxicology In Vitro*, vol. 27, no. 1, pp. 257–263, 2013.
- [145] X. Huang, Z. Zhang, L. Jia, Y. Zhao, X. Zhang, and K. Wu, "Endoplasmic reticulum stress contributes to vitamin E succinate-induced apoptosis in human gastric cancer SGC-7901 cells," *Cancer Letters*, vol. 296, no. 1, pp. 123–131, 2010.
- [146] J. Ahn, J. S. Lee, and K. M. Yang, "Ultrafine particles of *Ulmus davidiana* var. *japonica* induce apoptosis of gastric cancer cells via activation of caspase and endoplasmic reticulum

stress," *Archives of Pharmacal Research*, vol. 37, no. 6, pp. 783–792, 2014.

- [147] M. L. Chan, J. W. Liang, L. C. Hsu, W. L. Chang, S. S. Lee, and J. H. Guh, "Zerumbone, a ginger sesquiterpene, induces apoptosis and autophagy in human hormone-refractory prostate cancers through tubulin binding and crosstalk between endoplasmic reticulum stress and mitochondrial insult," *Naunyn-Schmiedeberg's Archives of Pharmacology*, vol. 388, no. 11, pp. 1223–1236, 2015.

Research Article

Excessive Oxidative Stress Contributes to Increased Acute ER Stress Kidney Injury in Aged Mice

Xiaoyan Liu ¹, Ruihua Zhang,¹ Lianghu Huang,² Zihan Zheng,¹ Helen Vlassara,³ Gary Striker,³ Xiaoyan Zhang,¹ Youfei Guan,¹ and Feng Zheng ¹

¹Department of Nephrology, The Second Hospital and Center for Renal Diseases, Advanced Institute for Medical Sciences, Dalian Medical University, Dalian, Liaoning 116044, China

²Department of Urology, Dongfang Hospital, Fujian Medical University, Fuzhou, Fujian 350009, China

³Department of Geriatrics, Mount Sinai School of Medicine, New York City, NY 10029, USA

Correspondence should be addressed to Feng Zheng; zhengfeng@dmu.edu.cn

Received 5 July 2018; Revised 30 September 2018; Accepted 13 November 2018; Published 28 January 2019

Guest Editor: Tomasz Poplawski

Copyright © 2019 Xiaoyan Liu et al. This is an open access article distributed under the Creative Commons Attribution License, which permits unrestricted use, distribution, and reproduction in any medium, provided the original work is properly cited.

The aged kidney is susceptible to acute injury due presumably to its decreased ability to handle additional challenges, such as endoplasmic reticulum (ER) stress. This was tested by giving tunicamycin, an ER stress inducer, to either old or young mice. Injection of high dose caused renal failure in old mice, not in young mice. Moreover, injection of low dose resulted in severe renal damage in old mice, confirming the increased susceptibility of aged kidney to ER stress. There existed an abnormality in ER stress response kinetics in aged kidney, characterized by a loss of XBP-1 splicing and decreased PERK-eIF2 α phosphorylation at late time point. The presence of excessive oxidative stress in aged kidney may play a role since high levels of oxidation increased ER stress-induced cell death and decreased IRE1 levels and XBP-1 splicing. Importantly, treatment with antioxidants protected old mice from kidney injury and normalized IRE1 and XBP-1 responses. Furthermore, older mice (6 months old) transgenic with antioxidative stress AGER1 were protected from ER stress-induced kidney injury. In conclusion, the decreased ability to handle ER stress, partly due to the presence of excessive oxidative stress, may contribute to increased susceptibility of the aging kidney to acute injury.

1. Introduction

Older individuals are more susceptible to renal failure caused by drug toxicity and ischemic injury [1, 2]. Several factors, such as the existence of mild to moderate renal function decline, abnormalities in drug turnover, and dysregulation of the vasculature, have been implicated in the pathogenesis of aging-related susceptibility [2–5]. Since the kidney naturally also faces an increased oxidant load with declining antioxidant activity over the course of aging [4–6], we postulated that the above factors in combination may lead to a decreased capability in aging kidney to defend against acute stressors.

Endoplasmic reticulum (ER) stress is a common form of cell stress. The accumulation of unmodified or unfolded proteins in the ER induces a stress response called the unfolded protein response (UPR) [7–9]. The UPR serves to reduce

protein synthesis, accelerates the folding machinery, and increases the degradation of unfolded proteins to prevent buildup of unfolded proteins. Thus far, three separate pathways have been identified that regulate the UPR, including pancreatic ER kinase (PERK), activating transcription factor 6 (ATF6), and the inositol requiring enzyme 1 (IRE1) and X-box binding protein 1 (XBP-1) pathways [10–12]. These three pathways are activated in an attempt to reduce the stress. Failure to suppress ER stress may result in increased generation of reactive oxygen species (ROS), inflammation, and cell death. Increased acute stress has been shown to contribute to various diseases including diabetes mellitus, neurodegenerative diseases, cardiac disease, and atherosclerosis [9, 13, 14].

ER stress in the kidney has recently been shown to be an underlying cause of acute drug-induced nephrotoxicity

[15–19]. Moreover, hypoxia and ischemia have been shown to generate ER stress [20–22]. We postulate that the aged kidney has a decreased capability to cope with acute increases in ER stress due to the presence of factors such as oxidative stress [4, 5, 23]. This loss in coping capability may contribute to the increased susceptibility of the aged kidney to drug and ischemic injury.

2. Methods

2.1. Mice. 18–22-month-old C57B6 female mice, purchased from the National Institute on Aging, National Institutes of Health, Bethesda, MD, were housed in a specific pathogen-free facility with free access to regular diet and water. Since aged C57B6 mice may develop malignancies, we examined all mice and excluded those with tumors from the study. 3–6-month-old C57B6 female mice were purchased from Jackson Laboratories (Bar Harbor, ME). AGER1 transgenic mice were generated, bred to C57B6 background, and characterized as previously described [24]. 6-month-old female mice were used for the study. All experiments and animal care procedures were performed according to the Guide to Animal Use and Care of the Dalian Medical University, and every effort was made to minimize suffering. This study was approved by the Institutional Animal Care Use Committee of Dalian Medical University.

2.2. Tunicamycin Induced Acute ER Stress. To select a dose of tunicamycin that would induce renal damage but not mortality, 3–6-month-old female C57B6 mice were injected intraperitoneally with the following doses of tunicamycin: 0.6, 0.8, 1.0, 1.2, and 1.4 $\mu\text{g/g}$ /body weight in 0.9% NaCl ($n = 2$ /dose). Mice were followed for 4 days. Renal histology and renal function indicators of blood urea nitrogen (BUN) levels were examined. Severe proximal tubular injury and increased BUN levels were found in young mice at a dose above 1.2 $\mu\text{g/g}$. Since a 0.8 $\mu\text{g/g}$ dose generated moderate renal proximal tubular injury, without increasing serum BUN levels, this dose (designated as high dose) was chosen to determine if the response to ER stress injury differed between old ($n = 22$) and young mice ($n = 22$). Mice were sacrificed at 24 hours ($n = 8$ /age), 48 hours ($n = 6$ /age), and 72 hours ($n = 8$ /age) after injection. After examining tunicamycin doses from 0.2 to 0.6 $\mu\text{g/g}$ to find a dose that would induce significant kidney damage in old mice but not in young mice, the dose of 0.2 $\mu\text{g/g}$ was selected. Both old ($n = 18$) and young mice ($n = 18$) were injected with this dose of tunicamycin. Mice were sacrificed 24, 48, and 72 hours after injection for blood and tissue collection. Additionally, 6-month-old AGER1 transgenic and wild-type mice ($n = 14$ /group) were given 0.8 $\mu\text{g/g}$ of tunicamycin and sacrificed at 24 hours ($n = 7$ /group) and 72 hours ($n = 7$ /group) after injection.

2.3. N-Acetylcysteine (NAC) and Butylated Hydroxyanisole (BHA) Treatment. 18–22 months and 3–6 months C57B6 mice ($n = 12$ /age group) received NAC (150 $\mu\text{g/g}$ /body weight) intraperitoneally 24 hours before the injection of tunicamycin (0.8 $\mu\text{g/g}$). Mice were sacrificed 48 hours or 72

hours after tunicamycin challenge. For BHA preventive treatment, BHA (0.7%) was added to regular mouse chow of old and young mice for 7 days before tunicamycin injection (0.8 $\mu\text{g/g}$). Mice were sacrificed 48 hours ($n = 6$ /age group) or 72 hours ($n = 6$ /age group) after tunicamycin challenge.

2.4. Analysis of Renal Function and Tunicamycin Blood Level. Blood samples were collected from animals at sacrifice. BUN was measured using a QuantiChrom assay kit (QuantiChrom™ Urea Assay Kit, BioAssay Systems, Hayward, Calif.) following the manufacturer's instructions. Serum creatinine was measured by high-performance liquid chromatography (HPLC) using creatinine (Sigma, Munich, Germany) as standard. Plasma tunicamycin levels were determined by HPLC using tunicamycin (Sigma, Munich Germany) as standard.

2.5. Histology and Morphometry. Kidneys were flushed with phosphate-buffered saline and then fixed in 4% paraformaldehyde for 48 hours. After fixation, tissues were washed and transferred to phosphate-buffered saline. Tissues were embedded in glycol methacrylate or low-melting point paraffin, and sections were cut at a thickness of 4 μm and stained with periodic acid Schiff (PAS) [25]. For electron microscopy, tissues were fixed for 1 hour in 1.0% osmium tetroxide, prestained in 1.25% uranyl acetate for 1 hour, dehydrated through a series of graded alcohol solutions, and embedded in EPON epoxy resin. The severity of histological lesions in tunicamycin-treated old and young mice was determined using a Meta Imaging software (Molecular Devices, Downingtown, PA, USA). The injured proximal tubules in the cortical area were digitized under a microscope connected with a Sony 3CCD color video camera. The ratio of the damaged to normal tubular area was measured [26].

2.6. Apoptotic Cell Staining. Paraffin sections were processed for staining as described [27, 28]. Briefly, tissues were digested with 20 $\mu\text{g/ml}$ of proteinase K for 2.5 minutes and then reacted with terminal deoxynucleotidyl transferase (TdT) for 1 hour. Positive reactions were revealed by peroxidase-conjugated antidigoxigenin and DAB. Nuclei were stained with hematoxylin. The number of apoptotic cells was counted under 400x magnification. At least 10 random fields in each section were examined.

2.7. Western Blots. Renal cortices were collected under microscope guidance. Tissue proteins were extracted using a lysis buffer containing proteinase inhibitors [27]. Equal amounts of protein were loaded in each lane of sodium dodecyl sulfate polyacrylamide gels. After electrophoresis, proteins were transferred to nitrocellulose membrane and blotted with antibody against GRP78 (1:5000, Affinity BioReagents (ABR), Golden, CO), GRP-94 (1:5000, Affinity BioReagents (ABR), Golden, CO), phosphorylated eIF2 α (1:1000, Stressgen, Ann Arbor, MI), C/EBP homologous protein (CHOP, 1:1000, Alexis Biochemicals, San Diego, CA), nuclear poly ADP-ribose polymerase (PARP, 1:1000, Cell Signaling Technology, Danvers, MA), or caspase 12 (1:1000, Cell Signaling Technology, Danvers, MA) [26]. Membranes probed for phosphorylated eIF2 α were stripped to reblot with antibody against total eIF2 α (1:5000, Bethyl Laboratories,

Montgomery, TX). Finally, all membranes were stripped to reprobe for β -actin as an internal control. The blotting for each molecule was repeated at least twice. For the measurement of phosphorylated PERK, 100 μ g of tissue protein from the kidneys of young and old mice was immunoprecipitated with a rabbit anti-PERK antibody (Santa Cruz Biotechnology Inc., Santa Cruz, CA). The precipitates were recovered with protein A/G agarose (Pierce Biotechnologies, Rockford, IL). After denaturation, the immunoprecipitated protein was examined by Western blots for phosphorylated PERK with a specific antibody (SC32577-R, 1:200, Santa Cruz Biotechnology Inc., Santa Cruz, CA).

2.7.1. Real-Time PCR. Total RNA was isolated from the renal cortex using a PureYield RNA Midiprep kit (Promega, Madison, WI). The preparation was free of DNA contamination. 500 ng of total RNA from each sample was reverse transcribed and amplified using SYBR[®] Premix Ex Taq[™] II reagent kit and ABI Prism 7700 sequence detection system (PerkinElmer Applied Biosystems, Foster City, CA) as previously described [27]. The GRP78, GRP94, oxygen-regulated protein 150 (ORP150), ER degradation-enhancing α -mannosidase I-like protein (EDEM1), CHOP, and IRE1 mRNA levels were determined. The primers were from previous reports [26, 29]: GRP78, forward, 5'-TACTCGGGCCA AATTTGAAG, reverse, 5'-CATGGTAGAGCGGAACAGG T; GRP94, 5'-TGAAGGAGAAGCAGGACAAAA, reverse, 5'-AGTCGCTCAACAAAGGGAGA; ORP150 forward, 5'-GAAGCCAACCGGCTTAAAAC, reverse, 5'-CCGAGT TACTTTGGCCTTGA; EDEM1 forward, 5'-TGTGAAAGC CCTCTGGAAC, reverse, 5'-AATGGCCTGTCTGGAT GTTC; CHOP forward, 5'-TATCTCATCCCCAGGAAACG, reverse, 5'-GGACGCAGGGTCAAGAGTAG. IRE1 forward, 5'-TGAAACACCCCTTCTTCTGG, reverse, 5'-CAGGGG GACAGTGATGTTCT. The mRNA levels were corrected by the levels of β -actin mRNA. Triplicates for each sample were done to increase accuracy of the measurement. However, since both previous reports [26, 29] had not described a 5-log dilution for primers and we had not specifically optimized PCR conditions, the levels of gene expression measured here were only semiquantitative in nature although the $\Delta\Delta$ Ct values were calculated after real-time PCR.

2.8. Spliced XBP-1. Total RNA was extracted from the renal cortex and reverse transcribed as described [23]. When we screened for dosages of tunicamycin for experiments, we noticed that X-box binding protein 1 (XBP-1) splicing occurred at 48 hours after tunicamycin treatment. Thus, this time point was chosen for examining XBP-1. The presence of the spliced XBP-1 mRNA levels was measured by standard PCR using the following primers: forward, 5'-TTACGGGAGAAAACACGGC; reverse, 5'-GGGT CCAACTTGTCCAGAATGC. 40 cycles of PCR were performed with the annealing temperature of 58°C. GAPDH mRNA levels were measured at the same sample using the previously described primers [26, 27].

2.9. Analysis of Oxidative Stress. Lipid peroxidation in the kidney was determined by a thiobarbituric acid-reactive substance assay that measures the formation of malondialdehyde (MDA) (Cayman Chemical, Ann Arbor, MI) [25]. The quantity of protein carbonyls in the kidney was measured by first reacting kidney extracts with dinitrophenylhydrazine (DNP). Protein-bound DNP was then detected by a biotinylated anti-DNP antibody followed by streptavidin-linked horseradish peroxidase. Absorbances were related to a standard (Chemicon International, Temecula, CA). To determine the levels of glutathione, kidney extracts were processed and deproteinized. A chemical reaction kit (Cayman Chemical, Ann Arbor, MI) was used to measure glutathione. Both the levels of reduced and total glutathione were determined. Kidney AGE levels were determined by ELISA and corrected for protein levels as previously described [30].

2.10. Oxidative Stress and Unfolded Protein Response in Proximal Tubular Cells. A proximal tubular cell line obtained from mice transgenic for SV40 T antigen was grown in DMEM containing 10% FBS [31]. To determine if oxidative stress could directly affect UPR, proximal tubular cells were treated with H₂O₂ (0.5–3 mM) in the presence or absence of NAC (15 mM, adding 1 hour before H₂O₂) for 6–24 hours. IRE1 mRNA and protein and XBP-1 splicing and protein were determined.

2.11. Proximal Tubule Isolation and Tunicamycin-Induced Cell Death. Three mice from young or old mice were sacrificed, and renal cortical proximal tubules (PT) were isolated by a standard method [25, 32]. Briefly, renal cortexes were freed from the medulla under a dissecting microscope. Tissues were then cut into 1–2 mm³ pieces and digested with collagenase. Proximal tubules were obtained from gradient Percoll centrifugation. Proximal tubules were suspended in DMEM containing 2% FBS, allocated to a 24-well plate, and incubated with increasing concentration of tunicamycin (0.5–5 μ g/ml). Both media and tubular segments were collected 24 hours after tunicamycin treatment to determine LDH activity.

2.12. Statistical Analysis. Data were expressed as mean \pm SD. ANOVA or the two-tailed unpaired *t*-test was used to evaluate differences between the means. For comparison with more than two subgroups, the nonparametric Kruskal-Wallis ANOVA followed by Dunnett's test was performed. Significance was defined as *p* < 0.05.

3. Results

3.1. Tunicamycin-Induced Acute ER Stress Is more Severe in Older Mice. Tunicamycin, an inhibitor of protein N-glycosylation, which has been used extensively to induce ER stress *in vitro* and *in vivo* [33–35], was given to mice (0.8 μ g/g). A sharp decrease in renal function as reflected by elevated BUN and Scr levels was observed in older mice (Figures 1(a) and 1(b)). Results from several of our experiments including this study on young AGER1 transgenic wild-type controls indicated that the BUN and Scr levels remained unchanged in most of young mice treated with

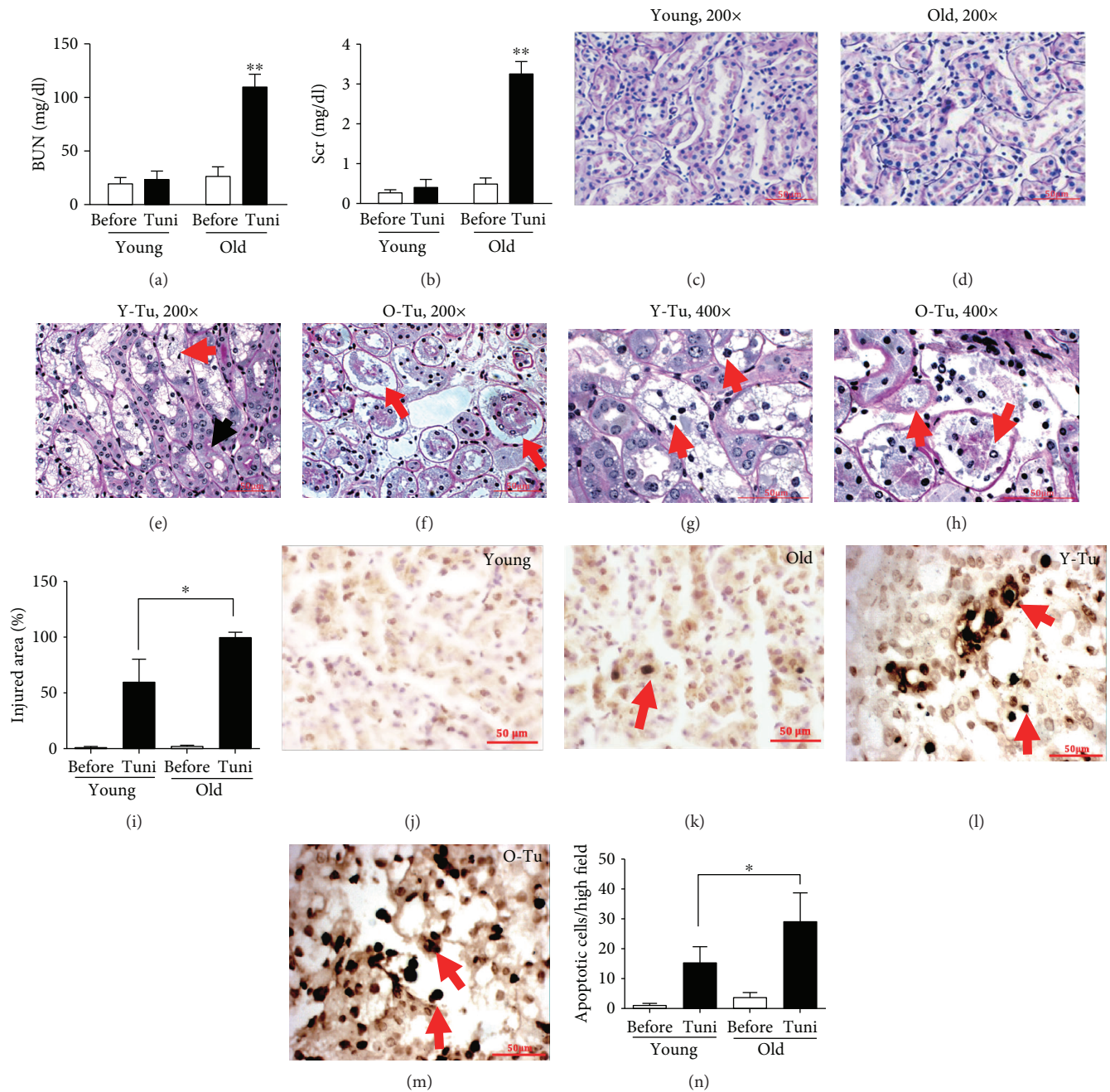


FIGURE 1: Differences in kidney function and renal lesions between old and young mice after high dose of tunicamycin injury ($0.8 \mu\text{g/g BW}$, $n = 8/\text{age group}$). (a, b) Increased BUN and Scr levels in old mice after high dose of tunicamycin injection: serum samples were obtained from 18–22-month- or 3–6-month-old mice prior to and after 72 hours of high dose of tunicamycin injection. (c, d) Representative kidney sections from (c) young and (d) old mice without receiving tunicamycin seem normal. (e, g) Extensive tubular vacuolation was present in young mice at 72 hours of high dose tunicamycin injury (PAS, (e) 200x, and (g) 400x). The lesions were localized in proximal tubules (red arrow) while the descending tubules extended from the injured proximal tubule were relatively normal as indicated by a (e) black arrow. (g) Nuclear pyknosis (condensation) and fragmentation were widely present (arrows). (f) Large vacuoles were less common in the kidneys of tunicamycin-treated old mice (200x). (f) However, the cellular damage was more severe with detachment of the whole segment of proximal tubular cells from the basement membrane in old mice (arrows). (h) Higher power magnification (400x) showed that cells in the injured tubules in aging kidney contained many small or fine vacuoles. Nuclear damages were also prominent. (i) Morphometry analysis revealed that tubular damage occurred nearly in all proximal tubules in old mice after high dose of tunicamycin injection. More apoptotic cell death in aging kidney after high dose of tunicamycin injury: apoptotic TUNEL staining was performed in kidney sections obtained from (l) young or (m) old mice at 72 hours of high-dose tunicamycin injection. Kidneys without tunicamycin treatment for (j) young and (k) old mice were as controls (400x). Nuclei with brown or black staining (DAB) were apoptotic cells (arrows). (n) More apoptotic cell counts in the kidneys from tunicamycin-treated old mice. * $p < 0.05$ vs. young mice. ** $p < 0.01$ vs. the levels before tunicamycin injection. Data was expressed as mean \pm SD. Scale bar = $50 \mu\text{m}$.

0.8 $\mu\text{g/g}$ of tunicamycin (data not shown), demonstrating that younger mice can better tolerate acute ER stress. Detailed pathological and histological investigations further revealed the age-related differences in acute ER stress response. The renal tubulointerstitial area appears normal in both young and old mice before the tunicamycin challenge (Figures 1(c) and 1(d)). Cortical enlargement caused by swelling and vacuolation of proximal tubular cells was observed in young mice after tunicamycin treatment, while other tubular segments remained largely intact (Figure 1(e)). Cell death under light microscopy, as evidenced by chromatin condensation, pyknosis, and nuclear fragmentation (Figure 1(g)), could be seen in the main lesions in tunicamycin-treated young mice, which occurred in about 60% of proximal tubules (Figure 1(i)). In old mice treated with tunicamycin, tubular injury was very severe and occurred in 94% of the area (Figure 1(i)). Damages presented as the detachment of the whole proximal tubular epithelium from the basement membrane (Figures 1(f) and 1(h)). TUNEL staining showed a 2-fold increase in apoptosis in tubular cells in old mice (Figures 1(j)–1(n)). Taken together, these results demonstrate that older mice are much more susceptible to ER stress than younger mice.

3.2. Low-Dose Tunicamycin-Induced Acute ER Stress Leading to Renal Lesions in Old Mice. Since tunicamycin at a dose of 0.8 $\mu\text{g/g}$ also caused kidney injury in young mice, we then sought to reduce the dosage of tunicamycin to rule out the possibility that results observed were solely because of the extreme degree of ER stress received. At a dose of 0.2 $\mu\text{g/g}$, young mice developed very trivial tubular lesions (affecting less than 5% proximal tubules) (Supplementary Figures 1(a) and (c)). However, the kidney lesions in old mice were widespread, with 60% of the areas showing extensive proximal tubular damage consisting of vacuolation, cell swelling, and cell death (Supplementary Figures 1(b) and (c)). TUNEL staining showed more apoptotic cells in the kidneys of old mice (14.3 ± 6.7 per high-power field) than in the kidneys of young mice (3.7 ± 2.8 per high-power field, $**p < 0.01$) (Supplementary Figures 1(d)–(f)).

3.3. ER Stress Induces Proximal Tubular Injury in Old Mice. The above results clearly showed that old mice were more susceptible to ER stress-induced kidney injury *in vivo*. One of the primary reasons for increased drug nephrotoxicity experienced by older individuals is their decreased ability to eliminate drugs, leading to higher blood/tissue concentration and/or prolonged exposure. To find out if this is the case for tunicamycin, we measured its concentration in plasma from young or old mice at 1, 2, and 24 hours after 0.8 $\mu\text{g/g}$ of tunicamycin intraperitoneal injection. Plasma tunicamycin was detectable at 1 hour after drug injection, and there was no difference in the levels between old and young mice (Supplementary Figure 2), which argues against delayed drug excretion as a major cause of increased tunicamycin nephrotoxicity in old mice. Our current and previous studies have shown that proximal tubules are major sites for ER stress-induced kidney injury [26]. Thus, we isolated proximal tubules from either old or young mice to test directly their

response to acute ER stress injury. Tunicamycin caused a dose-dependent increase in proximal tubular cell death (Supplementary Figure 3). When exposed to the same dose of tunicamycin, more cell death occurred in proximal tubules from old mice (Supplementary Figure 3), suggesting that proximal tubules from the old are more susceptible to injury.

On the organelle level, electron microscopy examination showed that changes of proximal tubular cells in young mice were mild (Supplementary Figure 4(a)), while there were extensive vacuolar changes in old mice (Supplementary Figure 4(b)). Higher definition further showed that abnormal ER and mitochondria were widely present in old mice (Supplementary Figures 4(c) and (d)). Mitochondria were condensed with many electron-dense bodies absent of their cristae (Supplementary Figure 4(c)). Additionally, the vacuoles in proximal tubular cells observed under light microscopy and low magnification of electron microscopy seemed to be dilated rough ER, as evidenced by the presence of ribosomes on the surface of the vacuoles (Supplementary Figure 4(d)). Overall, it is clear that proximal tubular cells in older mice are much more susceptible to acute ER stress, while those of younger mice are able to tolerate it.

3.4. Prolonged UPR Responses in the Kidneys of Old Mice after Low Dose of Tunicamycin Injury (0.2 $\mu\text{g/g}$). Chemical and genetic manipulations of UPR have been shown to directly affect the outcome of acute ER stress-induced injury, and aging has been linked with changes in UPR mechanisms [35–40]. Based on these reports, we next examined the expression of UPR-related genes before and after tunicamycin treatment that might explain the age-linked difference in ER stress. Prior to tunicamycin treatment, the mRNA baseline levels of ER chaperones GRP78 and GRP94 were about 50% and 60% lower, respectively, in the kidneys of old mice than in the kidneys of young mice ($n = 6/\text{age group}$, Supplementary Figure 5). Additionally, the mRNA levels of protective ORP150 and IRE1 were also lower in the kidneys from old mice (Supplementary Figure 5). Surprisingly however, the baseline levels of GRP78 and GRP94 proteins were similar between the kidneys of old and young mice (Supplementary Figure 7(b)), despite a sizeable difference in mRNA expression. The cause of the discrepancies between mRNA and protein levels is not clear. One of the reasons may be that our real-time PCR conditions especially the primers have not been optimized by 5-log dilutions and may affect the accuracy of mRNA quantitation. Another reason may be the unparallel expression between mRNAs and proteins of GRP78 and GRP94 in the kidney. To test this, we dissected out proximal and distal tubules for PCR and performed immunostaining of proteins in different nephron segments. We found by both regular and real-time PCR that GRP78 and GRP94 mRNA levels were higher in proximal tubules than in distal tubules (data not shown), while the proteins were higher in distal tubules than in proximal tubules (Supplementary Figure 6), suggesting that posttranscriptional modification or transport mechanism was in play in different nephron segments.

Low dose (0.2 $\mu\text{g/g}$) of tunicamycin was sufficient to induce ER stress in both the kidneys of young and old mice

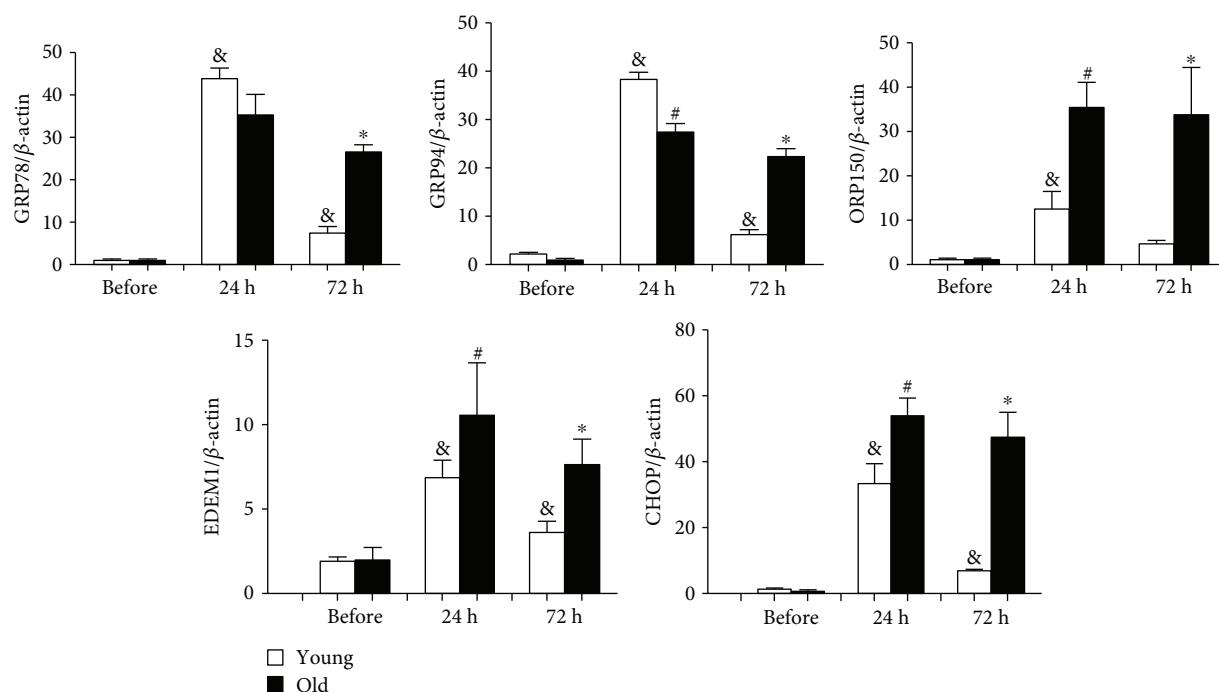


FIGURE 2: Differences in mRNA levels of UPR-related genes between the kidneys of old and young mice after high dose of tunicamycin injury: renal cortex RNA was obtained from young and old mice at baseline, 24 hours, and 72 hours after high dose of tunicamycin ($0.8 \mu\text{g/g}$) injection. The levels of GRP78, GRP94, ORP150, EDEM1, and CHOP mRNAs were measured by real-time PCR, and data was expressed as the ratio after dividing with β -actin mRNA levels at the same sample. & $p < 0.05$ vs. young mice at baseline. # $p < 0.05$ vs. young mice at 24 hours. * $p < 0.05$ vs. young mice at 72 hours.

as indicated by the appearance of spliced XBP-1 at 48 hours (Supplementary Figure 7(a)). However, the levels of GRP78, GRP94, ORP150, EDEM1, and CHOP mRNAs were higher in the kidneys of old mice after 72 hours (Supplementary Figure 7(a)). GRP78 and GRP94 protein levels were also elevated in old kidneys. Moreover, CHOP and cleaved caspase 12 were present in old kidneys (Supplementary Figures 7(b) and (c)), consistent with *in vivo* observations of higher tubular apoptosis and severe renal injury in old mice 72 hours after acute ER stress (Supplementary Figure 1).

3.5. Dysregulated UPR Responses in the Kidneys of Old Mice after High Dose of Tunicamycin Injury ($0.8 \mu\text{g/g}$). To further explore the differences in UPR response in the kidneys of old and young mice, we also examined mice treated with a high dose of tunicamycin ($0.8 \mu\text{g/g}$). The mRNAs GRP78 and GRP94 were increased in both old and young mice 24 hours after tunicamycin injection (Figure 2). Similarly, ORP150, EDEM1, and CHOP mRNAs were upregulated in both old and young mice at 24 hours but the increases were more pronounced in the old (Figure 2). 72 hours later, the levels of GRP78, GRP94, ORP150, EDEM1, and CHOP mRNAs had significantly reduced in young mice while they remained high in old mice (Figure 2). However, at the protein levels, GRP78 and GRP94 proteins were similarly increased in the kidneys from old and young mice at both 24- and 72-hour time points (Figures 3(a)–3(d)). Thus, the unparallel expression between mRNA and protein levels of GRP78 and GRP94 in the kidneys still existed after being exposed to high

dose of tunicamycin. Nevertheless, XBP-1 splicing was found missing in old mice receiving high dose of tunicamycin (Figure 3(g)). Additionally, the increase in phosphorylated PERK, although occurring in old mice at 24 hours (Figure 3(a)), was largely lost at 72 hours (Figure 3(e)). Subsequently, phosphorylated eIF2 α was also largely missed in old mice at 72 hours (Figure 3(e)). These were associated with highly elevated proapoptotic CHOP, cleaved caspase 12, and cleaved PARP proteins in old mice (Figures 3(f) and 3(h)). In contrast, XBP-1 splicing was clearly present (Figure 3(g)) and phosphorylated PERK were increased at both 24- and 72-hour time points in young mice (Figures 3(a) and 3(e)), which were accompanied by increased phosphorylated eIF2 α (Figure 3(e)).

3.6. Inhibition of Oxidative Stress Largely Protected Old Mice from High-Dose Tunicamycin-Induced Renal Injury. Oxidative stress has been shown elevated in aging kidney [11, 12]. Since ER stress causes oxidative stress and oxidative stress in turn contributes to ER stress-induced cell death, we postulated that excessive oxidative stress might play a role in severe ER stress-induced kidney injury in old mice. We first assessed the state of oxidative stress in kidneys from old and young mice prior to and after tunicamycin treatment. Although baseline levels of malondialdehyde (MDA), one of the parameters for lipid peroxidation, were comparable between old and young mice (Figure 4(a)), the levels of oxidized proteins and advanced glycation end products (AGEs) were significantly elevated in the kidneys of old mice

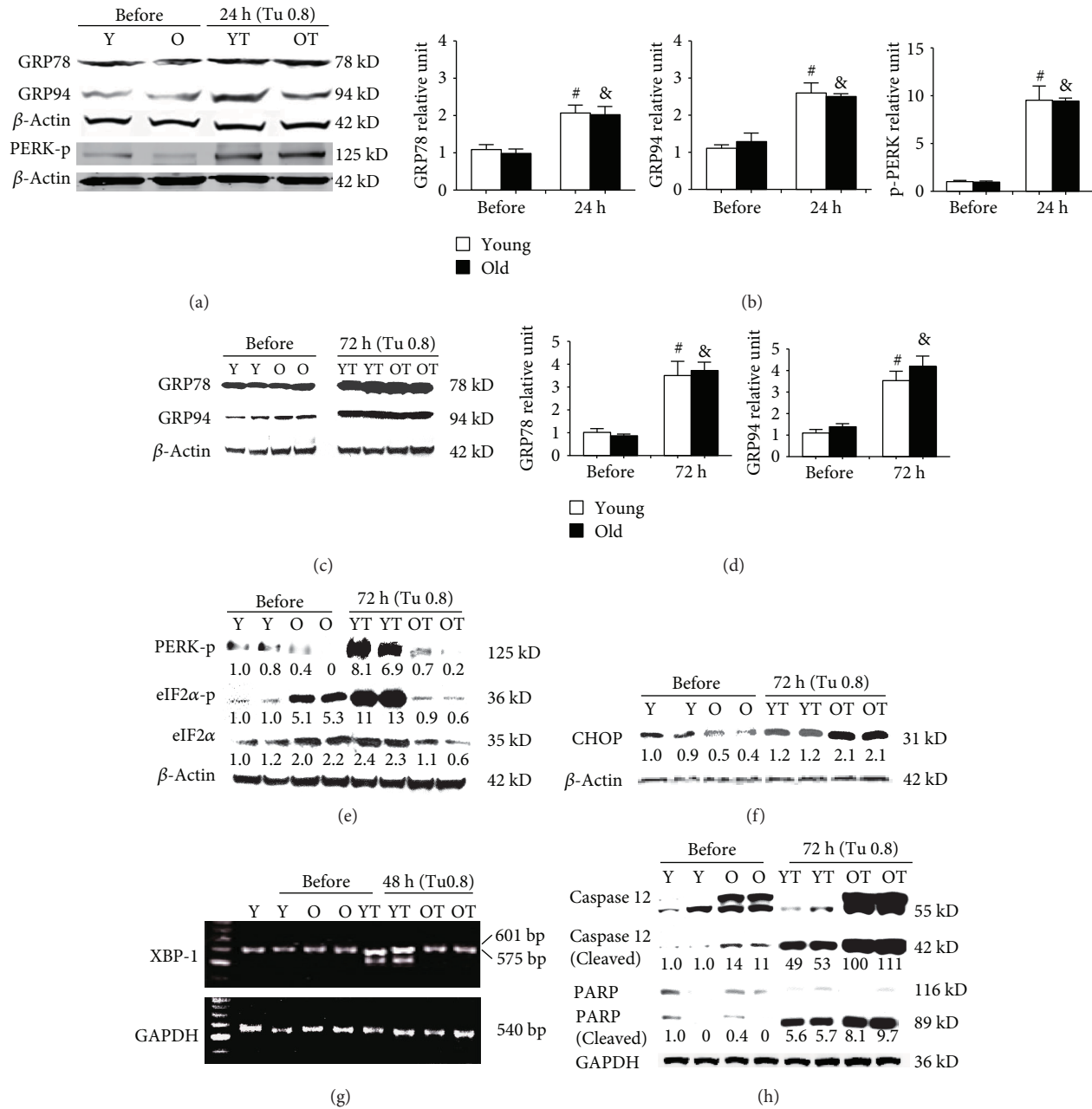


FIGURE 3: Abnormalities in UPR in the kidneys of old mice: renal cortex RNA was obtained from young and old mice at baseline, 24 hours, 48 hours, and 72 hours after high dose of tunicamycin (0.8 $\mu\text{g/g}$) injection. The levels of GRP78, GRP94, phosphorylated PERK (PERK-p), phosphorylated eIF2 α (eIF2 α -p), total eIF2 α , CHOP, caspase 12, and PARP were measured in eight animals from each group by Western blots. XBP-1 and GAPDH mRNA expression in kidneys at baseline and 48 hours after tunicamycin injection was determined by RT-PCR ($n = 6$). Results from two representative animals of baseline and tunicamycin-treated young and old mice were shown. The intensity of each blot band was quantitated using a densitometer. Data from the untreated kidneys of young mice was arbitrarily defined as 1 after correcting with the intensity of the individual β -actin band of the same sample. Lanes Y (baseline) and YT (tunicamycin treated) were samples from young mice. Lanes O (baseline) and OT (tunicamycin treated) were samples from old mice. Both GRP78 and GRP94 were significantly increased in the kidneys of both young and old mice at 24 (a, b) and 72 hours (c, d) after tunicamycin treatment. No differences were found between young and old mice. At baseline, phosphorylated PERK levels were low (a, e). The levels were significantly elevated in both old and young mice 24 hours after high dose of tunicamycin injection (a). Phosphorylated PERK remained high in young mice but was largely lost in old mice at 72 hours (e). Subsequently, at 72 hours, phosphorylated eIF2 α was increased in young mice while it was decreased in old mice (e). High-dose tunicamycin treatment was associated with more increased kidney CHOP protein levels in old mice (f). XBP-1 mRNA splicing occurred only in the kidneys of young mice after treatment (g). Cleaved caspase 12 levels were increased in old mice at baseline and were further increased after tunicamycin treatment (h). The increase in cleaved PARP was also more robust in old mice (h). [#] $p < 0.05$ vs. young mice at baseline. [&] $p < 0.05$ vs. old mice at baseline.

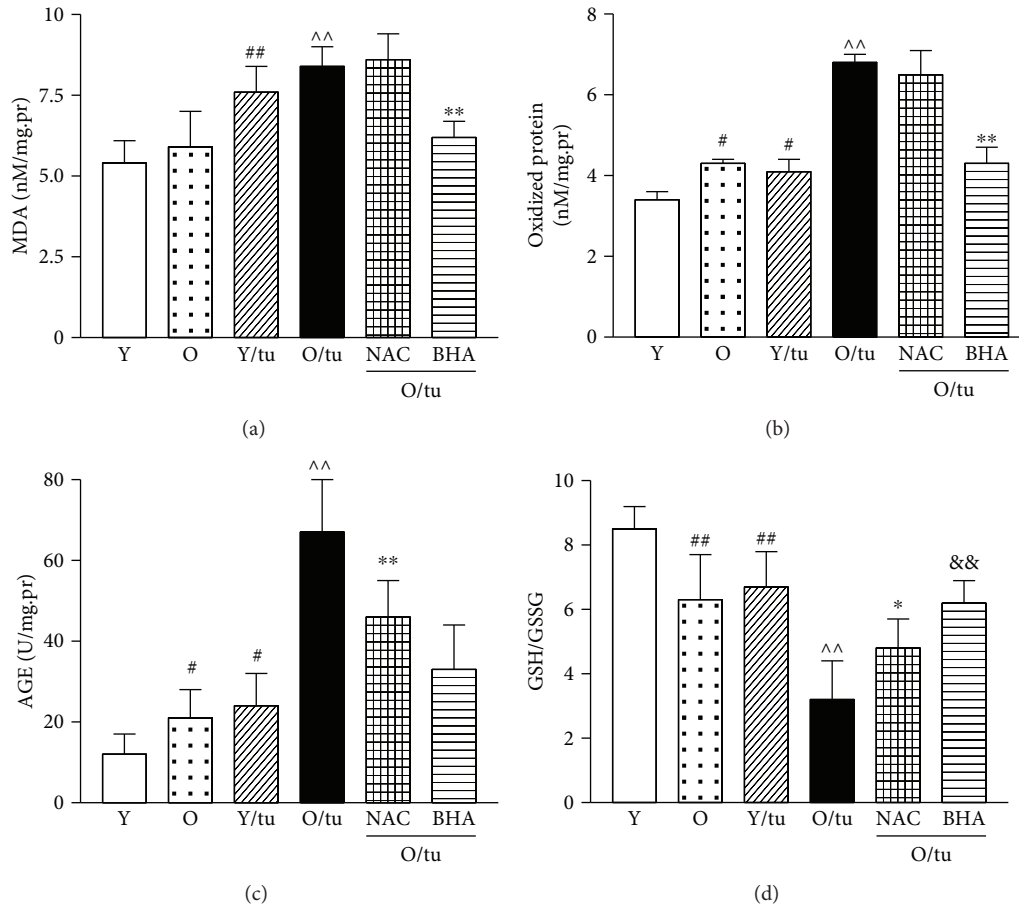


FIGURE 4: ER stress-induced severe oxidative stress in the kidneys of old mice is prevented by antioxidants. Renal tissue was obtained from young and old mice at baseline, 72 hours after tunicamycin (0.8 $\mu\text{g/g}$) injection and old mice pretreatment with BHA for 7 days or NAC 24 hours before tunicamycin injection. ER stress caused elevation in MDA, oxidized protein, and AGEs and decreased reducing glutathione (GSH)/glutathione disulfide (GSSG). (a) Levels of MDA, (b) levels of oxidized protein, (c) levels of AGEs, and (d) the ratio of GSH and GSSG. Y: young mice; O: old mice; Y/tu: young mice with tunicamycin injury; O/tu: old mice with tunicamycin injury; NAC: old mice treated with NAC; BHA: old mice treated with BHA. # $p < 0.05$ and ## $p < 0.01$ vs. young mice at baseline; ^ $p < 0.05$ and ^^ $p < 0.01$ vs. old mice at baseline; * $p < 0.05$ and ** $p < 0.01$ vs. old mice that received tunicamycin; and && $p < 0.01$ vs. old mice treated with NAC.

(Figures 4(b) and 4(c)). Additionally, the ratio of reduced to oxidized glutathione (GSH/GSSG) was decreased in the kidneys of old mice, confirming the presence of increased oxidative stress in the kidneys of old mice (Figure 4(d)). After high dose of tunicamycin injection, the levels of MDA in the kidneys were increased comparably by about 44% in both old and young mice (Figure 4(a)). However, the levels of oxidized protein and AGEs were more elevated in old mice following treatment (Figures 4(b) and 4(c)). At the same time, the GSH/GSSG ratio for older mice was halved by ER stress, while younger mice exhibited a modest decline (Figure 4(d)). To determine if high levels of oxidative stress directly contribute to increased ER stress-induced kidney injury in old mice, old mice were given antioxidants butylated hydroxyanisole (BHA) or N-acetyl cysteine (NAC) before tunicamycin. Interestingly, both BHA treatment and NAC treatment helped to preserve reduced glutathione levels in the kidneys (Figure 4(d)). In addition, BHA treatment seemed to have a better antioxidant effect, because it also significantly downregulated MDA

(Figure 4(a)). Consequently, the elevation of oxidized protein levels after tunicamycin injury was completely blocked by BHA (Figure 4(b)). The levels of AGEs were also significantly decreased by antioxidants, with much higher reduction in BHA-treated than in NAC-treated old mice (Figure 4(c)).

Importantly, both NAC and BHA prevented renal function decline induced by severe ER stress. Unlike untreated old mice that had significantly elevated BUN and Scr after tunicamycin injury (Figures 5(a) and 5(b)), the BUN and Scr levels were normal in mice receiving NAC or BHA. Renal histological examination results were consistent with the functional data, demonstrating substantial improvements upon treatment with either NAC or BHA. The severe lesions featuring proximal tubular cell sloughing were not seen in NAC- or BHA-treated old mice (Figures 5(d) and 5(e)). The main lesions in NAC-treated old mice (Figure 5(d)) were the vacuoles in proximal tubular cells instead of severe damages characterized by detachment of tubular cells seen in controls (Figure 5(c)). Only mild lesions were present in BHA-treated old mice (Figure 5(e)). Quantitative

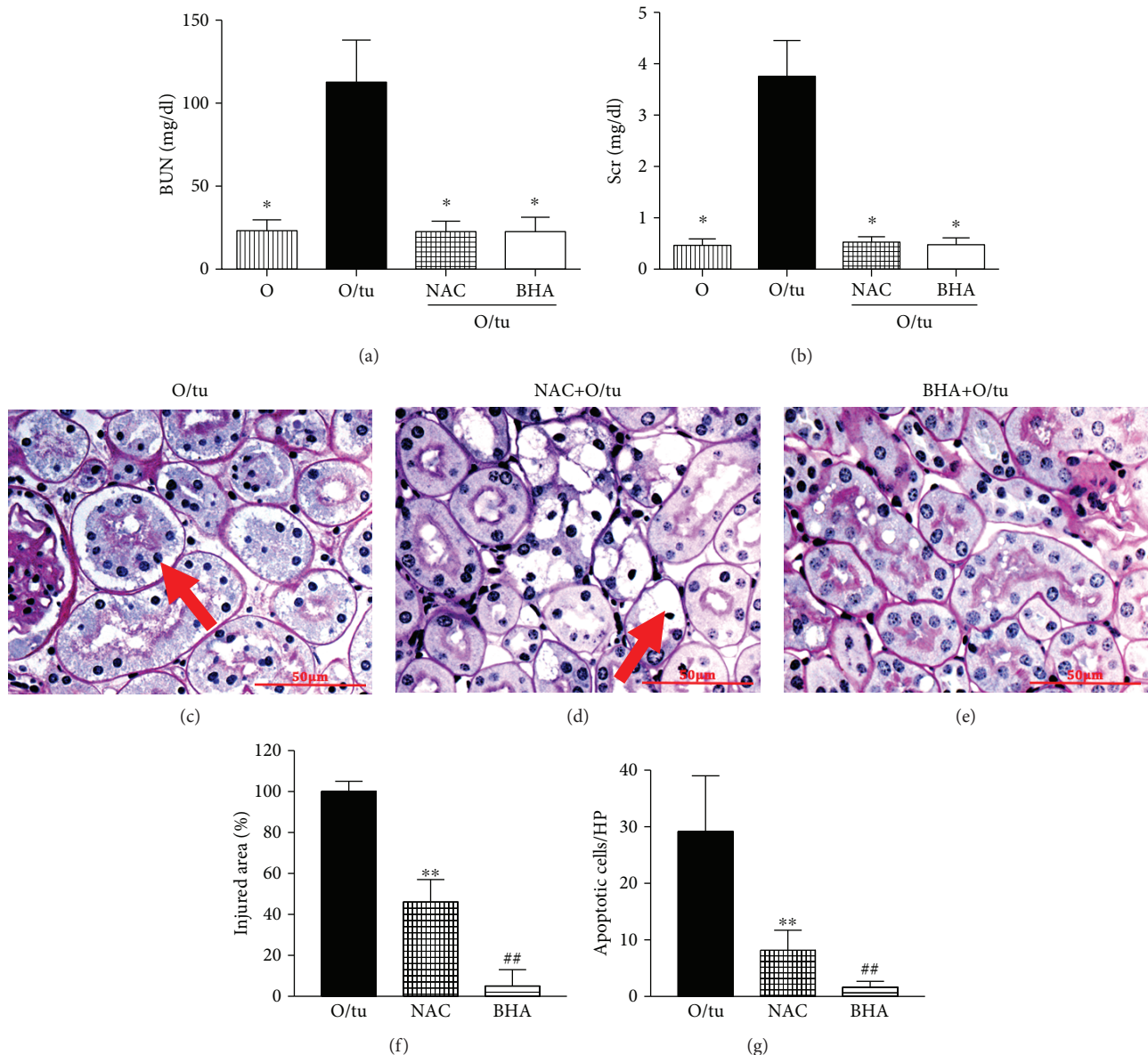


FIGURE 5: Prevention of ER stress renal injury in old mice by antioxidants. NAC or BHA treatment blocked high dose of tunicamycin-induced elevation (0.8 $\mu\text{g/g}$) of BUN (a) and Scr (b). Histologically, while severe renal injury characterized by sloughing of tubular cells (arrow) was frequently seen in old mice that received tunicamycin alone (c), NAC treatment resulted in a partial protection against tunicamycin-induced renal injury in old mice (d). There is no tubular cell sloughing, but vacuolation and nuclear damage (arrow) were seen in NAC-treated mice (d). BHA treatment gave a nearly complete protection, and renal histology was essentially normal in this group (e). Morphometry quantitation of the injured area in the renal cortex revealed a significant reduction in ER stress renal injury by antioxidants, and the effect was especially prominent by BHA (f). Counting the number of TUNEL-positive cells in kidney sections showed that BHA and NAC decreased tunicamycin-induced apoptotic cell death (g). ** $p < 0.01$ vs. old mice that received tunicamycin alone (O/tu) and ## $p < 0.01$ vs. NAC-treated mice. Scale bar = 50 μm .

measurement of the area of injury showed that BHA treatment was able to reduce the coverage from 98% to 5%, while NAC treatment was able to halve it (Figure 5(f)). The number of apoptotic cells remained directly correlated with the severity of renal lesions (Figures 5(f) and 5(g)). Old mice treated only with tunicamycin exhibited extensive apoptotic cell death, which was largely prevented by antioxidants, with BHA being more effective than NAC (Figure 5(g)). Collectively, these results demonstrate that BHA treatment is

highly effective for reducing the impact of severe ER stress on proximal tubular cells in aged mice.

3.7. Inhibition of Oxidative Stress Largely Corrected the Altered UPR in Aging Kidney. Since antioxidant treatment significantly improved the outcome of ER stress renal injury in old mice, we then examined if antioxidant treatment also corrected dysregulated UPR dynamics. Real-time PCR results showed that mRNA levels of GRP78, GRP94, EDEM,

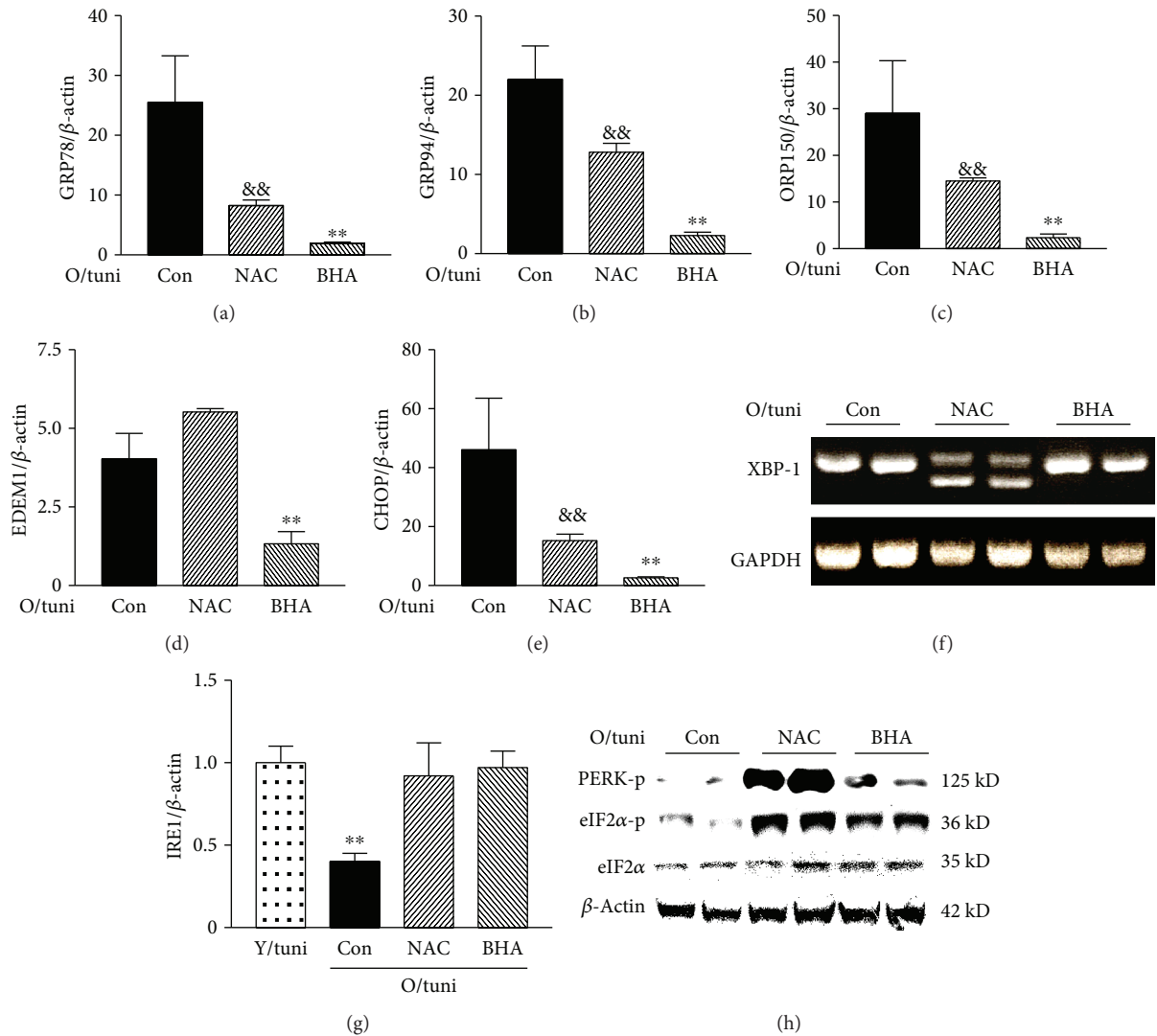


FIGURE 6: Antioxidant treatment corrects UPR dysregulation in old mice. RNA was collected from the kidneys of controls that received tunicamycin alone ($0.8 \mu\text{g/g}$) or treated with NAC or BHA before tunicamycin injection ($n = 6/\text{group}$). mRNA levels of GRP78 (a), GRP94 (b), OPR150 (c), EDEM1 (d), and CHOP (e) in the kidneys at 72 hours after tunicamycin injection were determined by real-time PCR and corrected for β -actin mRNA levels. O/tuni: old mice challenged with high dose of tunicamycin. $\&\&p < 0.01$ vs. old mice treated with tunicamycin alone (Con). $**p < 0.01$ vs. mice pretreated with NAC. XBP-1 splicing (f). Regular PCR was performed in the kidneys from tunicamycin alone (Con) and NAC- and BHA-treated mice at 48 hours after tunicamycin injection ($n = 6/\text{group}$). Representative gels from two mice of each group were shown. The loss of XBP-1 splicing in tunicamycin alone (Con) mice reappears in NAC-treated mice. IRE1 mRNA levels (g). $**p < 0.01$ vs. young mice treated with high dose of tunicamycin or old mice pretreated with NAC or BHA. The levels of phosphorylated PERK, phosphorylated eIF2 α , and total eIF2 α in the kidneys from control and NAC- and BHA-treated old mice (h). Renal protein was obtained from these mice 72 hours after tunicamycin injection ($n = 6/\text{group}$). Representative gel shows two samples from each group. The levels of phosphorylated PERK and eIF2 α were highest in the NAC-treated group. Phosphorylated eIF2 α was also visibly higher in the BHA group than in the control group.

and CHOP were significantly lower in old mice that received BHA or NAC treatment ($p < 0.01$, Figures 6(a)–6(e)). Importantly, NAC treatment led to the appearance of XBP-1 splicing (Figure 6(f)), a loss in untreated old mice after higher levels of acute ER stress kidney injury. However, no XBP-1 splicing was observed in BHA-treated mice (Figure 6(f)), one of the reasons may be that BHA treatment nearly completely protected the kidneys of old mice from acute ER stress injury. Both NAC treatment and BHA treatment prevented the decrease in IRE1 mRNA levels (Figure 6(g)).

Additionally, NAC treatment and BHA treatment both restored the PERK-eIF2 α pathway response to high dose of tunicamycin at the 72-hour time point (Figure 6(h)), providing the aged kidneys with another UPR pathway to relieve stress. Taken together, these data suggest that antioxidant treatment is highly effective to restore the kinetics of UPR pathways in response to severe ER stress in old mice.

3.8. Oxidants Decreased IRE1 and XBP-1 Splicing in Proximal Tubular Cells. Since ER stress-induced kidney injury

occurred predominantly in proximal tubules and the injury could be prevented by antioxidant prophylaxis, we next asked if oxidative stress causes UPR dysregulation in proximal tubular cells. We tested this in a proximal tubular cell line with known overactive XBP-1 splicing. Cells were exposed to H_2O_2 in the presence or absence of NAC. As shown in Supplementary Figure 8, NAC blocked the suppression of IRE1 and XBP-1 on both mRNA and protein levels by H_2O_2 . These results suggest that oxidative stress may have a direct effect on UPR regulation in proximal tubular cells.

3.9. Mice Transgenic for *AGER1* Were Resistant to Tunicamycin-Induced ER Stress Kidney Injury. An aging kidney has an elevated oxidative stress due to decreased antioxidants/anticarboxyls and excessive oxidants/carboxyls. Since the above results show a clear role played by oxidative stress in driving acute ER stress renal injury, we then sought to determine whether overexpression of *AGER1*, one of the antioxidants/anticarboxyls that is decreased in aging kidney while the oxidants/carboxyls are more prevalent [30], was protective against acute ER stress kidney injury. Mice transgenic for *AGER1* have been shown to be resistant to acute arterial wire injury [24]. *AGER1* transgenic mice, which have a nearly 5-fold increase in *AGER1* expression in the kidney [24], and wild-type mice were treated with tunicamycin ($0.8 \mu\text{g/g}$). As shown above, renal injury characterized by extensive vacuolation and tubular cell death was widely present in wild-type mice (Supplementary Figure 9(a)) while *AGER1* transgenic mice had an obvious reduction in injury lesions (Supplementary Figure 9(b)). The injured area was reduced by 50% in the kidneys of transgenic mice (Supplementary Figure 9(c)), demonstrating a significant protection from tunicamycin-induced acute ER stress kidney injury in *AGER1* transgenic mice.

4. Discussion

It is well-known that the aging kidney is more susceptible to acute kidney injury and it develops more severe postinjury outcome due to the preexisting structural and functional deterioration [1, 41–43]. We show here that old mice, but not young mice, developed severe renal failure after high dose of tunicamycin injection. Even low dosage of tunicamycin (reduced as to cause minimal or no kidney damage in young mice) was sufficient to induce extensive injury and apoptosis in the kidneys of old mice. Since ER stress is commonly associated with acute kidney injury caused by infection, drug toxicity, and ischemia [16, 18, 19, 32, 44], the inability to handle ER stress may be another mechanism for increased susceptibility to and severity of acute injury in aging kidney.

There were noticeable differences in magnitude and temporality of GRP78, GRP94, and ORP150 expression between the kidneys of old and young mice at baseline and after tunicamycin treatment although there were inconsistencies between the levels of mRNAs and those of proteins in GRP78 and GRP94 due partly to posttranscription modifications. Nevertheless, based on the more severe kidney injury seen in old mice, we speculate that there may be a difference in UPR between the kidneys of old and young mice. Indeed,

we found a dysregulated UPR dynamic in old mice: while UPR at 24 hours after high dose of tunicamycin treatment was similar between the kidneys of old and young mice, XBP-1 splicing was lost at 48 hours and phosphorylated PERK and eIF2 α were not elevated at 72 hours in old mice. PERK and eIF2 α phosphorylation along with XBP-1 splicing are two key steps in ER stress regulation. Although inhibition of IRE-1 has been shown to reduce apoptosis [36] and activation of PERK-eIF2 α may promote apoptosis by inducing CHOP [36], these may not be a general phenomenon since both IRE1-XBP-1 signaling and PERK-eIF2 α phosphorylation pathways have also been shown to be critical in maintaining cell survival during ER stress [36, 45]. Additionally, since high dose of tunicamycin caused extensive renal damage at 72 hours in the kidneys of old mice, the results of missing PERK and eIF2 α phosphorylation and XBP-1 at a relative late time point likely reflected the failure of dynamic ER stress responses. The causes of this failure are not clear. Oxidative stress is one of the key factors in aging, along with a number of human pathological conditions, and has been shown to play an important role in ER stress-induced cell death [46–48]. Unsurprisingly, the kidneys from old mice had higher basal levels of oxidative stress. ER stress induced by tunicamycin caused an increase in oxidative stress in both the kidneys of old and young mice, but the increase was more prominent in those of old mice. When old mice were pretreated with antioxidant NAC or BHA before tunicamycin challenge, renal injury was largely prevented. Moreover, the degree of renal protection was closely related to the extent of oxidative stress inhibition. BHA treatment, which resulted in a more extensive decrease in oxidative stress compared to NAC treatment in this experiment, offered a better renal protection than NAC treatment. It is unclear if different mechanisms of antioxidant actions of NAC and BHA, with NAC serving as a cysteine precursor that increases reduced glutathione [49] and BHA acting against lipid oxidation [50], contribute to the different degrees of protection conferred. Overall, these data suggest that excessive oxidative stress initiated by acute ER stress may cause renal damage.

Since the protection against ER stress-induced renal injury in old mice by antioxidants was associated with improved UPR dynamics, including the recovery of XBP-1 splicing and of the PERK-eIF2 α pathway, excessive oxidative stress may be one of the reasons for aging kidney failing in UPR. This is partly supported by our finding that high levels of H_2O_2 decreased IRE1 levels and XBP-1 splicing, which were largely prevented in the presence of an antioxidant. Future studies are required to determine if oxidants could affect the kinetics of UPR especially PERK phosphorylation and if specific phosphatases are involved in dephosphorylation of PERK in aging kidney under a late time point of acute ER stress. However, since old mice receiving low dose of tunicamycin had the UPR in XBP-1 and phosphorylated PERK similar to those of young mice, it is likely that a different magnitude of oxidative stress may dictate UPR kinetics.

Interestingly, our experiments using young *AGER1* transgenic mice showed that a reduction of oxidative stress was sufficient to protect against ER stress in an aging-independent

manner. AGER1 is a receptor of AGEs and AGER1 can decrease prooxidant action [51]. Previous reports have demonstrated that the levels of AGEs were increased in cases of acute kidney injury caused by various reasons including ischemia or endotoxin [45, 51, 52]. Since inhibition of AGEs by aminoguanidine has been shown to decrease acute kidney injury caused by various diseases [53, 54], these data, together with our findings from AGER1 transgenic mice, further support the proposition that AGEs are an important source of oxidative stress that is directly involved in acute kidney injury.

Drug nephrotoxicity is increased in elderly patients due partly to the decreased capability to metabolize and excrete drugs [55]. Theoretically, this may also be the case for tunicamycin and thus lead to increased ER stress kidney injury in old mice. However, we did not find tunicamycin accumulation in old mice in the dosage used in this study. Moreover, we found that the same dose of tunicamycin caused more cell death directly in proximal tubules isolated from old mice, suggesting that aging kidney is intrinsically more susceptible to severe ER stress-induced renal injury even though we still need to rule out a possibility that tunicamycin acts more strongly to inhibit protein N-glycosylation in the kidneys of old mice.

Data Availability

The data used to support the findings of this study are available from the corresponding author upon request.

Conflicts of Interest

The authors declare no conflicts of interest.

Authors' Contributions

Authors Xiaoyan Liu, Ruihua Zhang, Lianghu Huang, and Feng Zheng designed the experiments herein, and authors Xiaoyan Liu, Ruihua Zhang, and Lianghu Huang executed the experiments and performed data analysis. Each author contributed significantly to the intellectual content presented in our manuscript. Authors Xiaoyan Liu and Feng Zheng were responsible for drafting the manuscript, and all authors participated in the revision and finalization process. All authors approve this manuscript for publication. Xiaoyan Liu, Ruihua Zhang, and Lianghu Huang contributed equally to this work.

Acknowledgments

This work was supported by the National Natural Science Foundation of China (nos. 81370460 and 81670668), Liaoning Key R&D Program Guidance Plan (no. 2017225041), and Natural Science Foundation of Liaoning Province (no. 20180550411).

Supplementary Materials

Supplementary Figure 1: severe ER stress-induced kidney injury in old mice. Both old and young mice were injected with 0.2 $\mu\text{g/g}$ of tunicamycin. Renal histology was examined

72 hours after injection ($n=6/\text{age group}$). While renal tubules remained relative intact in young mice ((a) 200x, PAS), the formation of a big vacuole in proximal tubules was prominent in old mice ((b) 200x, PAS), which affected 61% of proximal tubules in the cortex (c). TUNEL staining showed more apoptotic cells (arrows) in the kidneys of old mice ((d) representative section of young mice; (e) representative section of old mice, 400x). (f) The number of apoptotic cells per high-power field was more in old mice. Scale bar = 50 μm . $**p < 0.01$ vs. young mice. Supplementary Figure 2: no differences in blood tunicamycin levels between old and young mice. Old and young mice were injected with 0.8 $\mu\text{g/g}$ of tunicamycin, and blood was obtained from mice 0.5, 1, and 2 hours after injection. Plasma tunicamycin levels were determined by HPLC. Peak drug levels were observed in both old and young mice at 1 hour after injection and were comparable between young and old mice. Supplementary Figure 3: tunicamycin induced more cell death in proximal tubules isolated from old mice: proximal tubules isolated from old and young mice were exposed to increasing concentration of tunicamycin (0.5–5 $\mu\text{g/ml}$) for 24 hours. Cell death was determined by LDH release from the cells, and the data was expressed as the ratio of LDH in medium to total LDH from both cells and medium. $*p < 0.05$ vs. young proximal tubules treated with the same dose of tunicamycin. Supplementary Figure 4: electron microscopic examination of renal lesions of old mice with ER stress injury: extensive vacuolation was present in old, but not in young, proximal tubular cells of mice ((a) young; (b) old). Scale bar = 2.0 μm . Higher magnification further revealed the abnormalities in mitochondria and rough ER in old mice (scale bar = 500 nm). Mitochondria contained condensed body and lost the regular structure of cristae ((c) arrow). (d) Many round-shaped dilated ER with ribosomes still attached to the outside membrane were seen (red arrow) and may appear as a vacuole under a light microscope. The yellow arrow points to a membrane-bounded, multilayered inclusion body and an inclusion body containing incompletely digested organelles. Supplementary Figure 5: differences in mRNA expression of UPR-related genes in the kidneys of old and young mice at baseline. Renal cortex RNA was obtained from normal old and young mice ($n=4/\text{age group}$). mRNA levels of GRP78, GRP94, OPR-150, IRE1, XBP-1, and CHOP were measured by real-time PCR and corrected for β -actin mRNA levels. The levels in the kidneys from young mice were arbitrarily defined as 1. $*p < 0.05$ and $**p < 0.01$ vs. the levels in the kidneys from young mice. Supplementary Figure 6: GRP78 and GRP94 immunohistochemistry: renal sections from normal young mice ($n=3$) were stained with anti-GRP78 or anti-GRP94, and the positive staining was revealed by FITC. To visualize the segment of tubules positive for GRP78 and GRP94, AQP1 that marks proximal tubules and THP that marks thick ascending limbs and distal convoluted tubules were stained and labeled (Cy5). Additionally, cell nuclei were stained with blue DAPI. (a) and (b) panels clearly showed that the relatively strong GRP78 and GRP94 staining colocalized with THP-positive tubules. (c) and (d) panels indicated that neither GRP78 nor GRP94 strong staining was present in AQP1-positive tubules. Scale bar = 25 μm . Supplementary

Figure 7: differences in expression of UPR-related genes between the kidneys of old and young mice after low dose of tunicamycin injury: renal cortex RNA was obtained from young and old mice at baseline and 72 hours after low dose (0.2 $\mu\text{g/g}$) of tunicamycin injection. The levels of GRP78, GRP94, ORP150, EDEM1, and CHOP mRNAs were measured by real-time PCR, and the results were corrected by β -actin mRNA levels. The presence of spliced XBP-1 was visualized by regular PCR. GRP78, GRP94, CHOP, and caspase 12 protein levels were determined by Western blots. β -actin levels were measured at the same membrane. The intensity of Western blot band was quantified using a densitometer. (a) mRNA levels at baseline and 72 hours after tunicamycin injection. $**p < 0.01$ vs. mRNA levels in young mice at 72 hours. XBP-1 splicing, which was not seen in young control (Y/c) and old control (O/c) mice, was clearly present in tunicamycin-treated young mice (Y/tuni) and old mice (O/tuni). (b) GRP78 and GRP94 protein levels were determined (8 mice/age/time point). Representative gels from two kidneys of young and old mice at baseline and 72 hours after tunicamycin injection. Y: young mice control; O: old mice control; YT: young mice with 0.2 $\mu\text{g/gBW}$ tunicamycin; OT: old mice with 0.2 $\mu\text{g/gBW}$ tunicamycin. Density of the specific band was quantitated. $*p < 0.05$ and $**p < 0.01$ vs. protein levels in young mice at 72 hours. (c) CHOP and caspase 12 protein levels at 72 hours after tunicamycin injection. Two representative gels from the kidneys of old and young mice showed that CHOP protein levels were higher in old mice and cleaved caspase 12 was only present in old mice. Supplementary Figure 8: oxidative stress and IRE1-XBP-1. (a) Severe oxidative stress decreased IRE1 mRNA levels. RNA was collected from proximal tubular cells treated with 1 and 3 mM of H_2O_2 in the presence or absence of NAC. mRNA levels of IRE1 were determined by real-time PCR and corrected for β -actin mRNA levels. The levels in cells without receiving H_2O_2 were arbitrarily defined as 1. $**p < 0.01$ vs. cells without receiving H_2O_2 (0). $##p < 0.01$ vs. cells treated with 1 mM of H_2O_2 . (b) Severe oxidative stress decreased the levels of spliced XBP-1 in proximal tubular cells. Spliced XBP-1 was readily present in cultured proximal tubular cells. Adding high dose of H_2O_2 (1–3 mM) into these cells for 6 hours caused a decrease in spliced XBP-1 mRNA levels. Pretreatment of cells with 15 mM of NAC 1 hour before adding H_2O_2 blocked the effect of H_2O_2 . (c) Severe oxidative stress decreased protein levels of spliced XBP-1 and IRE1. Proximal tubular cells were treated with different concentrations of H_2O_2 (0.5–3 mM) for 24 hours, in the presence or absence of NAC pretreatment. Nuclear protein was collected for the measurement of spliced XBP-1, and protein from total cell lysate was collected for the determination of IRE1. The blots used for IRE1 Western blot were reprobated with β -actin. High concentration of H_2O_2 decreases the levels of both spliced XBP-1 and IRE1. The presence of NAC blocked the effect of H_2O_2 . Supplementary Figure 9: protection against ER stress renal injury by overexpressing AGER1. AGER1 transgenic and wild-type mice were treated with high dose of tunicamycin. Severe renal injury characterized by extensive vacuolation and tubular cell death was present

in wild-type mice (a) while the injury was much less in AGER1 transgenic mice (b). (c) Morphometry analysis revealed that tubular damage occurred in 62% of proximal tubules in wild-type mice while the injured area was reduced by 50% in the kidneys of transgenic mice. $*p < 0.05$ vs. AGER1 transgenic mice. Data was expressed as mean \pm SD. (Supplementary Materials)

References

- [1] T. Brunnler, M. Drey, G. Dirrigl et al., "The oldest old in the emergency department: impact of renal function," *The Journal of Nutrition, Health & Aging*, vol. 20, no. 10, pp. 1045–1050, 2016.
- [2] F. Liaño, J. Pascual, and The Madrid Acute Renal Failure Study Group, "Epidemiology of acute renal failure: a prospective, multicenter, community-based study," *Kidney International*, vol. 50, no. 3, pp. 811–818, 1996.
- [3] G. Chen, E. A. Bridenbaugh, A. D. Akintola et al., "Increased susceptibility of aging kidney to ischemic injury: identification of candidate genes changed during aging, but corrected by caloric restriction," *American Journal of Physiology-Renal Physiology*, vol. 293, no. 4, pp. F1272–F1281, 2007.
- [4] S. Adler, H. Huang, M. S. Wolin, and P. M. Kaminski, "Oxidant stress leads to impaired regulation of renal cortical oxygen consumption by nitric oxide in the aging kidney," *Journal of the American Society of Nephrology*, vol. 15, no. 1, pp. 52–60, 2004.
- [5] S. Anderson and B. M. Brenner, "The aging kidney: structure, function, mechanisms, and therapeutic implications," *Journal of the American Geriatrics Society*, vol. 35, no. 6, pp. 590–593, 1987.
- [6] F. Gunduz, U. K. Senturk, O. Kuru, B. Aktekin, and M. R. Aktekin, "The effect of one year's swimming exercise on oxidant stress and antioxidant capacity in aged rats," *Physiological Research*, vol. 53, no. 2, pp. 171–176, 2004.
- [7] S. G. Coca, K. C. Cho, and C. Y. Hsu, "Acute kidney injury in the elderly: predisposition to chronic kidney disease and vice versa," *Nephron Clinical Practice*, vol. 119, Supplement 1, pp. c19–c24, 2011.
- [8] A. S. Lee, "The ER chaperone and signaling regulator GRP78/BiP as a monitor of endoplasmic reticulum stress," *Methods*, vol. 35, no. 4, pp. 373–381, 2005.
- [9] K. Zhang and R. J. Kaufman, "The unfolded protein response: a stress signaling pathway critical for health and disease," *Neurology*, vol. 66, no. 1, Supplement 1, pp. S102–S109, 2006.
- [10] K. Mori, "Tripartite management of unfolded proteins in the endoplasmic reticulum," *Cell*, vol. 101, no. 5, pp. 451–454, 2000.
- [11] M. Bensellam, E. L. Maxwell, J. Y. Chan et al., "Hypoxia reduces ER-to-Golgi protein trafficking and increases cell death by inhibiting the adaptive unfolded protein response in mouse beta cells," *Diabetologia*, vol. 59, no. 7, pp. 1492–1502, 2016.
- [12] H. Yoshida, T. Matsui, A. Yamamoto, T. Okada, and K. Mori, "XBP1 mRNA is induced by ATF6 and spliced by IRE1 in response to ER stress to produce a highly active transcription factor," *Cell*, vol. 107, no. 7, pp. 881–891, 2001.
- [13] N. Hiramatsu, W. C. Chiang, T. D. Kurt, C. J. Sigurdson, and J. H. Lin, "Multiple mechanisms of unfolded protein

- response-induced cell death," *The American Journal of Pathology*, vol. 185, no. 7, pp. 1800–1808, 2015.
- [14] S. J. Marciniak and D. Ron, "Endoplasmic reticulum stress signaling in disease," *Physiological Reviews*, vol. 86, no. 4, pp. 1133–1149, 2006.
- [15] C. Lorz, P. Justo, A. Sanz, D. Subira, J. Egido, and A. Ortiz, "Paracetamol-induced renal tubular injury: a role for ER stress," *Journal of the American Society of Nephrology*, vol. 15, no. 2, pp. 380–389, 2004.
- [16] M. Yokouchi, N. Hiramatsu, K. Hayakawa et al., "Atypical, bidirectional regulation of cadmium-induced apoptosis via distinct signaling of unfolded protein response," *Cell Death and Differentiation*, vol. 14, no. 8, pp. 1467–1474, 2007.
- [17] A. Mandic, J. Hansson, S. Linder, and M. C. Shoshan, "Cisplatin induces endoplasmic reticulum stress and nucleus-independent apoptotic signaling," *The Journal of Biological Chemistry*, vol. 278, no. 11, pp. 9100–9106, 2003.
- [18] H. Liu and R. Baliga, "Endoplasmic reticulum stress-associated caspase 12 mediates cisplatin-induced LLC-PK1 cell apoptosis," *Journal of the American Society of Nephrology*, vol. 16, no. 7, pp. 1985–1992, 2005.
- [19] M. Peyrou, P. E. Hanna, and A. E. Cribb, "Cisplatin, gentamicin, and p-aminophenol induce markers of endoplasmic reticulum stress in the rat kidneys," *Toxicological Sciences*, vol. 99, no. 1, pp. 346–353, 2007.
- [20] N. Chaudhari, P. Talwar, A. Parimisetty, C. Lefebvre d'Hellen-court, and P. Ravanan, "A molecular web: endoplasmic reticulum stress, inflammation, and oxidative stress," *Frontiers in Cellular Neuroscience*, vol. 8, p. 213, 2014.
- [21] D. J. Thuerauf, M. Marcinko, N. Gude, M. Rubio, M. A. Sussman, and C. C. Glembofski, "Activation of the unfolded protein response in infarcted mouse heart and hypoxic cultured cardiac myocytes," *Circulation Research*, vol. 99, no. 3, pp. 275–282, 2006.
- [22] S. Ogawa, Y. Kitao, and O. Hori, "Ischemia-induced neuronal cell death and stress response," *Antioxidants & Redox Signaling*, vol. 9, no. 5, pp. 573–587, 2007.
- [23] F. Zheng, Q. L. Cheng, A. R. Plati et al., "The glomerulosclerosis of aging in females: contribution of the proinflammatory mesangial cell phenotype to macrophage infiltration," *The American Journal of Pathology*, vol. 165, no. 5, pp. 1789–1798, 2004.
- [24] M. Torreggiani, H. Liu, J. Wu et al., "Advanced glycation end product receptor-1 transgenic mice are resistant to inflammation, oxidative stress, and post-injury intimal hyperplasia," *The American Journal of Pathology*, vol. 175, no. 4, pp. 1722–1732, 2009.
- [25] J. Wu, R. Zhang, M. Torreggiani et al., "Induction of diabetes in aged C57B6 mice results in severe nephropathy: an association with oxidative stress, endoplasmic reticulum stress, and inflammation," *The American Journal of Pathology*, vol. 176, no. 5, pp. 2163–2176, 2010.
- [26] L. Huang, R. Zhang, J. Wu et al., "Increased susceptibility to acute kidney injury due to endoplasmic reticulum stress in mice lacking tumor necrosis factor- α and its receptor 1," *Kidney International*, vol. 79, no. 6, pp. 613–623, 2011.
- [27] F. Zheng, A. R. Plati, M. Potier et al., "Resistance to glomerulosclerosis in B6 mice disappears after menopause," *The American Journal of Pathology*, vol. 162, no. 4, pp. 1339–1348, 2003.
- [28] S. J. Elliot, M. Karl, M. Berho et al., "Estrogen deficiency accelerates progression of glomerulosclerosis in susceptible mice," *The American Journal of Pathology*, vol. 162, no. 5, pp. 1441–1448, 2003.
- [29] L. Wang, W. chen, Y. Zhang et al., "Deletion of p18^{ink4c} aggravates cisplatin-induced acute kidney injury," *International Journal of Molecular Medicine*, vol. 33, no. 6, pp. 1621–1626, 2014.
- [30] W. Cai, J. C. He, L. Zhu et al., "Reduced oxidant stress and extended lifespan in mice exposed to a low glycotoxin diet: association with increased AGER1 expression," *The American Journal of Pathology*, vol. 170, no. 6, pp. 1893–1902, 2007.
- [31] G. Wolf and E. G. Neilson, "Angiotensin II induces cellular hypertrophy in cultured murine proximal tubular cells," *The American Journal of Physiology*, vol. 259, 5 Part 2, pp. F768–F777, 1990.
- [32] V. Esposito, F. Grosjean, J. Tan et al., "CHOP deficiency results in elevated lipopolysaccharide-induced inflammation and kidney injury," *American Journal of Physiology. Renal Physiology*, vol. 304, no. 4, pp. F440–F450, 2013.
- [33] M. Schroder and R. J. Kaufman, "The mammalian unfolded protein response," *Annual Review of Biochemistry*, vol. 74, no. 1, pp. 739–789, 2005.
- [34] D. T. Rutkowski, S. M. Arnold, C. N. Miller et al., "Adaptation to ER stress is mediated by differential stabilities of pro-survival and pro-apoptotic mRNAs and proteins," *PLoS Biology*, vol. 4, no. 11, article e374, 2006.
- [35] S. J. Marciniak, C. Y. Yun, S. Oyamomari et al., "CHOP induces death by promoting protein synthesis and oxidation in the stressed endoplasmic reticulum," *Genes & Development*, vol. 18, no. 24, pp. 3066–3077, 2004.
- [36] J. H. Lin, H. Li, Y. Zhang, D. Ron, and P. Walter, "Divergent effects of PERK and IRE1 signaling on cell viability," *PLoS One*, vol. 4, no. 1, article e4170, 2009.
- [37] J. H. Lin, H. Li, D. Yasumura et al., "IRE1 signaling affects cell fate during the unfolded protein response," *Science*, vol. 318, no. 5852, pp. 944–949, 2007.
- [38] D. T. Rutkowski, J. Wu, S. H. Back et al., "UPR pathways combine to prevent hepatic steatosis caused by ER stress-mediated suppression of transcriptional master regulators," *Developmental Cell*, vol. 15, no. 6, pp. 829–840, 2008.
- [39] J. Wu, D. T. Rutkowski, M. Dubois et al., "ATF6 α optimizes long-term endoplasmic reticulum function to protect cells from chronic stress," *Developmental Cell*, vol. 13, no. 3, pp. 351–364, 2007.
- [40] M. Boyce, K. F. Bryant, C. Jousse et al., "A selective inhibitor of eIF2 α dephosphorylation protects cells from ER stress," *Science*, vol. 307, no. 5711, pp. 935–939, 2005.
- [41] N. A. H. Sadik, W. A. Mohamed, and M. I. Ahmed, "The association of receptor of advanced glycated end products and inflammatory mediators contributes to endothelial dysfunction in a prospective study of acute kidney injury patients with sepsis," *Molecular and Cellular Biochemistry*, vol. 359, no. 1-2, pp. 73–81, 2012.
- [42] J. Himmelfarb, "Acute kidney injury in the elderly: problems and prospects," *Seminars in Nephrology*, vol. 29, no. 6, pp. 658–664, 2009.
- [43] C. G. Musso, V. Liakopoulos, I. Ioannidis, T. Eleftheriadis, and I. Stefanidis, "Acute renal failure in the elderly: particular characteristics," *International Urology and Nephrology*, vol. 38, no. 3-4, pp. 787–793, 2006.
- [44] X. Zhang, Y. Yuan, L. Jiang et al., "Endoplasmic reticulum stress induced by tunicamycin and thapsigargin protects

- against transient ischemic brain injury: involvement of PARK2-dependent mitophagy,” *Autophagy*, vol. 10, no. 10, pp. 1801–1813, 2014.
- [45] D. Zhang, Y. Wang, Z. Shi et al., “Metabolic reprogramming of cancer-associated fibroblasts by IDH3 α downregulation,” *Cell Reports*, vol. 10, no. 8, pp. 1335–1348, 2015.
- [46] S. E. Schriener, N. J. Linford, G. M. Martin et al., “Extension of murine life span by overexpression of catalase targeted to mitochondria,” *Science*, vol. 308, no. 5730, pp. 1909–1911, 2005.
- [47] T. Finkel and N. J. Holbrook, “Oxidants, oxidative stress and the biology of ageing,” *Nature*, vol. 408, no. 6809, pp. 239–247, 2000.
- [48] C.-H. A. Tang, S. Ranatunga, C. L. Kriss et al., “Inhibition of ER stress-associated IRE-1/XBP-1 pathway reduces leukemic cell survival,” *The Journal of Clinical Investigation*, vol. 124, no. 6, pp. 2585–2598, 2014.
- [49] J. Zhou, L. D. Cole, S. R. V. Kartha et al., “Intravenous administration of stable-labeled n-acetylcysteine demonstrates an indirect mechanism for boosting glutathione and improving redox status,” *Journal of Pharmaceutical Sciences*, vol. 104, no. 8, pp. 2619–2626, 2015.
- [50] M. Al-Hijazeen, E. Lee, A. Mendonca, and D. Ahn, “Effects of tannic acid on lipid and protein oxidation, color, and volatiles of raw and cooked chicken breast meat during storage,” *Antioxidants*, vol. 5, no. 2, p. 19, 2016.
- [51] N. Rabbani, K. Sebekova, K. Sebekova Jr., A. Heidland, and P. J. Thornalley, “Accumulation of free adduct glycation, oxidation, and nitration products follows acute loss of renal function,” *Kidney International*, vol. 72, no. 9, pp. 1113–1121, 2007.
- [52] A. Polat, H. Parlakpinar, S. Tasdemir et al., “Protective role of aminoguanidine on gentamicin-induced acute renal failure in rats,” *Acta Histochemica*, vol. 108, no. 5, pp. 365–371, 2006.
- [53] A. Heidland, K. Sebekova, and R. Schinzel, “Advanced glycation end products and the progressive course of renal disease,” *American Journal of Kidney Diseases*, vol. 38, no. 4, pp. S100–S106, 2001.
- [54] C. van Ypersele Strihou, “Advanced glycation in uraemic toxicity,” *EDTNA-ERCA Journal*, vol. 29, no. 3, pp. 148–150, 2003.
- [55] U. Klotz, “Pharmacokinetics and drug metabolism in the elderly,” *Drug Metabolism Reviews*, vol. 41, no. 2, pp. 67–76, 2009.

Review Article

Different Forms of ER Stress in Chondrocytes Result in Short Stature Disorders and Degenerative Cartilage Diseases: New Insights by Cartilage-Specific ERp57 Knockout Mice

Yvonne Rellmann  and Rita Dreier 

Institute of Physiological Chemistry and Pathobiochemistry, Waldeyerstraße 15, 48149 Münster, Germany

Correspondence should be addressed to Rita Dreier; dreierr@uni-muenster.de

Received 30 August 2018; Accepted 13 November 2018; Published 17 December 2018

Guest Editor: Tomasz Poplawski

Copyright © 2018 Yvonne Rellmann and Rita Dreier. This is an open access article distributed under the Creative Commons Attribution License, which permits unrestricted use, distribution, and reproduction in any medium, provided the original work is properly cited.

Cartilage is essential for skeletal development by endochondral ossification. The only cell type within the tissue, the chondrocyte, is responsible for the production of macromolecules for the extracellular matrix (ECM). Before proteins and proteoglycans are secreted, they undergo posttranslational modification and folding in the endoplasmic reticulum (ER). However, the ER folding capacity in the chondrocytes has to be balanced with physiological parameters like energy and oxygen levels. Specific cellular conditions, e.g., a high protein demand, or pathologic situations disrupt ER homeostasis and lead to the accumulation of poorly folded or misfolded proteins. This state is called ER stress and induces a cellular quality control system, the unfolded protein response (UPR), to restore homeostasis. Different mouse models with ER stress in chondrocytes display comparable skeletal phenotypes representing chondrodysplasias. Therefore, ER stress itself seems to be involved in the pathogenesis of these diseases. It is remarkable that chondrodysplasias with a comparable phenotype arise independent from the sources of ER stress, which are as follows: (1) mutations in ECM proteins leading to aggregation, (2) deficiencies in ER chaperones, (3) mutations in UPR signaling factors, or (4) deficiencies in the degradation of aggregated proteins. In any case, the resulting UPR substantially impairs ECM protein synthesis, chondrocyte proliferation, and/or differentiation or regulation of autophagy and apoptosis. Notably, chondrodysplasias arise no matter if single or multiple events are affected. We analyzed cartilage-specific ERp57 knockout mice and demonstrated that the deficiency of this single protein disulfide isomerase, which is responsible for formation of disulfide bridges in ECM glycoproteins, is sufficient to induce ER stress and to cause an ER stress-related bone phenotype. These mice therefore qualify as a novel model for the analysis of ER stress in chondrocytes. They give new insights in ER stress-related short stature disorders and enable the analysis of ER stress in other cartilage diseases, such as osteoarthritis.

1. Cartilage Enables Skeletal Development, Bone Growth, and Diarthrodial Joint Function

Cartilage is a connective tissue with essential functions in embryonic development and throughout life. During bone development by endochondral ossification, cartilaginous templates of future bones are formed and later gradually replaced by bone [1, 2]. The bone formation starts with the generation of cartilage condensations, consisting of prechondrogenic

mesenchymal cells. These cells differentiate into chondrocytes, produce a cartilage-specific ECM, and build bone templates (= bone anlagen), in which the central chondrocytes start to proliferate and progressively differentiate into metabolically highly active hypertrophic chondrocytes. During proliferation and hypertrophic differentiation, chondrocytes produce large amounts of extracellular proteins that form structural components of the ECM or act as local growth factors. Through a variety of these growth factors, the chondrocytes trigger the differentiation of osteoblasts from the

surrounding periosteum to form the bone collar [3]. In addition, vascular invasion is initiated and brings osteoblasts and osteoclasts into this so-called primary ossification center. These cells replace the cartilage by bone through removal of cartilaginous extracellular matrix and deposition of newly formed trabecular bone. Most hypertrophic chondrocytes die by apoptosis. However, recently, it was proven that some of the osteoblasts arise from hypertrophic chondrocytes by transdifferentiation [4]. All processes recur in the secondary ossification centers in both epiphyses of the long bones. Following ossification in the primary and secondary ossification centers, cartilaginous tissue remains on the bone surfaces as articular cartilage, where it is responsible for frictionless movement of the joints. Cartilage also remains in the growth plates between the ossification centers, where it is responsible for long bone growth until the growth plate fuses during puberty. Lengthening of a bone is dependent on proliferation and maturation of chondrocytes and the increasing production and secretion of ECM molecules by the chondrocytes. However, the largest contribution comes from a dramatic increase in the volume of hypertrophic chondrocytes in the growth plate as they undergo terminal differentiation [5]. Any imbalance between proliferation and hypertrophy can lead to skeletal defects and in particular to chondrodysplasias [6]. Chondrodysplasias comprise several hundred distinct forms of skeletal diseases from severe disorders that are perinatal lethal to milder conditions that are recognized postnatally [7]. The latter are characterized by a disproportionate short stature, eye abnormalities, cleft palate, and hearing loss [8]. In addition to skeletal development and bone growth, cartilage is involved in the maintenance and function of diarthrodial joints.

2. A Proper ER Function Is a Prerequisite for Effective Protein Synthesis and Secretion by Chondrocytes

To build and maintain cartilage, a proper function of the endoplasmic reticulum (ER) is essential in chondrocytes, as they are responsible for the production of large amounts of ECM proteins during skeletal development and growth. Due to avascularity of cartilage, the secretory chondrocytes experience a variety of stresses, such as low oxygen tension and limited nutrient conditions [9, 10], and consequently, the protein folding capacity in the cells has to be balanced with physiological parameters like energy and oxygen levels [11]. However, different cellular conditions, e.g., phases of high protein demand or pathologic situations, prevent ER homeostasis and lead to the accumulation of poorly folded proteins. This physiological or pathological state is called ER stress and induces a cellular quality control system, the so-called unfolded protein response (UPR), an adaptive mechanism to cope with ER stress to restore homeostasis [12].

Prior to their secretion, all proteins destined not only for the extracellular space but also for the plasma membrane or for secretory compartments undergo posttranslational

modification, folding, and maturation in the rough ER (Figure 1) [13]. For this purpose, the lumen of the ER contains resident molecular chaperones, protein disulfide isomerases (PDIs), and folding factors that multiply the rate of protein folding. The folding complexes are active in a specific environment of high Ca^{2+} concentration and oxidizing conditions [12, 14]. The chaperones and folding enzymes can be assigned to different protein families: (1) members of the heat shock family (e.g., BiP, GRP94), (2) serpins (e.g., HSP47), (3) lectins (e.g., calreticulin, calnexin, and EDEM), (4) oxidoreductases or protein disulfide isomerases (e.g., PDI, ERp57), and (5) peptidyl-prolyl cis/trans isomerases (cyclophilins, FK506-binding proteins, and parvulin-like peptidyl-prolyl cis/trans isomerases) [14–16]. Initially, the proteins to be folded are targeted to the ER by hydrophobic signal sequences that are cotranslationally recognized by signal recognition particles. After transition through a translocon complex in the ER membrane, the signal peptide is cleaved off by signal peptidases in the ER lumen and the nascent polypeptide is posttranslationally modified, e.g., by the oligosaccharyltransferase which is responsible for N-linked glycosylation. Attachment of carbohydrate moieties, called glycans, to asparagine within the Asn-X-Ser/Thr consensus sequence enhances the intrinsic solubility of nascent polypeptides during folding, potentially by masking hydrophobic patches, but also allows critical interactions with the lectin chaperones calnexin and calreticulin [17].

Via particular domains at their N-termini, the lectins calnexin and calreticulin specifically bind monoglycosylated N-linked glycans on the nascent proteins, after these were attached by the oligosaccharyltransferase and trimmed by glycosidases I and II and ER mannosidases [18]. The N-termini of calnexin and calreticulin in addition bind the PDI ERp57, assisting in folding by disulfide exchange reactions. Like other protein disulfide isomerases in the ER, ERp57 is responsible for correct disulfide bridge formation. After a first round of folding, calnexin or calreticulin releases the protein and glucosylase II removes the final glucose molecule from its glycan, thereby inhibiting the binding of lectin chaperones again. However, until the folding process is not completed, a uridine diphosphate-glucose-glycoprotein transferase adds a new glucose molecule to the glycan again, and the protein enters the calnexin/calreticulin cycle for a second time allowing another round of folding. Such glycosylation-folding reglycosylation cycles continue until the native conformation is finally achieved or proteins aggregate due to misfolding [12, 19]. This review focusses on ERp57, that is, as a part of the calnexin/calreticulin cycle, mainly engaged in folding of glycoproteins with unstructured disulfide-rich domains [20, 21]. An overview about these and other distinct functional roles of ERp57 in various cellular compartments playing a role under physiological and pathological conditions is given elsewhere [22].

Correctly folded proteins move via vesicular transport to the Golgi apparatus. There are additional modifications such as O-glycosylation occur, and sorting of the proteins into different kinds of vesicles is established to enable a further transport to different cellular compartments or

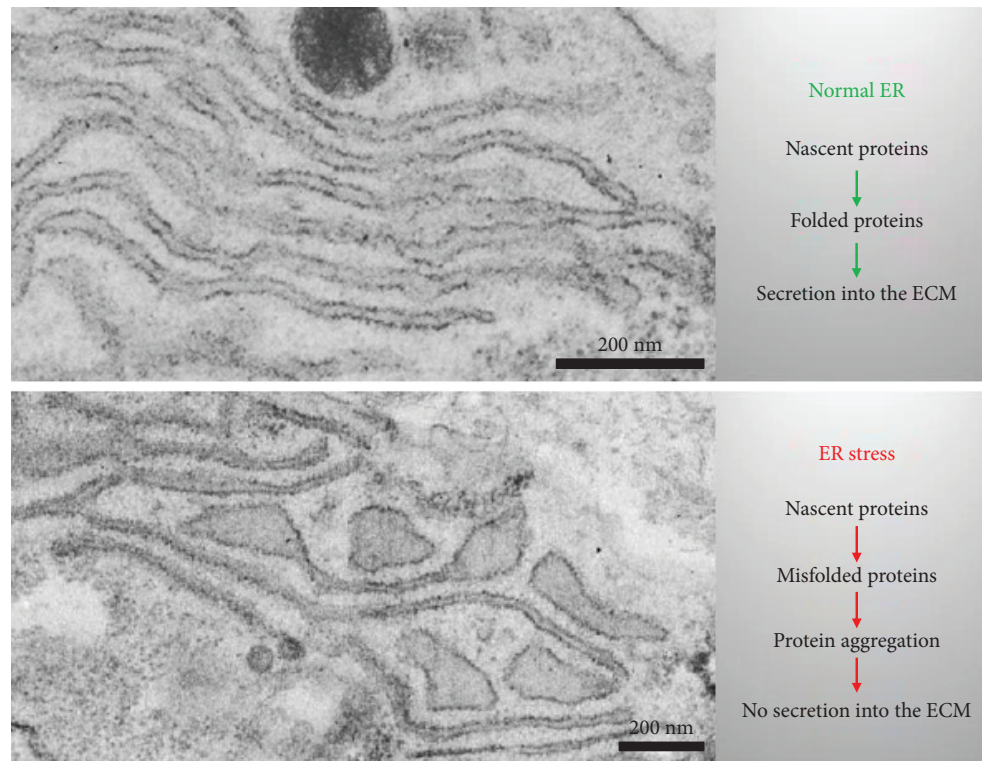


FIGURE 1: ER stress induces morphological and functional changes in chondrocytes. Normal chondrocytes produce large amounts of cartilage components. Before secretion into the ECM, these proteins undergo posttranslational modification and folding in the ER. If these processes fail, ER stress arises and misfolded proteins aggregate in the ER. This leads to a dilation of ER cisternae and a diminished protein secretion into the ECM.

secretion into the extracellular space. In case of incorrect folding of ECM proteins or protein overload in the ER, unfolded or misfolded proteins accumulate in the ER and subsequently activate the UPR. This complex quality control system leads to a general stop of cellular protein synthesis, an increased production of additional chaperones and other folding proteins, and to the degradation of aggregated proteins by ER-associated degradation (ERAD type I) or autophagy (ERAD type II). ERAD type II represents an autophagic pathway in which soluble and insoluble misfolded proteins are incorporated in autophagosomes, which then fuse with lysosomes. ERAD type I targets soluble misfolded proteins only. These are polyubiquitinated and translocated into the cytosol, where they are degraded in the proteasome [23]. However, when the combined efforts of UPR and ERAD do not readjust cellular homeostasis, cell death by apoptosis is initiated, in order to enable general tissue homeostasis. [24].

3. The UPR Initiates a Stepwise Rescue System for ER-Stressed Cells

The adaptive UPR comprises three parallel signaling pathways starting from ER stress sensor proteins located in the ER membrane: ATF6 α (activating transcription factor 6 alpha), IRE1 α (inositol-requiring enzyme 1 alpha), and PERK (protein kinase RNA-like endoplasmic reticulum

kinase) [25–27]. At the luminal side of the ER membrane, BiP (immunoglobulin heavy-chain-binding protein), also known as glucose-regulated protein 78 (GRP78), binds to these sensor proteins and keeps them inactive. Upon binding of BiP to unfolded or misfolded proteins accumulating in the ER, BiP is released from the ER stress sensors, which trigger the UPR signaling pathways. On the first route, BiP-free ATF6 α traffics to the Golgi apparatus, where it is processed by the site 1 and site 2 proteases (S1P and S2P). The released ATF6 α fragment acts as a transcription factor, enters the nucleus, and induces UPR genes encoding additional chaperones or initiators of ERAD [28]. On the second pathway, BiP-free IRE1 α is activated by oligomerization and autophosphorylation [29]. Active IRE1 α degrades certain mRNAs through regulated IRE1-dependent decay (RIDD) [30] and induces splicing of the transcription factor XBP1 (X-box-binding protein 1). The spliced transcription factor XBP1s (XBP1_{spliced}) then directly activates gene expression for folding proteins and quality control mechanisms in the ER. On the third route, oligomerized and autophosphorylated PERK acts as a kinase on eIF2 α (eukaryotic translation initiation factor 2A) and thereby stops global transcription, thus reducing the overall protein synthesis and decreasing the load of unfolded proteins in the ER [31]. However, due to preferential translation of mRNAs containing short open reading frames in the 5' UTRs, the amount of transcription factor ATF4 is

increased. ATF4 positively regulates the expression of UPR genes that are involved in amino acid metabolism, antioxidant response, folding, and regulation of autophagy and apoptosis. Examples of such ATF4-induced genes are CHOP (C/EBP homologous protein) and GADD34 (growth arrest and DNA damage-inducible 34) [32].

4. ER Stress in Cartilage Is Important under Physiological and Pathological Conditions

One should consider that ER stress or UPR signaling pathways play a crucial role in chondrocytes in phases of high protein synthesis, e.g., during bone development by endochondral ossification. As cartilage is a nonvascularized tissue, low energy levels and hypoxic conditions prevail. ER stress, therefore, is essential for normal differentiation and hypertrophic maturation of chondrocytes under these tough, but physiological conditions [33, 34].

In addition, ER stress is triggered by pathological conditions, such as metabolic dysfunction, Ca^{2+} ion imbalances, and expression of mutant proteins, or inducible by specific drugs. Under all circumstances, the direct consequence of ER stress is the initiation of UPR signaling in order to return to cellular homeostasis. However, this is not always possible, and thus, cellular imbalances occur that lead to ER stress-related pathological outcomes. Due to unresolved ER stress in chondrocytes, diseases of the skeletal system, such as chondrodysplasias, arise.

5. Various Mouse Models with ER Stress in Chondrocytes Display Phenotypes Resembling Skeletal Diseases Associated with Growth Plate Abnormalities and Dwarfism

Several whole-body knockout mouse models demonstrate the general necessity of a proper protein folding in the ER for developmental processes, organ function, and cellular homeostasis. Homozygous deletion of ER chaperones such as calreticulin, BiP, GRP94, ERp57, or UDP-glucosylglycoprotein glucosyltransferase results in embryonic lethality [14, 35]. Thus, the function of these proteins is exclusive and essential for embryonic development. Here, we focus on the impact of chondrocytes to the development and growth of long bones. Different actions of these cells are important for endochondral ossification, such as the finely tuned proliferation and maturation, the raising production and secretion of specific ECM molecules, the increase in the volume of hypertrophic chondrocytes, and the exact regulation of chondrocyte death by apoptosis at the lower end of the epiphyseal plate. If one or more of these processes fail, skeletal development is impaired and short stature diseases, like chondrodysplasias, may develop.

In order to specifically analyze the role of ER stress in chondrocytes and its relevance to chondrodysplasias, more and more mouse models with cartilage-specific changes in protein folding have been developed (Table 1) [36, 37]. From these mice, one can deduce that prolonged ER stress, e.g., due to a mutation of an ECM protein initiating poor folding and

aggregation in the ER, is a pathogenic mechanism behind short stature diseases like metaphyseal chondrodysplasia type Schmid (MCDS), multiple epiphyseal dysplasia (MED), or pseudoachondrodysplasia (PSACH). Similarly, mice with mutations in proteins of the ER folding machinery [38], mutations in UPR signaling factors [39, 40], or mutations in proteins of the secretory and degradative pathways eliminating aggregated proteins display related skeletal phenotypes. This substantiates that ER stress acts as a pathogenic factor in chondrodysplasias.

To get a well-defined overview about mouse models with ER stress in chondrocytes, one should discriminate between (1) transgenic mice with mutations in genes encoding ECM proteins, (2) transgenic mice with mutations in genes encoding exogenous proteins that are normally not expressed in cartilage, (3) mice with a knockout of genes encoding proteins of the ER folding machinery, (4) mice with a knockout of genes of UPR signaling factors, (5) mice with a knockout of proteins involved in the degradation of aggregated proteins, and (6) mice with a knockout of proteins essential for protein trafficking and secretion.

5.1. Transgenic Mice with Mutations in Genes Encoding Cartilage ECM Proteins. The extracellular matrix of cartilage is composed of a set of self-assembled secreted macromolecules that form a dynamic network of fibrillar and nonfibrillar structures. The key macromolecules of cartilage ECM are collagens II, IX, and XI, forming collagen fibrils and thus are mainly responsible for the tensile strength; proteoglycans, primarily aggrecan, responsible for the osmotic swelling and elastic properties; noncollagenous glycoproteins such as COMP and matrilins, connecting various ECM components; and hyaluronan, providing compression strength, lubrication, and hydration within the cartilaginous ECM [41]. Due to mutations in genes encoding such ECM proteins, misfolding may occur during its synthesis, which initiates ER stress. The following mouse models demonstrate that ER stress seems to be critically involved in the development of skeletal diseases, as all mice display chondrodysplasia-like phenotypes, no matter which deficiency they have.

5.1.1. Mouse Model of Chondrodysplasia Associated with a Mutation in the Col2a1 Gene (p.Gly1170Ser in Col2a1). Mutations in the $\alpha 1$ chain of procollagen type II initiate chondrodysplasias of different severity from lethal to mild forms [42]. Such disease-inducing mutations often occur in the triple-helical domain (Gly-X-Y domain) of collagen II alpha 1 chains and initiate intracellular retention of the targeted protein with induction of ER stress and activation of UPR signaling [37]. One prominent example is a knockin mouse model harboring a *col2a1*p.Gly1170Ser mutation, in which the growth plate develops abnormally because chondrocytes undergo apoptosis before hypertrophy. This leads to the disappearance of hypertrophic zones. The detailed investigation of this mouse model suggested that this early chondrocyte death is related to the ER stress-UPR-apoptosis cascade and that this is the main cause of the p.Gly1170Ser-induced chondrodysplasia in mice and men [43].

TABLE 1: Skeletal phenotypes in mice with ER stress in chondrocytes.

Reference	ERp57 KO	MED	PSACH	PSACH	MCDS	Chondrodysplasia	SED	Tg ^{Cre}	Tg ^{Cre}	Hsp47 KO	XBPI KO	ATF4 KO	SP1 KO	BMP2	Derlin-2	CTGF/CCN2	BBP2H7 KO	GMAP-210 KO
Genetic modification	Col2a1-ERp57 KO	p.Val194Asp in <i>MATN-3</i>	p.Thrs83Met in <i>COMP</i>	p-Asp469del in <i>COMP</i>	134del in <i>COL10a1</i>	p.Gly170Ser in <i>Col2a1</i>	p-Asp1192Cys in <i>Col2a1</i>	Col2a1-Tg ^{Cre}	Col2a1-Tg ^{Cre}	Col2a1-Hsp47 KO	Col2a1-XBPI KO	Af4 KO	Col2a1-SP1 KO	Col2a1-Bmp2 KO	Der2 KO	Ccn2 KO	Bb2h7 KO	Col2a1-Trip11 KO
Protein secretion	n/a	No secretion of targeted protein	Secretion of targeted protein	Reduced secretion of targeted protein	No secretion of targeted protein	Less col II secretion	Less col II secretion	No secretion of targeted protein	No secretion of targeted protein	Less col II and XI secretion	Normal secretion of Col II and Col X	Normal secretion of Col II	Less col II secretion	n/a	Retention of collagen matrix proteins	Fewer collagen fibrils in embryos E18.5	Less Col II and COMP secretion	Less proteoglycan secretion
Weight	↓-25% at the age of 4 wks	↓-9.5% at the age of 9 wks	↓-6% at the age of 9 wks	↓-6% at the age of 6 wks	n/a	No weight changes during embryogenesis	↓-30% at the age of 6 wks	↓At the age of 3, 6, and 9 wks	↓-17% in embryos E18.5	n/a	n/a	↓-50% at the age of 4 wks	n/a	n/a	↓In neonates	n/a	n/a	n/a
Bone length	↓-14% in the tibia at the age of 4 wks	↓-12.5% in the tibia at the age of 3 wks	↓-4% in the tibia at the age of 9 wks	↓-6% in the femur at the age of 9 wks	↓-15% in the tibia at the age of 10 wks	↓During embryogenesis and in neonates	↓At the age of 10 wks	↓-2, 3, and 7% in the femur at the age of 3, 6, and 9 wks	↓In embryos E15.0 and E18.5	↓-13% in the femur at the age of 2 wks	↓-50% in the femur at the age of 4 wks, ↓humerus in embryos	↓-50% in the femur at the age of 4 wks, ↓humerus in embryos	↓All skeletal elements in neonates	↓All skeletal elements in embryos E18.5	↓In neonates	n/a	↓In embryos E18.5	↓In embryos E17.5
Changes in the GP, PZ, or HZ	↓GP, ↑HZ at the age of 4 wks	Disorganized GP at the age of 1 and 3 wks	↑PZ, disorganized GP at the age of 3 wks	Disorganized GP at the age of 3 wks, areas of hypocalcemia in PZ	↑HZ at the age of 10 d	Disorganized GP, loss of HZ in embryos E19.5	Disorganized GP, cell-free areas at the age of 6 and 10 wks	Normal	n/a	Hypocellular areas, ↑PZ, ↓HZ (-45%), more cells per column at the age of 2 wks	↑HZ, disorganized GP in embryos E16	↑HZ, disorganized GP in embryos E16	Differentiation into hypertrophic cells disturbed	↓PZ, ↓HZ, disorganized HZ in embryos E18.5	n/a	↓HZ in neonates	Lack of columns in PZ, ↓HZ, decreased number and size of cells in HZ	↓HZ in embryos E15.5
ER structure	Dilated cisternae in neonates	Dilated cisternae at the age of 7 d	Dilated cisternae at the age of 7 d	Dilated cisternae in embryos E19.5	Dilated cisternae at the age of 10 d	Dilated cisternae in embryos E18.5	Dilated cisternae in embryos E19.5	n/a	Dilated cisternae in embryos E18.5	n/a	n/a	n/a	Dilated cisternae in embryos E18.5	n/a	Dilated cisternae in embryos E18.5	Dilated cisternae in embryos E18.5	Dilated cisternae in embryos E18.5	Dilated cisternae in embryos E15.5
UPR marker expression	↑BiP and CHOP at the age of 4 wks	↑BiP and CHOP at the age of 3 d	Normal	↑CHOP, XBPI, EDEM, CHOP at the age of 10 d	↑BiP, XBPI, EDEM, CHOP at the age of 10 d	↑BiP, processed ATF6 at the age of 3 wks	↑BiP at the age of 2 wks	↑BiP, phosphorylated eIF2α at the age of 3 wks, XBPIs at the age of 5 d	↑BiP in embryos E18.5	↑BiP in embryos E18.5	↑BiP, IRE1 at the age of 3 d	n/a	n/a	n/a	↑CHOP	↑BiP, CHOP, calnexin in embryos E18.5	↑BiP, PDI, GRP94, ATF4 in embryos E18.5	n/a
Proliferation	↓At the age of 4 wks	↓At the age of 3 wks	↓At the age of 3 wks	↓In embryos E18.5	n/a	↓In embryos E18.5	↓In neonates and at the age of 10 wks	↓At the age of 3 wks	n/a	↓At the age of 2 wks	↓In embryos E16 and in neonates	↓In embryos E16 and in neonates	Normal	↓In embryos E18.5	n/a	↓In embryos E16.5	n/a	n/a
Apoptosis	↑At the age of 4 wks	↑At the age of 3 wks	↑At the age of 3 wks	↑In embryos E18.5	Normal	↑In embryos E18.5	n/a	Normal	↑In embryos E18.5	Normal	↑In neonates	↑In embryos E15.5	↑In embryos E15.5	↑In embryos E18.5	n/a	↑In embryos E18.5	Normal	n/a
Osteoarthritis	Under investigation	n/a	n/a	n/a	n/a	n/a	n/a	n/a	n/a	n/a	n/a	n/a	n/a	n/a	n/a	n/a	n/a	n/a

n/a = not analyzed, GP = growth plate, PZ = proliferative zone, HZ = hypertrophic zone, Col = collagen, E = embryonal stage, ↓ = increased, ↑ = reduced, d = days, wks = weeks, and mo = months.

5.1.2. Mouse Model of Spondyloepiphyseal Dysplasia (SED) Associated with a Arg992Cys (p.Arg1192Cys) Mutation in the Col2a1 Gene. Another class of mutations within the human Col2a1 gene resulting in skeletal abnormalities is a single base substitution that converts codons for arginine in the Y position of the Gly-X-Y domain to codons for cysteine [44–46]. The most interesting is the SED model associated with an Arg992Cys (p.Arg1192Cys) substitution [45, 46]. These mice reveal ER stress and an altered linear bone growth. The growth plates display a disturbed columnar organization of chondrocytes, an altered collagenous matrix, an atypical cell polarization with unusual organization of primary cilia, and a reduced chondrocyte proliferation. Remarkably, this phenotype can be rescued by switching off the expression of mutated collagen II only during embryonic development or in newborn mice but not later, suggesting that possible therapies in human diseases with this mutation must be applied at prenatal or early postnatal stages in order to be successful [46]. Recently, the impact of arginine-to-cysteine mutations in collagen II on protein secretion and cell survival was described elsewhere [47].

5.1.3. Mouse Model of MED (p.Val194Asp in MATN-3). MED comprises a range of genetically and phenotypically heterogeneous skeletal dysplasias characterized by disorganized endochondral ossification of the epiphyses of long bones and early-onset osteoarthritis in large weight-bearing joints. Autosomal dominant forms of MED can result from mutations in genes encoding type IX collagen, oligomeric cartilage protein (COMP), and matrilin-3 [36]. The MED-causing mutant proteins are structurally unrelated, but all three comprise perifibrillar constituents and most likely form the structural basis for the mutual interaction of the cartilage fibrils with the extrafibrillar matrix [48]. In addition, the mutations lead at least to partial retention of the affected protein in the ER. Leighton et al. generated a murine model of MED by introducing a specific human disease-causing mutation (p.Val194Asp) into mouse matrilin-3 [49]. Homozygous mice of this genotype develop a progressive chondrodysplasia with weight loss and short-limbed dwarfism. Mutant matrilin-3 is retained within the rough ER of chondrocytes, and the aggregated proteins with aberrant disulfide bonding [50] initiate an unfolded protein response, with upregulation of the UPR marker proteins BiP and calreticulin. The mice display disorganized growth plates with reduced proliferation. In addition, spatially increased apoptosis of chondrocytes occurs. However, whether this chondrocyte death is directly linked to ER stress is unresolved yet, as CHOP expression is not correspondingly augmented [36, 51].

5.1.4. Mouse Models of PSACH (p.Thr583Met and p.D469del in COMP). Mutations in the cartilage oligomeric protein (COMP) can also cause PSACH. PSACH is a more severe skeletal dysplasia, characterized by a marked short stature, a deformation of the legs, and ligamentous laxity [52]. For a detailed analysis of PSACH, different mouse models were used. One harbors a single point mutation (Thr583Met) in the C-terminal domain of COMP [53] which in patients results in a mild form of the disease with typical radiographic

features and waddling gait, but normal or only mild short stature [54]. Mutant mice are normal at birth, but grow slower than their wild-type littermates and also develop a mild short-limbed dwarfism. The chondrocyte columns in the growth plates of these mice are poorly organized. Mutant COMP, however, is secreted into the extracellular matrix, but it is dislocated along with several COMP-binding proteins. Although mutant COMP is not retained within the rough ER, an unfolded protein response with upregulated expression of BiP, calreticulin, phosphorylated eIF2 α , and processed ATF6 is initiated. Chondrocyte proliferation is significantly reduced, while apoptosis is both generally increased and spatially dysregulated. By 16 months of age, mutant animals exhibit severe degeneration of articular cartilage, which is consistent with early-onset osteoarthritis seen in PSACH patients [55]. A second transgenic mouse model carries the most frequent mutation in humans, the deletion p.D469del [56]. In these mice, both wild-type and mutant COMP were detected throughout the growth plate. Mutant molecules were restricted to the pericellular matrix, while wild-type COMP showed a uniform distribution throughout the extracellular matrix. Mice expressing the mutant transgene showed a slight gender-specific growth retardation. In mutant animals, the columnar organization in the growth plate was disturbed, proteoglycans were lost, and improperly formed collagen fibrils were observed. In some chondrocytes, the ER was dilated, most probably due to an impaired secretion of mutant COMP similar to that observed in patients. Later in development, the growth plate was irregularly shaped and prematurely invaded by bony tissue [56]. A third mouse model harbors the D469del COMP mutation as a knockin and was generated by homologous recombination [57]. Most phenotypic characteristics were similar to the transgenic mouse, but in contrast, the knockin mouse showed no canonical UPR signaling although proteins aggregated in the ER. Instead, gene profiles of oxidative stress, cell cycle, apoptosis, and NF- κ B signaling changed, suggesting the involvement of UPR-independent stress pathways [57].

5.1.5. Mouse Model of MCDS (13del in COL10a1). MCDS is a dominant disease caused by mutations in the type X collagen gene. Collagen X is a short, nonfibrillar collagen expressed by hypertrophic chondrocytes in the growth plates of long bones. MCDS patients suffer from a relatively mild chondrodysplasia characterized by growth plate malfunction with a strong expansion of the hypertrophic zones [58]. Almost all patients with MCDS carry mutations in the NC1 domain of type X collagen [37]. Tsang et al. generated transgenic mice carrying a disease-causing 13 base pair deletion (13del) in this domain [59]. These mice display a chondrodysplasia phenotype including short limbs and expanded hypertrophic zones in growth plates of long bones. Collagen X is retained in the ER cisternae of hypertrophic chondrocytes, and UPR marker proteins such as BiP, XBP1s, CHOP, and processed ATF6 are upregulated, suggesting MCDS to be an ER stress-related skeletal disease. Furthermore, the authors described changes in the chondrocyte differentiation program as part of the adaptive response to the ER stress. The

hypertrophic chondrocytes are reprogrammed to a “prehypertrophic chondrocyte-like” cell showing proliferative characteristics to circumvent the expression of mutated collagen X. These aberrations from the normal differentiation processes during endochondral ossification then lead to the chondrodysplasia phenotype [59].

In all of these mouse models, mutations in ECM proteins result in the synthesis of misfolded proteins, which accumulate in the ER and induce the UPR. However, due to the intracellular retention of the mutated proteins, the ECM also lacks essential constituents or contains minor amounts of the affected ECM macromolecules. Therefore, it is hard to determine whether the ER stress itself, the loss of essential ECM components, or both is the underlying mechanism of the given chondrodysplasias.

5.2. Transgenic Mice with Mutations in Genes Encoding Exogenous Proteins That Are Normally Not Expressed in Cartilage. In order to analyze the effects of ER stress on bone development and long bone growth without loss of a single, essential cartilage ECM constituent, transgenic mice were generated in which mutated thyroglobulin (Tg^{COG}) is expressed in chondrocytes [60, 61]. The mutated thyroglobulin fails to be folded, accumulates in the ER, and induces ER stress. However, as thyroglobulin normally is only expressed in the thyroid gland, the cartilage of these transgenic mouse lines does not lack any specific essential cartilage component.

5.2.1. Tg^{COG} Mouse (Col2a1-Tg^{COG}). This mouse line was generated to investigate the generic role of ER stress and the UPR in the pathogenesis of the chondrodysplasia types MED and PSACH. Tg^{COG} was expressed as potential ER stress-inducing protein in proliferative chondrocytes under the control of the collagen II alpha 1 promoter. Due to its mutation, Tg^{COG} was retained in the ER cisternae, induced ER stress, and activated the UPR. This was detected by increased expression of the ER stress marker protein BiP, phosphorylation of eIF2 α , and appearance of XBP1s, the spliced form of XBP1. Col2a1Tg^{COG} mice displayed diminished long bone growth and a reduced rate of chondrocyte proliferation. However, morphology of the chondrocytes and architecture of the overall growth plate were normal. In addition, no increased apoptosis was detectable. Summarized, these data demonstrate that the targeted induction of ER stress in chondrocytes is sufficient to reduce the rate of bone growth and establishes that classical ER stress is a pathogenic factor that contributes to the disease mechanisms of MED and PSACH. However, as not all pathological features of MED and PSACH were recapitulated, a combination of intra- and extracellular factors is suggested to be responsible for disease pathology [60].

5.2.2. Tg^{COG} Mouse (Col10a1-Tg^{COG}). An analogous mouse model was established to examine the role of ER stress and the UPR in the pathogenesis of MCDS. Mutant thyroglobulin (Tg^{COG}) was expressed in hypertrophic chondrocytes under the control of the collagen X promoter. The hypertrophic chondrocytes in these mice exhibited ER stress with a characteristic UPR response. In addition, the hypertrophic zone was expanded, gene expression patterns were disrupted,

osteoclast recruitment to the vascular invasion front was reduced, and long bone growth decreased. Moreover, hypertrophic chondrocytes regain a prehypertrophic differentiation state comparable to chondrocytes of the MCDS mice. These data demonstrate that triggering ER stress in hypertrophic chondrocytes per se is sufficient to induce the essential features of the cartilage pathology associated with MCDS and confirm that ER stress is a central pathogenic factor in the disease mechanism [61].

Both Tg^{COG} mouse models prove that ER stress is centrally involved in the pathogenesis of chondrodysplasias. The advantage over mouse models with mutant ECM proteins is obvious, but the contribution of a possibly reduced concentration of numerous ECM components cannot clearly be ruled out as a potential factor in the pathogenesis of chondrodysplasias, as the induced UPR reduces the overall protein synthesis in affected chondrocytes. This is the reason why additional mouse models are important to confirm the direct link between ER stress and the pathogenesis of chondrodysplasias.

5.3. Mice with a Knockout of Genes Encoding Proteins of the ER Folding Machinery. To further characterize the role of ER stress as a pathogenic factor in chondrodysplasia, transgenic mice were generated with a cartilage-specific deficiency in proteins of the folding machinery or missing UPR signaling factors.

5.3.1. Hsp47 KO Mouse (Col2a1 Hsp47 KO). The most prominent knockout mouse model in this respect is the cartilage-specific Hsp47 KO mouse [38]. Masago et al. generated a mouse model with a conditionally inactivated Hsp47 gene in chondrocytes using Hsp47 floxed mice and mice carrying a chondrocyte-specific Col2a1-Cre transgene. Hsp47 binds Yaa-Gly-Xaa-Arg-Gly in triple-helical procollagen in the ER via hydrophobic and hydrophilic interactions. In cartilage, the binding of Hsp47 mainly stabilizes procollagen II by preventing unfolding of the triple helix. Thus, Hsp47 is crucial for efficient secretion, processing, fibril formation, and deposition of collagen type II in the ECM of cartilage [62]. These mice die just before or shortly after birth and exhibit a severe generalized chondrodysplasia and bone deformities with lower levels of type II and type XI collagen. Most long bones were severely twisted and shortened. First, these results demonstrate that Hsp47 is indispensable for well-organized cartilage fibril formation and normal endochondral bone formation. In addition, this mouse model displays numerous characteristics of ER stress. Cartilage collagens and other ECM components accumulated in the rough ER and induced the UPR with induction of the ER stress marker BiP. Moreover, the TUNEL assay revealed an elevated apoptosis rate. This ER stress induced chondrocyte death clearly contributes to the chondrodysplasia phenotype of cartilage-specific Hsp47 KO mice.

5.3.2. ERp57 KO Mouse (Col2a1 ERp57 KO). In our lab, the cartilage-specific ERp57 knockout mouse was intensively investigated [63]. ERp57 is a member of the protein disulfide isomerase family of ER chaperone proteins and is essentially

involved in the formation of disulfide bridges in newly formed glycoproteins [21]. Moreover, ERp57 accounts for a folding correction in misfolded proteins by elimination of disarranged and formation of new disulfide bridges [64]. The activity of ERp57 is dependent on interactions with calnexin and calreticulin, which mediate the recognition and binding of N-glycosylated substrates [20, 65]. As a total deficiency of ERp57 in mice is lethal at embryonic day 13.5, demonstrating that ERp57 action is indispensable for vertebrate development [66], a cartilage-specific KO mouse model was generated. We used ERp57 floxed mice and crossed these with Col2a1-Cre transgenic animals [63]. The cartilage-specific ERp57 KO animals (ERp57cKO) display an obvious chondrodysplasia-like bone phenotype. Four-week-old male mice reveal a reduced weight, shorter long bones, enlarged growth plates, and a decreased proliferation and increased apoptotic cell death in growth plate chondrocytes. Most likely, this bone phenotype is pronounced especially at this age because of an extremely high protein demand due to the pubertal growth spurt. The significantly reduced tibia lengths and the enlarged growth plates were confirmed by μ -computer tomography analysis. By this method, also altered trabecular structures and a reduced bone volume compared to the total volume were detectable. With respect to the function of ERp57 in protein folding, chondrocytes were analyzed by electron microscopy. Dilated ER structures, which are most likely a consequence of accumulating misfolded proteins and therefore represent a sign of ER stress in these cells, were evident. Immunofluorescence staining of chondrocytes of the tibial growth plate indeed displayed higher amounts of the ER stress markers BiP and CHOP. This demonstrates that ER stress, triggered by the knockout of the protein disulfide isomerase ERp57, is the basic reason of the chondrodysplasia phenotype in these mice [63]. Therefore, mice with a cartilage-specific knockout of the protein disulfide isomerase ERp57 qualify as a novel model for the analysis of ER stress in chondrocytes and ER stress-related skeletal diseases. We wondered that the knockout of this single PDI led to this pronounced phenotype and started to examine ERp57 substrates. In preliminary studies, we observed that the secretion of collagen II by ERp57 KO chondrocytes was almost normal, whereas the proteoglycans were diminished as seen by alcian blue staining of micromass-cultured cells. These analyses, however, are far from accurate and should be expanded in future. Jessop et al. analyzed ERp57 substrates by biochemical means and found common structural domains which are important for the interaction of ERp57 with the proteins to be folded [67]. These specific domains may also be one reason why other protein disulfide isomerases, such as PDI or ERp72, could not efficiently compensate for the loss of ERp57. The superior function of the calreticulin-calnexin ERp57 cycle over other protein folding mechanisms [20] might also play a role in this context. The complex of multiple proteins that work together is important for speeding up the folding process. If the calreticulin-calnexin-ERp57 cycle fails, this cannot be compensated by individual PDIs. These results and additional detailed analyses of the ERp57 KO mouse in the future will provide access to new insights into ER stress-related cartilage diseases.

As these mice also display chondrodysplasia-like phenotypes, ER stress gets more and more likely as a pathogenic factor in chondrodysplasia.

5.4. Mice with a Knockout of Genes Encoding Proteins Influencing UPR Signaling. ER stress initiates the UPR to restore cellular homeostasis by expression of additional chaperones, reduction of translation, and initiation of the degradation of aggregated proteins. Whenever the UPR fails or is not able to counteract the ER stress, cellular homeostasis cannot be restored and apoptosis is initiated. In mice with deficiencies in UPR signaling factors, this restoration system is reduced, and consequently, the ER stress remains high for a longer period. Therefore, the initiation of pathologic outcomes is anticipated. However, if only one UPR signaling route is blocked, the others probably can substitute for this loss. Here, different mouse models with a failure in ER stress-induced signaling processes in chondrocytes are described exemplarily.

5.4.1. XBP1 KO Mouse (Col2a1-XBP1 KO). In presence of aggregated proteins, the ER sensor protein IRE1 α is activated and then induces splicing of XBP1. The spliced form of XBP1 (XBP1s) acts as a transcription factor inducing the expression of different genes involved in quality control mechanisms of the ER. Cartilage-specific XBP1 knockout mice [39] display a mild form of chondrodysplasia with a delay in endochondral ossification. The main characteristics are dysregulation of chondrocyte proliferation and shortening of hypertrophic growth plate zones. Moreover, long bones reveal a delayed ossification. While ER stress was enhanced in the XBP1-deficient growth plate cartilage and was detectable by IRE1 hyperactivation, only minimal alterations in the expression of chondrocyte proliferation markers were observed and no changes in apoptotic cell death were detectable. The effects of a XBP1 deficiency in cartilage are rather low, but even small imbalances in chondrocytes induce changes in the timing of mineralization during endochondral ossification, ending in an ER stress-induced chondrodysplasia phenotype [39].

5.4.2. ATF4 KO Mouse (Total KO). ATF4 positively regulates the expression of UPR genes that are involved in folding and regulation of autophagy and apoptosis, e.g., CHOP and GADD34 [32]. Compared to XBP1 deficiency, the ablation of *Atf4* in mice leads to more severe skeletal defects. ATF4-deficient mice display a 50% reduction in body weight and in femoral bone length at the age of 1 month, indicating a severe limb dwarfism. In the growth plates, the typical columnar structure of proliferative chondrocytes is disturbed and the proliferative zone is shortened. In addition, the hypertrophic zone is abnormally expanded, suggesting a delay in the overall endochondral ossification process. Detailed analysis in chondrocytes showed that ATF4 acts as a transcriptional activator of Indian Hedgehog and therefore controls chondrocyte proliferation and differentiation during bone development and growth [40].

5.4.3. BMP2 KO Mouse (Col2a1-Bmp2 KO). During bone development by endochondral ossification, BMP2 activates

via Smad-4 the transcription of XBP1, which is involved in ER stress signaling and positively regulates bone formation by activating granulatin-epithelin precursor [68]. Both is essential, as mice with a conditional knockout of BMP2 develop a severe chondrodysplasia, with defects in proliferation, differentiation, and apoptosis of chondrocytes in the growth plate [69]. The phenotypes of cartilage-specific BMP2 and XBP1 KO mice are comparable.

5.4.4. S1P KO Mouse (*Col2a1-S1P*). The site 1 protease is essential in UPR signaling as well, as it is responsible for the processing and activation of the transcription factor ATF6. Due to a loss of active ATF6, one of the three UPR signaling pathways is completely shut down, and therefore, S1P KO mice exhibit a severe chondrodysplasia with a substantial increase in chondrocyte apoptosis. Ultrastructural analysis revealed that the ER in S1P KO chondrocytes displays characteristics of severe ER stress. This suggests that S1P activity is required for the genesis of normal cartilage by endochondral ossification [70].

These mouse models clearly demonstrate that UPR signaling factors play a role not only under pathological but also under physiological conditions in cartilage. Without a well-functioning ER quality control system, normal endochondral ossification and regular bone growth are disturbed.

5.5. Mice with a Knockout of Proteins Involved in the Degradation of Aggregated Proteins. In addition to other processes, the UPR initiates the degradation of aggregated proteins by ER-associated degradation (ERAD type I) or autophagy (ERAD type II). These mechanisms are commenced to liberate the chondrocytes from the overflow of unfolded or misfolded proteins in the ER. However, if the translocation processes into the cytosol or the degradation processes fail, the ER stress in affected chondrocytes remains and the initiation of apoptosis is the last chance to rescue cartilage homeostasis.

5.5.1. *Derlin-2* KO (*Total KO*). A multiprotein complex linking dislocation, ubiquitination, and extraction of misfolded proteins from the ER membrane mediates the dislocation process from the ER to the cytosol in the case that misfolded proteins should be degraded in the proteasome [71]. *Derlin-2* is one of the important players within this multiprotein complex. Whole-body deletion of *derlin-2* in mice results in perinatal death of most of the animals due to feeding failures. However, the few mice that survive to adulthood develop a severe chondrodysplasia with defects in ECM protein synthesis and secretion. *Derlin-2* KO mice were smaller, had reduced bone lengths, and displayed a striking involution of the rib cages with fusion of the third and fourth sternbrae. Chondrocytes of KO animals showed intracellular retention of ECM components, suggesting a defective protein secretion and degradation. In addition, higher CHOP RNA and protein levels suggest an increase in chondrocyte apoptosis in these animals [72].

5.5.2. *CTGF/CCN2* (*Total KO*). In addition to ERAD type I, autophagy (ERAD type II) is activated in case of ER stress. This mechanism is of great importance for the functionality

and homeostasis of the growth plates in mice, as the loss of the connective tissue growth factor (CTGF/CCN2), which is a positive regulator of autophagy, leads to a severe chondrodysplasia. CTGF/CCN2 KO chondrocytes displayed dilated ER cisternae, increased apoptosis, and increased BiP and CHOP expression levels [73]. Overall, autophagy is considered as a particularly important mechanism for the survival of highly secretory cells under hypoxic and other stressful conditions [74].

The occurrence of chondrodysplasias due to the loss of proteins engaged in ERAD I or II demonstrates the importance of a functional degradation system for unfolded or misfolded proteins. A retention of aggregated proteins in the ER induces ER stress in chondrocytes culminating in dysfunction of the skeletal system.

5.6. Mice with a Knockout of Proteins Which Are Essential for Protein Trafficking and Secretion. In addition to the above-mentioned processes, disturbed trafficking of proteins within the cells and to the cell surface and insufficient secretion induce skeletal phenotypes as well.

5.6.1. *BBF2H7* KO Mouse (*Total KO*). Under normal conditions, ER stress induces the activation of the transcription factor BBF2H7, which then, via Sec23, encodes a component that is responsible for the protein transport from the ER to the Golgi apparatus. If BBF2H7 and subsequently Sec23 are absent, the formation of vesicles for these transport processes fails and cartilage matrix secretion is impaired. BBF2H7 KO mice showed severe chondrodysplasia and died by suffocation shortly after birth because of an immature chest cavity. ECM proteins, type II collagen, and COMP remained in the ER; ER stress arose and a severe chondrodysplasia with characteristics, such as a lack of the typical columnar structure in the proliferating zone of growth plates and proliferating chondrocytes showing abnormally expanded ERs developed. This indicates that the ER stress-induced BBF2H7-Sec23a pathway is crucial in endochondral ossification as insufficient protein trafficking into the ECM results in ER stress counteracting proper cartilage proliferation and differentiation processes [75]. In addition, a C-terminal fragment of BBF2H7 accelerates chondrocyte proliferation by binding to Indian hedgehog and its receptor PTCH1, supporting their interaction and signaling [76]. If this acceleration is missing, the proliferative capacity of chondrocytes is reduced.

5.6.2. *GMAP-210* KO Mouse (*Col2a1-Trip11 KO*). Another trafficking component of interest is the golgin Golgi microtubule-associated protein of 210 kDa (*GMAP-210*). Like other golgins, *GMAP-210* is required for efficient trafficking from the ER to the Golgi. Studies by Bird et al. revealed that the skeletal phenotype of achondrogenesis type 1A is exclusively caused by defects in chondrocytes, but not osteoblasts, osteoclasts, or hematopoietic cells. Loss of *GMAP-210* led to a massive ER swelling and cell death in growth plate cells culminating in impaired bone formation. Notably, the intracellular accumulation of proteins applies only to specific ECM components such as perlecan, but is not a general secretion defect [77].

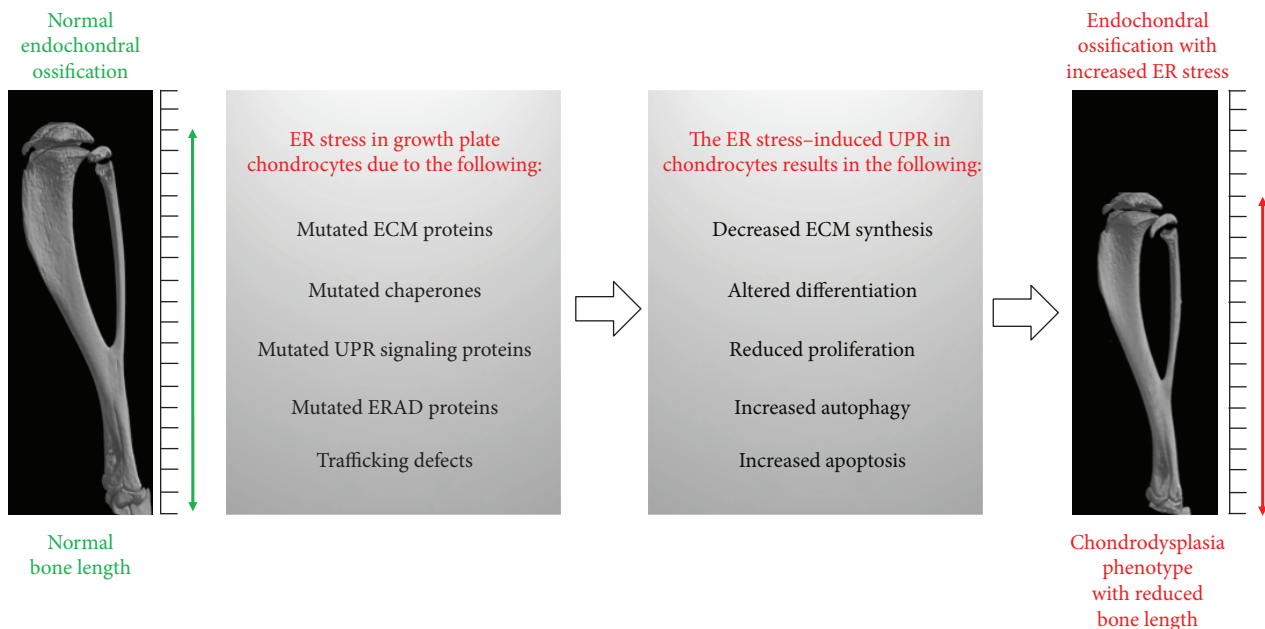


FIGURE 2: Causes and effects of ER stress in growth plate chondrocytes. ER stress in growth plate chondrocytes is induced by mutations in genes encoding ECM components, chaperones, UPR signaling factors, or ERAD proteins. The ER stress-induced unfolded protein response (UPR) substantially impairs essential processes of the endochondral ossification, such as ECM protein synthesis and chondrocyte proliferation and differentiation, and activates autophagy and apoptosis. This results in a chondrodysplasia phenotype with reduced lengths of long bones.

These examples show that mice with trafficking defects display ER stress. Consequently, it seems very likely that chondrodysplasias in mice with such defects are not induced by the loss of nonsecreted components in the ECM, but by the increasing ER stress in chondrocytes.

6. The Skeletal Phenotypes of Different ER Stress Mouse Models Show a High Degree of Similarity

Taken together, various mouse models with prolonged or high levels of ER stress in growth plate chondrocytes display chondrodysplasia phenotypes (Figure 2). However, the cause for this pathological outcome varies between the different ER stress mouse models. ER stress may arise due to misfolding of ECM proteins, failures in the ER folding machinery, malfunction of UPR signaling factors, or mutations in proteins involved in the degradation of aggregated proteins. All these cellular dysfunctions result in high levels of ER stress and are obvious, e.g., by dilation of ER cisternae due to the accumulation of unfolded or aggregated proteins. The cells react via UPR by a reduction of protein synthesis, an induction of additional folding enzymes, and by degradation of aggregated proteins. If these rescue mechanisms succeed, chondrocytes regain their normal function. If not, ECM protein synthesis is reduced for a longer period of time, proliferation decreases, differentiation of chondrocytes gets impaired, and apoptosis is augmented. All these changes critically impact bone development.

There are several essential steps in the endochondral ossification process and even slight imbalances at one or the other checkpoint affect the overall process. Long bone growth can be inhibited due to an ER stress-related reduced protein synthesis of cartilage ECM components by affected chondrocytes. The diminished ECM then leads to a reduced bone volume and manifests in a dwarfism disease. Another feature is an ER stress-induced change in chondrocyte proliferation or enhanced apoptosis. Together, this leads to a reduced number of chondrocytes in the growth plates affecting the overall process of endochondral ossification. In addition, ER stress-induced changes in the differentiation program of chondrocytes during endochondral ossification lead to dwarfism diseases. If only one of these necessary events fails, a normal bone development is impossible. This demonstrates that a finely tuned chondrocyte homeostasis with a distinct competence to cope with ER stress in all growth plate zones is essential for a regulated bone development and long bone growth.

7. ER Stress Also Affects Degenerative Cartilage Diseases Such As Osteoarthritis

ER stress, however, does not only affect temporary cartilage, which is involved in skeletal development. The function of permanent cartilage in various joints also is dependent on a regulated protein synthesis without enhanced ER stress levels. If this is altered, degenerative cartilage diseases, such as osteoarthritis (OA), may arise. OA is most likely associated with changes in protein synthesis and changes

in proliferation and differentiation of chondrocytes and enhanced apoptosis. These OA features are similar to ER stress-induced characteristics occurring during bone endochondral ossification.

In general, OA preferentially develops in the elderly. However, chondrodysplasias are often associated with cartilage degradation in young patients [37, 78]. Stickler syndrome, for example, is a dominantly inherited vitreoretinopathy and chondrodysplasia caused by mutations in the genes for types II and XI collagen [79, 80]. About 50% of all stickler syndrome patients develop severe cartilage erosion in diarthrodial joints before they get 30 years old, and this may be the result of ER stress in articular chondrocytes [81].

In the literature, various studies describe a link between osteoarthritis and ER stress [82–89]. During OA chondrocytes undergo activation, they proliferate and form cell clusters. In addition, the protein synthesis of both ECM molecules and matrix-degrading proteases increases [90], and thus, a high protein load arises in the ER. In late stages of OA, however, cartilage cells reduce their proliferation and die by apoptosis. With age, the expression and activity of folding enzymes for the ER and the UPR signaling decline [91]. Thus, an increased protein synthesis during OA and a weaker UPR response may induce ER stress, which cannot be compensated [92]. Moreover, the concentration of advanced glycation end products (AGEs) increases and AGEs are known to induce ER stress signaling [93, 94]. We assume that ER stress may contribute to the development of OA in young chondrodysplasia patients as well as in aged individuals.

In chondrocytes of osteoarthritis patients compared to cartilage cells of healthy controls, a 1.5-fold increase of ERp57 was detected. Simultaneously, calnexin and calreticulin were induced and the stimulation with thapsigargin, an ER stress inducer, increased the ERp57 expression in chondrocytes 2.8-fold [84]. Accordingly, ERp57 and the calnexin/calreticulin cycle appears to be particularly active during ER stress in osteoarthritic cartilage cells. We suggest to employ the cartilage-specific ERp57 KO mouse for a detailed analysis of the contribution of ER stress in the pathogenesis of different skeletal diseases, including OA.

8. Outlook/Conclusion

Various mouse models with prolonged or high levels of ER stress in growth plate chondrocytes display chondrodysplasia phenotypes suggesting ER stress as a pathogenic factor contributing to these skeletal diseases. We analyzed in detail the phenotype of the cartilage-specific ERp57 knockout mouse and demonstrated that the deficiency of this single ER-resident protein disulfide isomerase, which is responsible for the correct building of disulfide bridges in cartilage ECM glycoproteins, is sufficient to induce ER stress in chondrocytes and to cause an ER stress-related bone phenotype resembling a chondrodysplasia. This mouse line therefore qualifies as a novel model for the analysis of ER stress in chondrocytes. It may give new insights in ER stress-related short stature disorders and enables the analysis of the role

of ER stress in other cartilage diseases, such as osteoarthritis. By proteomic analysis, it would be possible to examine whether specific or all ECM proteins accumulate in the ER of ERp57 cKO mice. Comparable tests in different MED and PSACH mouse models with ER stress revealed genotype-specific differences, suggesting common and distinct disease signatures [95]. This shows that ER stress in different mouse models may have diverse effects. Therefore, multiple ER stress mouse models are valuable to examine cartilage diseases in further detail and to test therapeutics to intervene. Possible therapeutic options are as follows: (1) small molecular chemical chaperones, which efficiently support protein folding in the ER and ameliorate UPR signaling; (2) inhibitors of single UPR pathways, such as PERK signaling inhibitors [96]; (3) activators of ER-associated degradation and autophagy, such as carbamazepine [97]; or (4) inhibitors of excessive apoptosis. However, it is further to be tested whether such compounds alone or in combination are applicable to achieve improvement in ER stress-related cartilage disorders in patients.

Conflicts of Interest

The authors declare no conflicts of interests.

Acknowledgments

We would like to thank Uwe Hansen and Tobias Gronau for TEM and μ CT analyses of cartilage-specific ERp57 KO mice and Jeannine Wegner for proof reading the manuscript. The work was supported by the German Research Foundation (Grant DR455/3-1 to Rita Dreier).

References

- [1] H. M. Kronenberg, “Developmental regulation of the growth plate,” *Nature*, vol. 423, no. 6937, pp. 332–336, 2003.
- [2] E. J. Mackie, L. Tatarczuch, and M. Mirams, “The skeleton: a multi-functional complex organ. The growth plate chondrocyte and endochondral ossification,” *Journal of Endocrinology*, vol. 211, no. 2, pp. 109–121, 2011.
- [3] C. Hartmann, “Transcriptional networks controlling skeletal development,” *Current Opinion in Genetics & Development*, vol. 19, no. 5, pp. 437–443, 2009.
- [4] X. Zhou, K. von der Mark, S. Henry, W. Norton, H. Adams, and B. de Crombrughe, “Chondrocytes transdifferentiate into osteoblasts in endochondral bone during development, postnatal growth and fracture healing in mice,” *PLoS Genetics*, vol. 10, no. 12, article e1004820, 2014.
- [5] K. L. Cooper, S. Oh, Y. Sung, R. R. Dasari, M. W. Kirschner, and C. J. Tabin, “Multiple phases of chondrocyte enlargement underlie differences in skeletal proportions,” *Nature*, vol. 495, no. 7441, pp. 375–378, 2013.
- [6] E. Zelzer and B. R. Olsen, “The genetic basis for skeletal diseases,” *Nature*, vol. 423, no. 6937, pp. 343–348, 2003.
- [7] L. Bonafe, V. Cormier-Daire, C. Hall et al., “Nosology and classification of genetic skeletal disorders: 2015 revision,” *American Journal of Medical Genetics Part A*, vol. 167A, no. 12, pp. 2869–2892, 2015.

- [8] K. Gawron, "Endoplasmic reticulum stress in chondrodysplasias caused by mutations in collagen types II and X," *Cell Stress and Chaperones*, vol. 21, no. 6, pp. 943–958, 2016.
- [9] C. T. Brighton and R. B. Heppenstall, "Oxygen tension in zones of the epiphyseal plate, the metaphysis and diaphysis: an in vitro and in viro study in rats and rabbits," *The Journal of Bone & Joint Surgery*, vol. 53, no. 4, pp. 719–728, 1971.
- [10] I. A. Silver and A. Maroudas, "Measurement of pH and ionic composition of pericellular sites," *Philosophical Transactions of the Royal Society B: Biological Sciences*, vol. 271, no. 912, pp. 261–272, 1975.
- [11] S. Hisanaga, M. Miyake, S. Taniuchi et al., "PERK-mediated translational control is required for collagen secretion in chondrocytes," *Scientific Reports*, vol. 8, no. 1, p. 773, 2018.
- [12] M. Wang and R. J. Kaufman, "Protein misfolding in the endoplasmic reticulum as a conduit to human disease," *Nature*, vol. 529, no. 7586, pp. 326–335, 2016.
- [13] G. K. Voeltz, M. M. Rolls, and T. A. Rapoport, "Structural organization of the endoplasmic reticulum," *EMBO Reports*, vol. 3, no. 10, pp. 944–950, 2002.
- [14] L. Halperin, J. Jung, and M. Michalak, "The many functions of the endoplasmic reticulum chaperones and folding enzymes," *IUBMB Life*, vol. 66, no. 5, pp. 318–326, 2014.
- [15] Y. Ishida and K. Nagata, "Hsp47 as a collagen-specific molecular chaperone," *Methods in Enzymology*, vol. 499, pp. 167–182, 2011.
- [16] P. E. Shaw, "Peptidyl-prolyl isomerases: a new twist to transcription," *EMBO Reports*, vol. 3, no. 6, pp. 521–526, 2002.
- [17] M. Aebi, R. Bernasconi, S. Clerc, and M. Molinari, "N-glycan structures: recognition and processing in the ER," *Trends in Biochemical Sciences*, vol. 35, no. 2, pp. 74–82, 2010.
- [18] J. J. Caramelo and A. J. Parodi, "Getting in and out from calnexin/calreticulin cycles," *Journal of Biological Chemistry*, vol. 283, no. 16, pp. 10221–10225, 2008.
- [19] K. McCaffrey and I. Braakman, "Protein quality control at the endoplasmic reticulum," *Essays in Biochemistry*, vol. 60, no. 2, pp. 227–235, 2016.
- [20] C. E. Jessop, T. J. Tavender, R. H. Watkins, J. E. Chambers, and N. J. Bulleid, "Substrate specificity of the oxidoreductase ERp57 is determined primarily by its interaction with calnexin and calreticulin," *Journal of Biological Chemistry*, vol. 284, no. 4, pp. 2194–2202, 2009.
- [21] J. D. Oliver, F. J. Van der Wal, N. J. Bulleid, and S. High, "Interaction of the thiol-dependent reductase ERp57 with nascent glycoproteins," *Science*, vol. 275, no. 5296, pp. 86–88, 1997.
- [22] A. Hettinghouse, R. Liu, and C. J. Liu, "Multifunctional molecule ERp57: from cancer to neurodegenerative diseases," *Pharmacology & Therapeutics*, vol. 181, pp. 34–48, 2018.
- [23] E. Fujita, Y. Kouroku, A. Isoai et al., "Two endoplasmic reticulum-associated degradation (ERAD) systems for the novel variant of the mutant dysferlin: ubiquitin/proteasome ERAD(I) and autophagy/lysosome ERAD(II)," *Human Molecular Genetics*, vol. 16, no. 6, pp. 618–629, 2007.
- [24] R. J. Kaufman, "Orchestrating the unfolded protein response in health and disease," *The Journal of Clinical Investigation*, vol. 110, no. 10, pp. 1389–1398, 2002.
- [25] C. Hetz, "The unfolded protein response: controlling cell fate decisions under ER stress and beyond," *Nature Reviews Molecular Cell Biology*, vol. 13, no. 2, pp. 89–102, 2012.
- [26] Y. Kozutsumi, M. Segal, K. Normington, M. J. Gething, and J. Sambrook, "The presence of malfolded proteins in the endoplasmic reticulum signals the induction of glucose-regulated proteins," *Nature*, vol. 332, no. 6163, pp. 462–464, 1988.
- [27] P. Walter and D. Ron, "The unfolded protein response: from stress pathway to homeostatic regulation," *Science*, vol. 334, no. 6059, pp. 1081–1086, 2011.
- [28] K. Haze, H. Yoshida, H. Yanagi, T. Yura, and K. Mori, "Mammalian transcription factor ATF6 is synthesized as a transmembrane protein and activated by proteolysis in response to endoplasmic reticulum stress," *Molecular Biology of the Cell*, vol. 10, no. 11, pp. 3787–3799, 1999.
- [29] C. Y. Liu, M. Schroder, and R. J. Kaufman, "Ligand-independent dimerization activates the stress response kinases IRE1 and PERK in the lumen of the endoplasmic reticulum," *Journal of Biological Chemistry*, vol. 275, no. 32, pp. 24881–24885, 2000.
- [30] J. Hollien and J. S. Weissman, "Decay of endoplasmic reticulum-localized mRNAs during the unfolded protein response," *Science*, vol. 313, no. 5783, pp. 104–107, 2006.
- [31] H. P. Harding, Y. Zhang, A. Bertolotti, H. Zeng, and D. Ron, "Perk is essential for translational regulation and cell survival during the unfolded protein response," *Molecular Cell*, vol. 5, no. 5, pp. 897–904, 2000.
- [32] H. P. Harding, I. Novoa, Y. Zhang et al., "Regulated translation initiation controls stress-induced gene expression in mammalian cells," *Molecular Cell*, vol. 6, no. 5, pp. 1099–1108, 2000.
- [33] K. Hata, Y. Takahata, T. Murakami, and R. Nishimura, "Transcriptional network controlling endochondral ossification," *Journal of Bone Metabolism*, vol. 24, no. 2, pp. 75–82, 2017.
- [34] X. Kang, W. Yang, D. Feng et al., "Cartilage-specific autophagy deficiency promotes ER stress and impairs chondrogenesis in PERK-ATF4-CHOP-dependent manner," *Journal of Bone and Mineral Research*, vol. 32, no. 10, pp. 2128–2141, 2017.
- [35] M. Ni and A. S. Lee, "ER chaperones in mammalian development and human diseases," *FEBS Letters*, vol. 581, no. 19, pp. 3641–3651, 2007.
- [36] R. P. Boot-Handford and M. D. Briggs, "The unfolded protein response and its relevance to connective tissue diseases," *Cell and Tissue Research*, vol. 339, no. 1, pp. 197–211, 2010.
- [37] S. E. Patterson and C. N. Dealy, "Mechanisms and models of endoplasmic reticulum stress in chondrodysplasia," *Developmental Dynamics*, vol. 243, no. 7, pp. 875–893, 2014.
- [38] Y. Masago, A. Hosoya, K. Kawasaki et al., "The molecular chaperone Hsp47 is essential for cartilage and endochondral bone formation," *Journal of Cell Science*, vol. 125, no. 5, pp. 1118–1128, 2012.
- [39] T. L. Cameron, I. L. Gresshoff, K. M. Bell et al., "Cartilage-specific ablation of XBP1 signaling in mouse results in a chondrodysplasia characterized by reduced chondrocyte proliferation and delayed cartilage maturation and mineralization," *Osteoarthritis and Cartilage*, vol. 23, no. 4, pp. 661–670, 2015.
- [40] W. Wang, N. Lian, L. Li et al., "Atf4 regulates chondrocyte proliferation and differentiation during endochondral ossification by activating *Ihh* transcription," *Development*, vol. 136, no. 24, pp. 4143–4153, 2009.
- [41] C. Gentili and R. Cancedda, "Cartilage and bone extracellular matrix," *Current Pharmaceutical Design*, vol. 15, no. 12, pp. 1334–1348, 2009.

- [42] P. Kannu, J. Bateman, and R. Savarirayan, "Clinical phenotypes associated with type II collagen mutations," *Journal of Paediatrics and Child Health*, vol. 48, no. 2, pp. E38–E43, 2012.
- [43] G. Liang, C. Lian, D. Huang et al., "Endoplasmic reticulum stress-unfolding protein response-apoptosis cascade causes chondrodysplasia in a *col2a1* p.Gly1170Ser mutated mouse model," *PLoS One*, vol. 9, no. 1, article e86894, 2014.
- [44] M. Arita, S. W. Li, G. Kopen, E. Adachi, S. A. Jimenez, and A. Fertala, "Skeletal abnormalities and ultrastructural changes of cartilage in transgenic mice expressing a collagen II gene (COL2A1) with a Cys for Arg- α 1-519 substitution," *Osteoarthritis and Cartilage*, vol. 10, no. 10, pp. 808–815, 2002.
- [45] M. Arita, J. Fertala, C. Hou, A. Steplewski, and A. Fertala, "Mechanisms of aberrant organization of growth plates in conditional transgenic mouse model of spondyloepiphyseal dysplasia associated with the R992C substitution in collagen II," *The American Journal of Pathology*, vol. 185, no. 1, pp. 214–229, 2015.
- [46] J. Fertala, M. Arita, A. Steplewski, W. V. Arnold, and A. Fertala, "Epiphyseal growth plate architecture is unaffected by early postnatal activation of the expression of R992C collagen II mutant," *Bone*, vol. 112, pp. 42–50, 2018.
- [47] S. A. Chakkalakal, J. Heilig, U. Baumann, M. Paulsson, and F. Zaucke, "Impact of arginine to cysteine mutations in collagen II on protein secretion and cell survival," *International Journal of Molecular Sciences*, vol. 19, no. 2, 2018.
- [48] B. Budde, K. Blumbach, J. Ylostalo et al., "Altered integration of matrilin-3 into cartilage extracellular matrix in the absence of collagen IX," *Molecular and Cellular Biology*, vol. 25, no. 23, pp. 10465–10478, 2005.
- [49] M. P. Leighton, S. Nundlall, T. Starborg et al., "Decreased chondrocyte proliferation and dysregulated apoptosis in the cartilage growth plate are key features of a murine model of epiphyseal dysplasia caused by a *matn3* mutation," *Human Molecular Genetics*, vol. 16, no. 14, pp. 1728–1741, 2007.
- [50] C. L. Hartley, S. Edwards, L. Mullan et al., "Armet/Manf and Creld2 are components of a specialized ER stress response provoked by inappropriate formation of disulphide bonds: implications for genetic skeletal diseases," *Human Molecular Genetics*, vol. 22, no. 25, pp. 5262–5275, 2013.
- [51] S. Nundlall, M. H. Rajpar, P. A. Bell et al., "An unfolded protein response is the initial cellular response to the expression of mutant matrilin-3 in a mouse model of multiple epiphyseal dysplasia," *Cell Stress and Chaperones*, vol. 15, no. 6, pp. 835–849, 2010.
- [52] M. D. Briggs and K. L. Chapman, "Pseudoachondroplasia and multiple epiphyseal dysplasia: mutation review, molecular interactions, and genotype to phenotype correlations," *Human Mutation*, vol. 19, no. 5, pp. 465–478, 2002.
- [53] K. A. Pirog-Garcia, R. S. Meadows, L. Knowles et al., "Reduced cell proliferation and increased apoptosis are significant pathological mechanisms in a murine model of mild pseudoachondroplasia resulting from a mutation in the C-terminal domain of COMP," *Human Molecular Genetics*, vol. 16, no. 17, pp. 2072–2088, 2007.
- [54] M. D. Briggs, G. R. Mortier, W. G. Cole et al., "Diverse mutations in the gene for cartilage oligomeric matrix protein in the pseudoachondroplasia-multiple epiphyseal dysplasia disease spectrum," *American Journal of Human Genetics*, vol. 62, no. 2, pp. 311–319, 1998.
- [55] K. A. Pirog, A. Irman, S. Young et al., "Abnormal chondrocyte apoptosis in the cartilage growth plate is influenced by genetic background and deletion of CHOP in a targeted mouse model of pseudoachondroplasia," *PLoS One*, vol. 9, no. 2, article e85145, 2014.
- [56] M. Schmitz, A. Niehoff, N. Miosge, N. Smyth, M. Paulsson, and F. Zaucke, "Transgenic mice expressing D469 Δ mutated cartilage oligomeric matrix protein (COMP) show growth plate abnormalities and sternal malformations," *Matrix Biology*, vol. 27, no. 2, pp. 67–85, 2008.
- [57] F. Suleman, B. Gualeni, H. J. Gregson et al., "A novel form of chondrocyte stress is triggered by a COMP mutation causing pseudoachondroplasia," *Human Mutation*, vol. 33, no. 1, pp. 218–231, 2012.
- [58] M. S. P. Ho, K. Y. Tsang, R. L. K. Lo et al., "COL10A1 nonsense and frame-shift mutations have a gain-of-function effect on the growth plate in human and mouse metaphyseal chondrodysplasia type Schmid," *Human Molecular Genetics*, vol. 16, no. 10, pp. 1201–1215, 2007.
- [59] K. Y. Tsang, D. Chan, D. Cheslett et al., "Surviving endoplasmic reticulum stress is coupled to altered chondrocyte differentiation and function," *PLoS Biology*, vol. 5, no. 3, article e44, 2007.
- [60] L. H. W. Kung, M. H. Rajpar, R. Preziosi, M. D. Briggs, and R. P. Boot-Handford, "Increased classical endoplasmic reticulum stress is sufficient to reduce chondrocyte proliferation rate in the growth plate and decrease bone growth," *PLoS One*, vol. 10, no. 2, article e0117016, 2015.
- [61] M. H. Rajpar, B. McDermott, L. Kung et al., "Targeted induction of endoplasmic reticulum stress induces cartilage pathology," *PLoS Genetics*, vol. 5, no. 10, article e1000691, 2009.
- [62] S. Ito and K. Nagata, "Biology of Hsp47 (serpin H1), a collagen-specific molecular chaperone," *Seminars in Cell & Developmental Biology*, vol. 62, pp. 142–151, 2017.
- [63] A. Linz, Y. Knieper, T. Gronau et al., "ER stress during the pubertal growth spurt results in impaired long-bone growth in chondrocyte-specific ERp57 knockout mice," *Journal of Bone and Mineral Research*, vol. 30, no. 8, pp. 1481–1493, 2015.
- [64] L. Ellgaard and L. W. Ruddock, "The human protein disulphide isomerase family: substrate interactions and functional properties," *EMBO Reports*, vol. 6, no. 1, pp. 28–32, 2005.
- [65] J. D. Oliver, H. L. Roderick, D. H. Llewellyn, and S. High, "ERp57 functions as a subunit of specific complexes formed with the ER lectins calreticulin and calnexin," *Molecular Biology of the Cell*, vol. 10, no. 8, pp. 2573–2582, 1999.
- [66] H. Coe, J. Jung, J. Groenendyk, D. Prins, and M. Michalak, "ERp57 modulates STAT3 signaling from the lumen of the endoplasmic reticulum," *Journal of Biological Chemistry*, vol. 285, no. 9, pp. 6725–6738, 2010.
- [67] C. E. Jessop, S. Chakravarthi, N. Garbi, G. J. Hammerling, S. Lovell, and N. J. Bulleid, "ERp57 is essential for efficient folding of glycoproteins sharing common structural domains," *The EMBO Journal*, vol. 26, no. 1, pp. 28–40, 2007.
- [68] F. J. Guo, Z. Xiong, X. Han et al., "XBP1S, a BMP2-inducible transcription factor, accelerates endochondral bone growth by activating GEP growth factor," *Journal of Cellular and Molecular Medicine*, vol. 18, no. 6, pp. 1157–1171, 2014.
- [69] B. Shu, M. Zhang, R. Xie et al., "BMP2, but not BMP4, is crucial for chondrocyte proliferation and maturation during endochondral bone development," *Journal of Cell Science*, vol. 124, no. 20, pp. 3428–3440, 2011.

- [70] D. Patra, X. Xing, S. Davies et al., "Site-1 protease is essential for endochondral bone formation in mice," *The Journal of Cell Biology*, vol. 179, no. 4, pp. 687–700, 2007.
- [71] B. N. Lilley and H. L. Ploegh, "Multiprotein complexes that link dislocation, ubiquitination, and extraction of misfolded proteins from the endoplasmic reticulum membrane," *Proceedings of the National Academy of Sciences of the United States of America*, vol. 102, no. 40, pp. 14296–14301, 2005.
- [72] S. K. Dougan, C. C. A. Hu, M. E. Paquet et al., "Derlin-2-deficient mice reveal an essential role for protein dislocation in chondrocytes," *Molecular and Cellular Biology*, vol. 31, no. 6, pp. 1145–1159, 2011.
- [73] F. Hall-Glenn, A. Aivazi, L. Akopyan et al., "CCN2/CTGF is required for matrix organization and to protect growth plate chondrocytes from cellular stress," *Journal of Cell Communication and Signaling*, vol. 7, no. 3, pp. 219–230, 2013.
- [74] V. Srinivas, J. Bohensky, A. M. Zahm, and I. M. Shapiro, "Autophagy in mineralizing tissues: microenvironmental perspectives," *Cell Cycle*, vol. 8, no. 3, pp. 391–393, 2009.
- [75] A. Saito, S. Hino, T. Murakami et al., "Regulation of endoplasmic reticulum stress response by a BBF2H7-mediated Sec23a pathway is essential for chondrogenesis," *Nature Cell Biology*, vol. 11, no. 10, pp. 1197–1204, 2009.
- [76] A. Saito, S. Kanemoto, Y. Zhang, R. Asada, K. Hino, and K. Imaizumi, "Chondrocyte proliferation regulated by secreted luminal domain of ER stress transducer BBF2H7/CREB3L2," *Molecular Cell*, vol. 53, no. 1, pp. 127–139, 2014.
- [77] I. M. Bird, S. H. Kim, D. K. Schweppe et al., "The skeletal phenotype of achondrogenesis type 1A is caused exclusively by cartilage defects," *Development*, vol. 145, no. 1, 2018.
- [78] A. Hughes, A. E. Oxford, K. Tawara, C. L. Jorczyk, and J. T. Oxford, "Endoplasmic reticulum stress and unfolded protein response in cartilage pathophysiology; contributing factors to apoptosis and osteoarthritis," *International Journal of Molecular Sciences*, vol. 18, no. 3, 2017.
- [79] N. N. Ahmad, L. Ala-Kokko, R. G. Knowlton et al., "Stop codon in the procollagen II gene (COL2A1) in a family with the Stickler syndrome (arthro-ophthalmopathy)," *Proceedings of the National Academy of Sciences of the United States of America*, vol. 88, no. 15, pp. 6624–6627, 1991.
- [80] A. J. Richards, J. R. Yates, R. Williams et al., "A family with Stickler syndrome type 2 has a mutation in the *COL11A1* gene resulting in the substitution of glycine 97 by valine in $\alpha 1(XI)$ collagen," *Human Molecular Genetics*, vol. 5, no. 9, pp. 1339–1343, 1996.
- [81] T. Couchouron and C. Masson, "Early-onset progressive osteoarthritis with hereditary progressive ophthalmopathy or Stickler syndrome," *Joint, Bone, Spine*, vol. 78, no. 1, pp. 45–49, 2011.
- [82] K. Horiuchi, T. Tohmonda, and H. Morioka, "The unfolded protein response in skeletal development and homeostasis," *Cellular and Molecular Life Sciences*, vol. 73, no. 15, pp. 2851–2869, 2016.
- [83] A. Hosseinzadeh, S. K. Kamrava, M. T. Joghataei et al., "Apoptosis signaling pathways in osteoarthritis and possible protective role of melatonin," *Journal of Pineal Research*, vol. 61, no. 4, pp. 411–425, 2016.
- [84] Y. H. Li, G. Tardif, D. Hum et al., "The unfolded protein response genes in human osteoarthritic chondrocytes: PERK emerges as a potential therapeutic target," *Arthritis Research & Therapy*, vol. 18, no. 1, p. 172, 2016.
- [85] R. Liu-Bryan and R. Terkeltaub, "Emerging regulators of the inflammatory process in osteoarthritis," *Nature Reviews Rheumatology*, vol. 11, no. 1, pp. 35–44, 2015.
- [86] A. E. Nugent, D. M. Speicher, I. Gradisar et al., "Advanced osteoarthritis in humans is associated with altered collagen VI expression and upregulation of ER-stress markers Grp78 and bag-1," *Journal of Histochemistry & Cytochemistry*, vol. 57, no. 10, pp. 923–931, 2009.
- [87] K. Takada, J. Hirose, K. Senba et al., "Enhanced apoptotic and reduced protective response in chondrocytes following endoplasmic reticulum stress in osteoarthritic cartilage," *International Journal of Experimental Pathology*, vol. 92, no. 4, pp. 232–242, 2011.
- [88] Y. Uehara, J. Hirose, S. Yamabe et al., "Endoplasmic reticulum stress-induced apoptosis contributes to articular cartilage degeneration via C/EBP homologous protein," *Osteoarthritis and Cartilage*, vol. 22, no. 7, pp. 1007–1017, 2014.
- [89] X. Yuan, H. Liu, L. Li et al., "The roles of endoplasmic reticulum stress in the pathophysiological development of cartilage and chondrocytes," *Current Pharmaceutical Design*, vol. 23, no. 11, pp. 1693–1704, 2017.
- [90] M. B. Goldring and K. B. Marcu, "Cartilage homeostasis in health and rheumatic diseases," *Arthritis Research & Therapy*, vol. 11, no. 3, p. 224, 2009.
- [91] M. K. Brown and N. Naidoo, "The endoplasmic reticulum stress response in aging and age-related diseases," *Frontiers in Physiology*, vol. 3, p. 263, 2012.
- [92] C. Lopez-Otin, M. A. Blasco, L. Partridge, M. Serrano, and G. Kroemer, "The hallmarks of aging," *Cell*, vol. 153, no. 6, pp. 1194–1217, 2013.
- [93] C. Adamopoulos, E. Farmaki, E. Spilioti, H. Kiaris, C. Piperi, and A. G. Papavassiliou, "Advanced glycation end-products induce endoplasmic reticulum stress in human aortic endothelial cells," *Clinical Chemistry and Laboratory Medicine*, vol. 52, no. 1, pp. 151–160, 2014.
- [94] S. Yamabe, J. Hirose, Y. Uehara et al., "Intracellular accumulation of advanced glycation end products induces apoptosis via endoplasmic reticulum stress in chondrocytes," *FEBS Journal*, vol. 280, no. 7, pp. 1617–1629, 2013.
- [95] P. A. Bell, R. Wagener, F. Zaucke et al., "Analysis of the cartilage proteome from three different mouse models of genetic skeletal diseases reveals common and discrete disease signatures," *Biology Open*, vol. 2, no. 8, pp. 802–811, 2013.
- [96] C. Wang, Z. Tan, B. Niu et al., "Inhibiting the integrated stress response pathway prevents aberrant chondrocyte differentiation thereby alleviating chondrodysplasia," *eLife*, vol. 7, 2018.
- [97] L. A. Mullan, E. J. Mularczyk, L. H. Kung et al., "Increased intracellular proteolysis reduces disease severity in an ER stress-associated dwarfism," *The Journal of Clinical Investigation*, vol. 127, no. 10, pp. 3861–3865, 2017.

Research Article

Methane-Rich Saline Ameliorates Sepsis-Induced Acute Kidney Injury through Anti-Inflammation, Antioxidative, and Antiapoptosis Effects by Regulating Endoplasmic Reticulum Stress

Yifan Jia,¹ Zeyu Li,¹ Yang Feng,² Ruixia Cui³,³ Yanyan Dong,¹ Xing Zhang,¹ Xiaohong Xiang,¹ Kai Qu¹,¹ Chang Liu^{1,4},^{1,4} and Jingyao Zhang^{1,4}

¹Department of Hepatobiliary Surgery, The First Affiliated Hospital of Xi'an Jiaotong University, Xi'an Shaanxi 710061, China

²Department of Immunology, Shaanxi University of Chinese Medicine, Xianyang Shaanxi 712046, China

³Department of ICU, The First Affiliated Hospital of Xi'an Jiaotong University, Xi'an Shaanxi 710061, China

⁴Department of SICU, The First Affiliated Hospital of Xi'an Jiaotong University, Xi'an Shaanxi 710061, China

Correspondence should be addressed to Kai Qu; joanne8601@163.com, Chang Liu; liuchangdoctor@163.com, and Jingyao Zhang; you12ouy@163.com

Received 14 July 2018; Accepted 14 September 2018; Published 15 November 2018

Guest Editor: Dariusz Pytel

Copyright © 2018 Yifan Jia et al. This is an open access article distributed under the Creative Commons Attribution License, which permits unrestricted use, distribution, and reproduction in any medium, provided the original work is properly cited.

Sepsis-induced acute kidney injury (AKI) is a severe complication of sepsis and an important cause of mortality in septic patients. Previous investigations showed that methane had protective properties against different diseases in animal models. This study is aimed at investigating whether methane-rich saline (MRS) has a protective effect against sepsis-induced AKI. Sepsis was induced in wild-type C57BL/6 mice by cecal ligation and puncture (CLP), and the mice were divided into three groups: a sham control group (sham), a surgery group with saline intraperitoneal injection (i.p.) treatment (CLP + NS), and a surgery group with MRS i.p. treatment (CLP + MRS). 24 h after the establishment of the sepsis, the blood and kidney tissues of mice in all groups were collected. According to the serum levels of blood urea nitrogen (BUN) and creatinine (CRE) and a histologic analysis, which included hematoxylin-eosin (H&E) staining and periodic acid-Schiff (PAS) staining, MRS treatment protected renal function and tissues from acute injury. Additionally, MRS treatment significantly ameliorated apoptosis, based on the levels of apoptosis-related protein makers, including cleaved caspase-3 and cleaved PARP, and the levels of Bcl-2/Bax expression and TUNEL staining. In addition, the endoplasmic reticulum (ER) stress-related glucose-regulated protein 78 (GRP78)/activating transcription factor 4 (ATF4)/C/EBP homologous protein (CHOP)/caspase-12 apoptosis signaling pathway was significantly suppressed in the CLP + MRS group. The levels of inflammation and oxidative stress were also reduced after MRS treatment. These results showed that MRS has the potential to ameliorate sepsis-induced acute kidney injury through its anti-inflammatory, antioxidative, and antiapoptosis properties.

1. Introduction

Sepsis-induced acute kidney injury (AKI) is a severe complication of sepsis and a leading cause of mortality in intensive care unit (ICU) patients. Among critically ill patients, the morbidity of acute renal injury can be up to 70%, and approximately 5% of these patients progress to acute renal failure during their hospital stays. The overall ICU mortality rate of acute renal failure is approximately 50%, and 15% of survivors continued to rely on renal replacement therapy

(RRT) after they were discharged. The leading cause of acute kidney injury is sepsis, which contributes to the 50% of the incidence [1–4]. Despite advances in clinical treatment and intensive care, there is currently no specific therapy for septic AKI; however, the early onset of RRT may reduce mortality [5]. Septic AKI is the result of a series of complex interactions between vascular endothelial cell dysfunction, subsequent inflammation, and tubular cell damage [6]. Additionally, recent research has suggested that apoptosis and immune suppression, especially the apoptosis of tubular cells, may

be involved in the pathological process of septic AKI, which is quite different from the other types of AKI [7].

During the sepsis process, the accumulation of unfolded protein in endoplasmic reticulum (ER), which is called ER stress, triggers an evolutionarily conserved unfolded protein response (UPR) to reestablish cellular homeostasis. Three transmembrane proteins, including inositol-requiring enzyme 1 (IRE1 α), PKR-like ER kinase (PERK), and activating transcription factor 6 (ATF6), are initially activated and accelerate the unfolded protein response by activating downstream signaling pathways. However, prolonged UPR can lead to an excessive ER stress and result in C/EBP homologous protein-(CHOP-) mediated apoptosis [8]. During sepsis-induced acute kidney injury, ER stress also plays an important role [9, 10].

Methane, the simplest organic compound, can be detected in 30%–50% of healthy adults around the world and has been deemed to have little physiological activity for decades. However, many recent studies have discovered that methane has several important biological effects that can protect cells and organs from inflammation, oxidative stress, and apoptosis [11–14]. It is notable that methane could play a protective role in the cellular apoptosis process. Methane could remarkably attenuate the expression of the proapoptotic protein Bax and increase the expression of Bcl-2, which resulted in the downregulation of caspase-3 and other downstream caspases, thus suppressing the activation of the mitochondrial apoptotic pathway [15]. Based on these protective effects, methane has been considered a possible therapeutic agent for several diseases, including acute lung injury, autoimmune hepatitis, and spinal cord injury [13, 16, 17]. However, there has been little investigation regarding whether methane can protect the kidney from septic AKI. Accordingly, we hypothesize that methane has a protective effect against septic AKI and aim to prove it using a CLP-induced sepsis model. We also examined whether ER stress played a key role in the mechanism underlying this effect and provided some suggestions for the use of methane in clinical practice.

2. Materials and Methods

2.1. Animals. Healthy female wild-type C57BL/6 mice (6–7 weeks old, weighing 20–25 g) were obtained from the Animal Feeding Center of Xi'an Jiaotong University Health Science Center. All the mice were maintained at a constant temperature of 25°C and a humidity of 50% and fed with a standard diet with open access to tap water under a 12:12 day/night cycle for 7 days before the experiments. The animal experiment was performed in accordance with the Guide of Laboratory Animal Care and Use from the United States National Institution of Health and was approved and supervised by the Institutional Animal Care and Use Committee of the Ethics Committee of Xi'an Jiaotong University Health Science Center, China.

2.2. Animal Model of CLP. The sepsis model was established as previously described [18]. Mice were anesthetized by 50 mg/kg pentobarbital sodium (i.p.), and laparotomy was performed to isolate the cecum of mice along the midline of

the abdomen, ligating the 1/3 cecal tip with a 4-0 silk suture. The cecum was separated with forceps and punctured twice, and one column of fecal material was squeezed out. The cecum was returned to its original location, and the abdomen closed in layers with a 4-0 silk suture. The mice were put back in their cages until they completely recovered. The sham operation was performed by only incising the abdomen, separating and exposing the cecum for 5 minutes, then closing it in layers.

2.3. Experimental Groups and Drug Treatment. Mice were randomly divided into the three groups: (1) sham group ($n = 6$): the C57BL/6 mice received a sham laparotomy operation. (2) Normal saline group ($n = 12$): the C57BL/6 mice underwent a laparotomy operation with CLP; meanwhile, the normal saline was administered at 10 mL/kg dosage every 4 hours as a control (CLP+NS group). (3) Methane-rich saline group ($n = 12$): the C57BL/6 mice received a laparotomy operation with CLP and were given an intraperitoneal injection (i.p.) of methane-rich saline (MRS) at 10 mL/kg (CLP+MRS group) every 4 hours after a successful sepsis model establishment [14]. 24 hours after the surgery, all animals were euthanized; kidney and blood samples were collected for quantification of biochemical analysis.

2.4. Methane-Rich Saline Production. The production method of the MRS was described by Ye et al. [19]. Briefly, normal saline was saturated with pure methane (>99.999%) in a high-pressure vessel (Wuhan Newradar Special Gas Co. Ltd., Wuhan, China) under 0.4 MPa for 4 h, stored at 4°C, and freshly prepared 24 h before administration to the animals to ensure the methane concentration. The concentration of the methane was detected as previous described [20].

2.5. Renal Function Analysis. Blood samples ($n = 6$) were collected from the eyeballs of the mice and centrifuged at 4°C for 15 min at 1500 $\times g$ in tubes. Renal functions were evaluated by BUN and CRE levels, which were detected by a Hitachi 7600-20 automatic biochemical analyzer (Clinical Laboratory of the First Affiliated Hospital of Xi'an Jiaotong University, Xi'an, China).

2.6. Histopathological Examination. Kidney tissue samples ($n = 6$) were gathered 24 h after surgery and fixed in 10% formalin solution. Serial 5 μ m sections were stained with hematoxylin and eosin (H&E). The histologic changes and the quantity of infiltrated neutrophils were assessed in a double-blinded way to randomly select five different fields in each sample through the light microscope. Then, the samples were embedded in paraffin and sectioned into 5 μ m thick sections and stained with periodic acid-Schiff (PAS). Histological changes in the cortex and in the outer stripe of the outer medulla (OSOM) were assessed by quantitative measures of tissue damage by a blind observation. Tubular damage was defined as tubular epithelial swelling, loss of brush border, vacuolar degeneration, necrotic tubules, cast formation, and desquamation. The degree of kidney damage was estimated at $\times 200$ magnification, using five randomly selected fields for each animal, by the following criteria: 0, normal; 1, area of damage < 25% of tubules; 2, damage

involving 25–50% of tubules; 3, damage involving 50–75% of tubules; and 4, damage involving 75–100% of tubules [21].

2.7. Cytokine Detection. Kidney tissues from different groups ($n = 6$) were homogenized with PBS on ice and then centrifuged at 4°C for 40 min at 12,000 rpm. Subsequently, the supernatants were collected to perform ELISA. We used commercially available ELISA kits to detect the levels of inflammatory cytokines, including TNF- α , IL-6, and IL-1 β (Jiancheng Bioengineering Institute, Nanjing, China), in kidney tissue according to the manufacturer's recommendation.

2.8. Reactive Oxidative Stress Activity Assay. The kidney tissue ($n = 6$) homogenate produced was previously described to measure the oxidative stress indexes. The level of malondialdehyde (MDA) in the tissue was taken as the level of lipid oxidation in the tissue, while the superoxide dismutase (SOD) was the index of the tissue antioxidant. The levels of MDA and the activities of SOD in kidney tissues were detected by commercial biochemical kits (Jiancheng Bioengineering Institute, Nanjing, China) following the manufacturer's instructions.

2.9. Detection of ROS Activation. Tissue samples ($n = 6$) were fixed with 10% formaldehyde and dehydrated using 30% sucrose solution. The sections (4 μ m thick) were incubated with dihydroethidium (DHE; 10 μ M) (Vigorous Biotechnology Co. Ltd., Beijing, China). After 60 min in the dark, the specimens were washed with adequate volumes of PBS. DHE oxidized by ROS in the cells could show red emission.

2.10. Western Blot Assay. The protein expression in kidney tissue ($n = 6$) was detected by Western blot. In brief, RIPA lysis buffer was used to extract the total protein and nucleoprotein at 14000g for 15 min at 4°C. After the protein concentration was determined, the lysates were separated using sodium dodecyl sulfate-polyacrylamide gel electrophoresis (SDS-PAGE). The proteins were transferred onto polyvinylidene difluoride (PVDF) membranes. The resulting blots were blocked with 8% skim milk and incubated with an anti-GRP78 antibody (1:5000; Proteintech, China), an anti-ATF4 antibody (1:1000; Proteintech, China), anti-caspase-12 antibodies (1:1000; Cell Signaling Technology (CST), USA), anti-IL-1 β antibodies (1:1000; Abcam, USA), anti-TNF- α (1:500; Abcam, USA), anti-Bcl2 antibodies (1:1000; Bioss, China), anti-Bax antibodies (1:2000; Proteintech, China), anti-cleaved-caspase-3 antibodies (1:1000; Cell Signaling Technology (CST), USA), anti-PARP antibodies (1:1000; Cell Signaling Technology (CST), USA), and anti- β -actin antibodies (1:10000; Santa Cruz Biotechnology, USA) overnight at 4°C. Subsequently, the blots were washed three times with PBS and incubated with anti-rabbit and anti-mouse horseradish peroxidase-conjugated secondary antibodies (1:10000; Abmart, China) for 1 h at 37°C. The proteins were detected with the chemiluminescence (ECL) system. The expressions of proteins were normalized to β -actin as a reference.

2.11. Immunohistochemical Analysis. Twenty-four hours after the CLP operation, the kidney tissues ($n = 6$) were

gathered and processed for immunohistochemistry to estimate the activation of CHOP and IL-1 β . Briefly, the kidney tissues were fixed into 4% paraformaldehyde and then embedded in paraffin and cut into 4 μ m thick sections. The sections were deparaffinized with xylene and rehydrated with serial gradient ethanol. After incubation with 3% hydrogen peroxide for 15 min to block endogenous peroxidase activity, the sections were blocked with goat serum and then incubated with primary antibodies against CHOP (1:500; Bioss, China) and IL-1 β (1:150; Proteintech, China) overnight at 4°C. After those procedures, the sections were washed with PBS three times and incubated with biotinylated secondary antibodies at room temperature for 40 min. Finally, the sections were incubated with diaminobenzidine tetrahydrochloride (DAB), counterstained with hematoxylin, and mounted for microscopic examination. The images were selected at 200 \times magnification, and five fields were captured randomly.

2.12. Detection of the Apoptosis Rate by TUNEL Staining. The apoptosis rate of the kidney tissue ($n = 6$) was detected by TdT-mediated dUTP nick-end labeling (TUNEL) staining 24 h after sepsis. The experiment was carried out strictly according to the instructions of the TUNEL kit (Roche Molecular Biochemicals, Indianapolis, IN, USA). The images were selected at 200 \times magnification, and five fields were captured randomly.

2.13. Statistical Analysis. The measurement data were described as the mean \pm standard deviation (SD). All statistical analyses were performed by the SPSS 18.0 software (SPSS Inc., Chicago, USA). Student's *t*-test or one-way analysis of variance (ANOVA) was used for the comparison among the groups. The figure was made by GraphPad (version 7) Prism software (GraphPad Software, La Jolla, CA). All tests were two sided, and significance was accepted at $P < 0.05$.

3. Results

3.1. Methane-Rich Saline Protected Kidney Functions in CLP Mice. First, we investigated whether MRS can improve kidney function during the sepsis process. Blood urea nitrogen (BUN) and serum creatinine (CRE) are the products of protein metabolism and are used as indicators of kidney function. Elevated levels of BUN and CRE were observed after the establishment of the CLP model, confirming that the sepsis model was successfully constructed (Figure 1). However, in the CLP + MRS group, the levels of BUN and CRE were reduced dramatically compared to those of the CLP + NS group ($P < 0.05$).

3.2. Methane-Rich Saline Attenuated Histopathological Damage in the Kidneys of CLP Mice. We then attempted to confirm the histopathological damage among the different groups. The H&E staining was performed on kidney tissue slices. There was little histopathological damage observed in the sham group. Widespread degeneration and necrosis were observed in tubular epithelial cells in the CLP + NS group. However, there was slight damage, including tubular epithelial swelling and brush border injury, in the CLP + MRS group (Figure 2(a)). We calculated the number of infiltrated

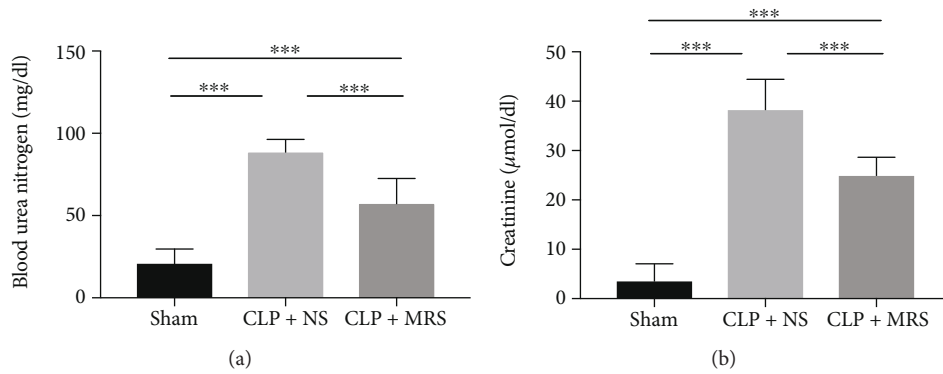


FIGURE 1: Methane-rich saline protected kidney function in CLP mice. (a) The blood urea nitrogen level in mouse serum. (b) The creatinine level in mice serum. * $P < 0.05$, ** $P < 0.01$, and *** $P < 0.001$.

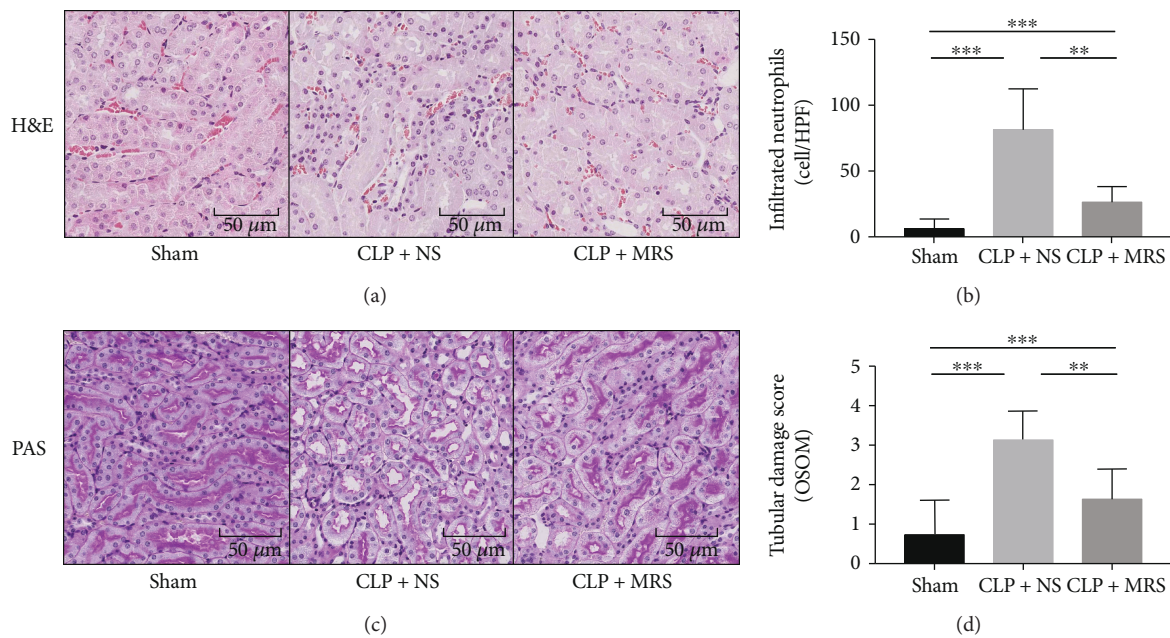


FIGURE 2: Methane-rich saline attenuated kidney histopathological damage in CLP mice. (a) H&E staining was performed on kidney tissue slices 24 h after CLP. (b) The infiltrated neutrophil granulocytes were counted. (c) PAS staining was performed on kidney tissue slices 24 h after CLP. (d) The tubular damage scores of kidney tissue were calculated. Representative sections; original magnification, 200x. * $P < 0.05$, ** $P < 0.01$, and *** $P < 0.001$.

neutrophils (Figure 2(b)) and found that the MRS treatment could greatly ameliorate the severity of kidney destruction. Moreover, the PAS staining and the tubular damage score also showed the same protective effect of MRS on kidney histology (Figures 2(c) and 2(d)).

3.3. Anti-Inflammation Effects of Methane-Rich Saline on Septic AKI. An unresolved inflammation response plays a crucial role in sepsis. As previous research has reported, MRS can attenuate organism damage by suppressing the overactivation of the inflammatory response. We detected the levels of proinflammatory cytokines in kidney tissues from the different groups, including IL-1 β , IL-6, and TNF- α by ELISA (Figures 3(a), 3(b), and 3(c)) and Western blot (Figures 3(f) and 3(g)). According to the results, the levels of IL-1 β , IL-6, and TNF- α were all increased after CLP

surgery. Compared with the CLP + NS group, the levels of the proinflammatory cytokines were reduced in the CLP + MRS group, which confirmed the anti-inflammation effect of MRS. Then, we performed an immunohistochemical analysis of IL-1 β in kidney tissues from the different groups (Figures 3(d) and 3(e)). The results of the immunohistochemical analysis demonstrated similar results to those from the ELISA and the Western blot. According to the results, the sham group had few IL-1 β -positive cells. However, the CLP + NS group had a more obvious emergence of IL-1 β -positive cells than the CLP + MRS group. All these results showed that MRS has a very strong inflammatory suppression effect.

3.4. Antioxidative Effects of Methane-Rich Saline on Septic AKI. The activation of oxidative stress, including reactive

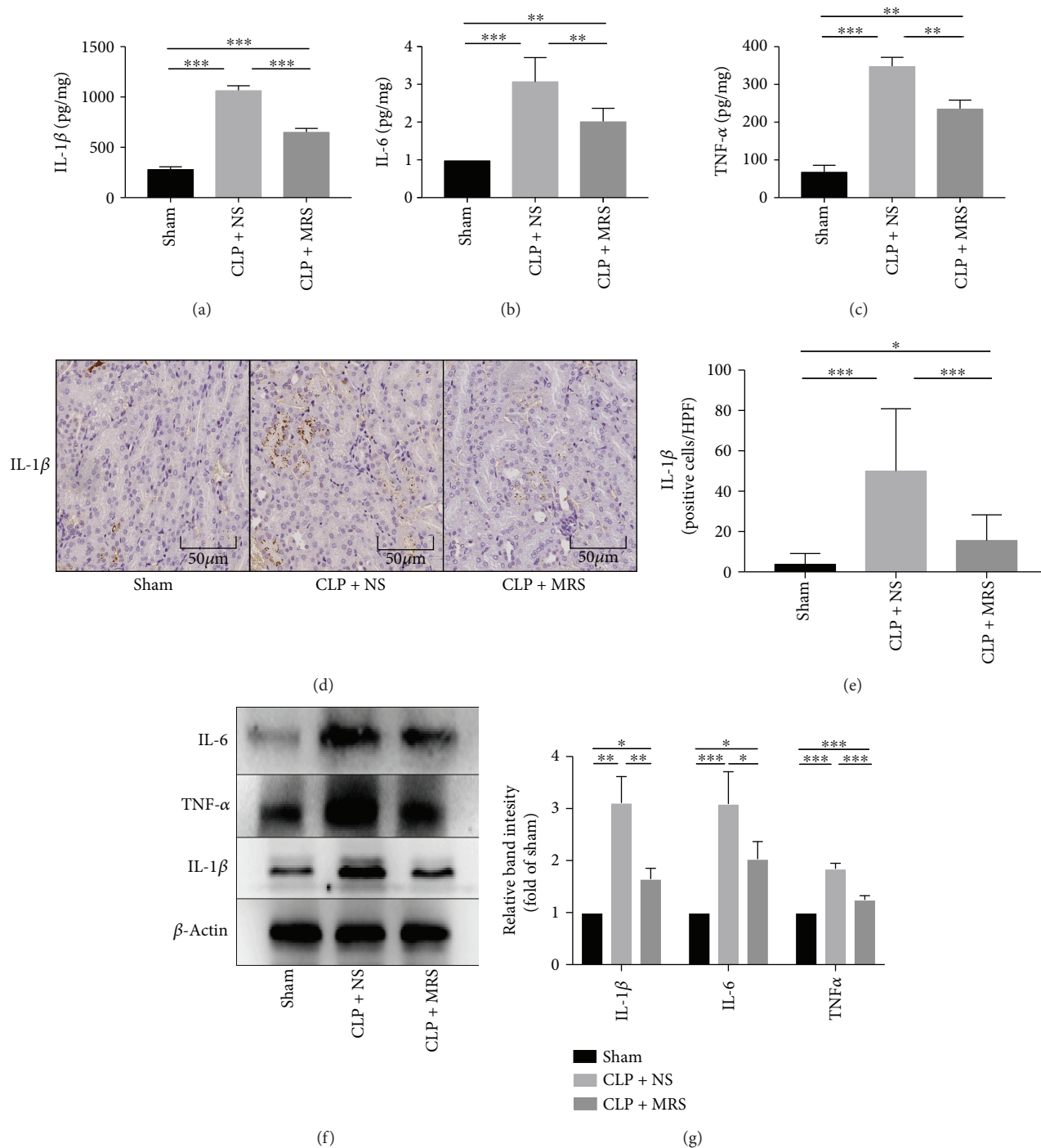


FIGURE 3: Methane-rich saline suppressed inflammation response in kidney tissue after CLP. The levels of (a) IL-1 β , (b) IL-6, and (c) TNF- α in kidney tissue were assessed by ELISA. (d) The expression of IL-1 β was detected by immunohistochemistry. (e) The quantity of IL-1 β -positive cells was counted in a high-power field. (f) The kidney protein expression levels of IL-1 β , IL-6, and TNF- α were detected by Western blot. (g) The relative band intensity (fold of the sham group) were shown. Representative sections; original magnification, 200x. * $P < 0.05$, ** $P < 0.01$, and *** $P < 0.001$.

oxygen species (ROS), also occurs during sepsis and induces organ and tissue damage. Oxidative stress levels above a certain threshold can trigger an ER stress overload and induce the activation of CHOP-mediated apoptosis. Simultaneously, excessive ER stress can also lead to harmful oxidative stress. We detected the serum MDA and SOD levels 24 h after the

CLP operation (Figures 4(a) and 4(b)). The results showed that the CLP + NS group had the highest MDA level among the three groups, and the level in the CLP + MRS group was significantly reduced compared to that in the CLP + NS group. Moreover, the results indicated that SOD activity of the CLP + MRS group was greater than that of the

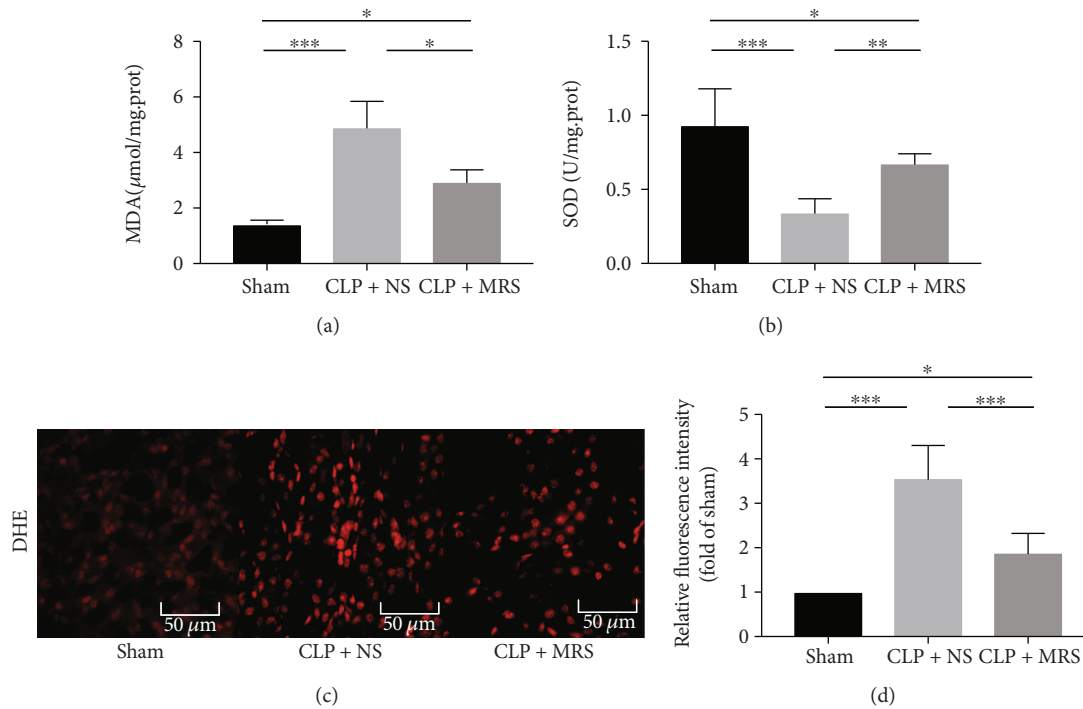


FIGURE 4: Methane-rich saline attenuated oxidative stress in kidney tissue after CLP. The levels of (a) MDA and (b) SOD in kidney tissue were assessed. (c) The DHE fluorescent probe was performed on kidney tissue slices. (d) The relative fluorescence intensities (fold of sham) of ROS were shown. Representative sections; original magnification, 200x. * $P < 0.05$, ** $P < 0.01$, and *** $P < 0.001$.

CLP + NS group. To reveal the different levels of oxidative stress in a visual way, we measured the ROS levels in kidney tissues by DHE, and different levels of fluorescence intensity revealed different levels of ROS activity (Figures 4(c) and 4(d)). The results demonstrated that the ROS activity in the CLP + MRS group was attenuated when compared with that of the CLP + NS group, as the DHE fluorescence intensity was decreased in the CLP + MRS group compared with the CLP + NS group. According to these results, MRS has an antioxidative effect on the kidney during sepsis.

3.5. Antiapoptosis Effects of Methane-Rich Saline on Septic AKI. As an important link in sepsis-related acute kidney injury, apoptosis of the cells in the kidney, especially tubular endothelial cells, could lead to major damage in the septic kidney. We examined apoptotic cells using a TUNEL system (Figures 5(a) and 5(b)). Two researchers counted the number of TUNEL-positive cells. A significant increase was observed in the number of TUNEL-positive tubular cells in the CLP + NS group compared with the sham group. However, the CLP + MRS group had a greatly reduced number of TUNEL-positive cells compared with the CLP + NS group. In agreement with the TUNEL assay results, the CLP operation also led to a significant augmentation of Bax and a decline in Bcl-2 expression in comparison with the sham group, and MRS treatment reduced the level of Bax and increased the level of Bcl-2 (Figures 5(c) and 5(d)). In addition, MRS could also attenuate the high expression of cleaved caspase-3 and PARP induced by CLP (Figures 5(e) and 5(f)). These results revealed that there was significant

apoptotic activity in the cells of the kidney during sepsis and that MRS treatment could dramatically reduce apoptosis.

3.6. Methane-Rich Saline Ameliorated the ER Stress-Related Apoptosis Process in Septic AKI. ER stress played an important role in sepsis-induced AKI; therefore, we tested the expression levels of the ER stress proteins and related components of apoptosis signaling pathways. We examined the levels of GRP78/ATF4/CHOP/caspase-12 by Western blot (Figures 6(a) and 6(b)). An increasing trend could be identified in the CLP + NS group, which showed the activation of ER stress-related apoptosis. However, there was an obvious decreasing trend in the CLP + MRS group when compared to the CLP + NS group. Moreover, we also assessed the level of CHOP using immunohistochemical analysis (Figures 6(c) and 6(d)). As the immunohistochemical analysis images show, the methane-rich saline effectively reduced the number of the CHOP-positive cells. Hence, we suggest that methane has a downregulating effect on ER stress-related apoptosis.

4. Discussion

Sepsis-related AKI is a severe complication following sepsis and leads to high mortality [22]. Although many studies have been performed on sepsis-related AKI, they have mostly focused on the pathophysiological mechanisms and risk factors. However, the treatment of sepsis-related AKI is still limited, and thus, the mortality is still a challenging problem in clinical practice.

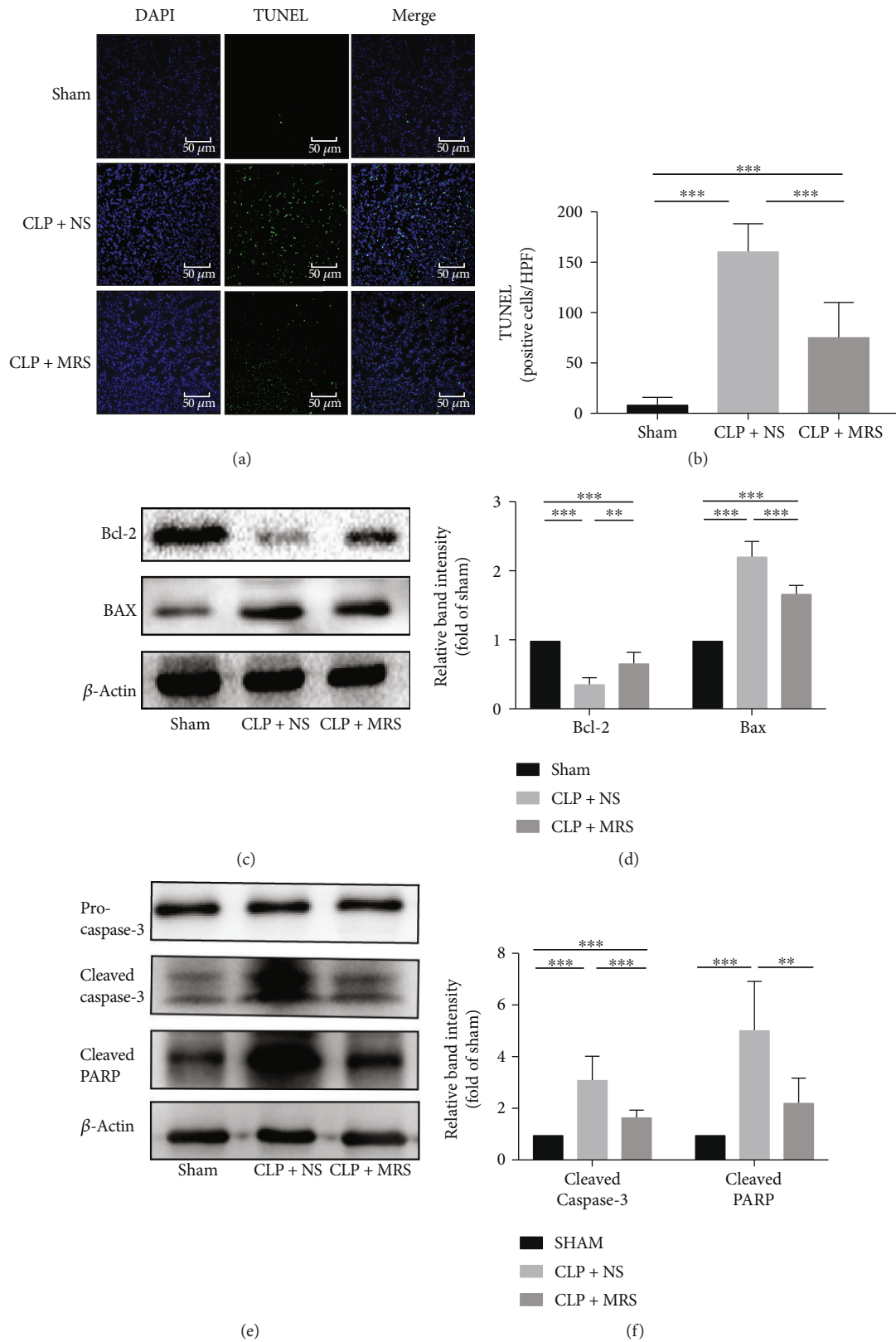


FIGURE 5: Antiapoptosis effects of methane-rich saline on septic AKI. (a) TUNEL assay was performed on kidney tissue slices. (b) The quantity of TUNEL-positive cells was counted in a high-power field. (c) The kidney protein expression levels of Bcl-2 and Bax were detected by Western blot, and the relative band intensities (fold of the sham group) were shown in (d). (e) The protein levels of cleaved caspase-3 and cleaved PARP were detected, and the relative band intensities (fold of the sham group) were shown in (f). * $P < 0.05$ versus CLP + NS group; representative sections; original magnification, 200x. * $P < 0.05$, ** $P < 0.01$, and *** $P < 0.001$.

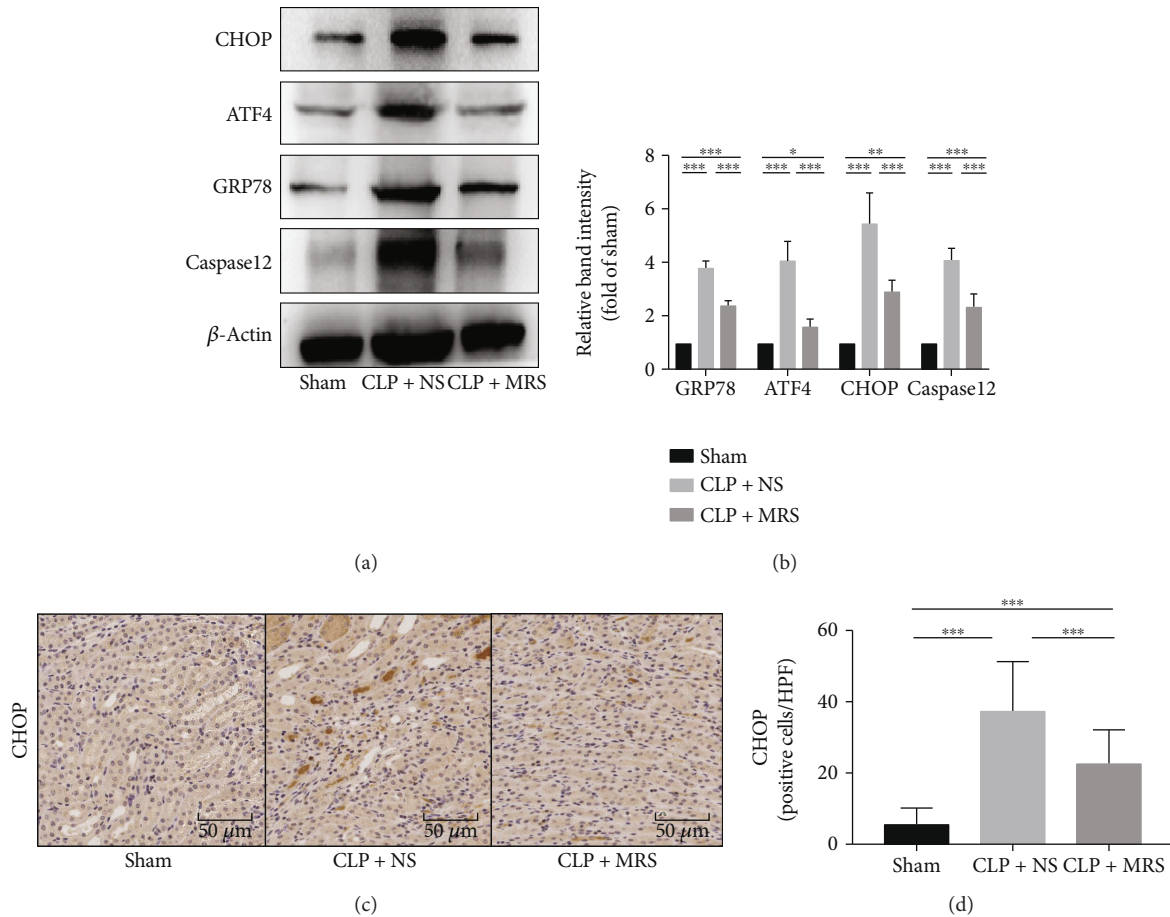


FIGURE 6: Methane-rich saline ameliorated the ER stress-related apoptosis process in septic AKI. (a) The protein levels of ER stress-related apoptosis signaling components (GRP78/ATF4/CHOP/caspase-12) were detected by Western blot, and the relative band intensities (fold of the sham group) were shown in (b). CHOP was detected by immunohistochemistry, and the quantity of CHOP-positive cells was counted in a high-power field (c). Representative sections; original magnification, 200x. * $P < 0.05$, ** $P < 0.01$, and *** $P < 0.001$.

Methane, the simplest alkane and likely the most abundant organic compound on earth, has been used as gas fuel by people for hundreds of years. Recently, scientists have focused on the clinical properties of methane and have suggested that methane can influence several pathological processes, including inflammation, oxidation, and apoptosis in different diseases [12–14]. However, the mechanisms behind these effects could be complex and have yet to be investigated. Some researchers, when examining a carbon tetrachloride-induced liver injury, have suggested that methane exhibits an anti-inflammatory effect through the activation of the PI3K-AKT-GSK-3 β pathway, which induces IL-10 expression and produces anti-inflammatory effects via the NF- κ B and MAPK pathways. In addition, Nrf2 and its downstream pathway have been suggested to be involved in the anti-inflammation and antioxidant effects in spinal cord ischemia-reperfusion injury [14].

There has been little research regarding the protective effects of methane on serious sepsis-induced acute kidney injury. Some previous studies have demonstrated that inflammation, oxidative stress, and apoptosis, especially the apoptosis of tubular endothelial cells, play important roles in sepsis-related AKI [23]. This study is aimed at revealing

the protective effects of methane on sepsis-related AKI and at determining the underlying mechanisms.

We created a sepsis mouse model using a CLP operation and gathered the blood and kidney tissue samples after 24 hours. First, we evaluated the renal functions of all groups and the levels of BUN and CRE after CLP to confirm the establishment of a sepsis model. The MRS treatment demonstrated protective properties for kidney function during serious sepsis, and the results were confirmed using histopathological damage analysis. We next attempted to investigate which parts of pathophysiological process had been influenced by MRS. We assessed the levels of the inflammatory response and oxidative stress among the different groups and found a significantly decreasing trend in the CLP + MRS group, which suggested that MRS treatment has strong anti-inflammation and antioxidative effects. As a crucial part of sepsis-related AKI, we examined cell apoptosis in renal tissues, especially the expression of cleaved caspase-3, PARP, and Bcl-2/Bax, and demonstrated an antiapoptosis effect of MRS treatment. We revealed a protective effect for MRS treatment against sepsis-related AKI that was mediated through anti-inflammation, antioxidative, and antiapoptosis effects.

Apoptosis is a process of programmed cell death that occurs in multicellular organisms and is important for homeostasis in multicellular life forms. The apoptosis of mammalian cells can be triggered by various stimuli via the intrinsic pathways, mitochondrial pathway and ER pathway.

Endoplasmic reticulum (ER) stress is a stress condition in which unfolded or misfolded proteins amass in the endoplasmic reticulum. While a mild ER stress-induced UPR signaling pathway can be considered a maintenance mechanism, chronically prolonged ER stress can deteriorate cellular functions and transform the adaptation programmed into CHOP-mediated apoptosis, activating the caspase-12 and Bcl-2/Bax system to clean irreversibly injured cells [24, 25]. We further investigated the level of ER stress-related apoptosis and discovered that MRS treatment could attenuate ER stress-related apoptosis, which is consistent with the previous results demonstrating the antiapoptosis effects of MRS. The levels of CHOP and caspase-12 were both reduced in the CLP + MRS group when compared with the CLP + NS group. In addition, the levels of cleaved caspase-3 and PARP as well as Bax were suppressed in the CLP + MRS group.

The exact molecular mechanisms of methane have not been clarified. Several scholars have proposed different hypotheses to explain the protective functions of methane, including the regulation of embedded proteins in the cell membrane, an interaction with a specific receptor, or ion channel kinetics [26, 27]. According to our research, we found that the reduction of ER stress may be involved in the protective mechanism of methane and could inhibit cell apoptosis directly. Therefore, we hypothesize that methane might block some signaling pathway triggers of ER stress and raise the threshold of the ER stress-related apoptosis, so that methane could also stop the downstream inflammation and oxidative signals. Many studies have confirmed that ER stress is involved in several pathological processes and contributes to tissue damage. As a potential ER stress-related apoptosis inhibitor and a promising medicinal treatment for sepsis-induced AKI, MRS could be applied as a valid intervention during the early stages of sepsis and for establishing a protective effect on the kidney and other organs. In conclusion, this study demonstrated that methane treatment reduced the inflammatory response, oxidative stress, and apoptosis during sepsis-induced AKI, suggesting that the reduction of ER stress may be the underlying protective mechanism.

Data Availability

The histological examination, biochemical index detection, results of IHC and TUNEL staining, and WB data used to support the findings of this study are included within the article.

Conflicts of Interest

We declare that there is no conflict of interest regarding the publication of this article.

Authors' Contributions

Jia YF participated in the research design, animal research and writing of the paper; Li ZY participated in IHC and WB performance; Feng Y participated in the animal research and IHC performance; Jia YF, Li ZY and Feng Y contributed equally to the paper. Cui RX participated in the revision; Dong YY participated in the language improvement. Zhang X participated in data analysis; Xiang XH participated in the WB performance; Qu K, Liu C and Zhang JY provided substantial advice in designing the study and assisting in the division of labor, writing and revising the paper. Yifan Jia, Zeyu Li, and Yang Feng contributed equally to the paper.

Acknowledgments

We are indebted to all individuals who participated in or helped with this research project. This study was supported by funding from “the National Nature Science Foundation of China” (Grant No. 81601672, 81272644, 81402022 and 81472247), “the Project of Innovative Research Team for Key Science and Technology in Shaanxi province” (Grant No.2013KCJ-23) and “the Fundamental Research Funds for the Central Universities” (Grant No.1191320114).

References

- [1] Z. Ricci, D. Cruz, and C. Ronco, “The RIFLE criteria and mortality in acute kidney injury: a systematic review,” *Kidney International*, vol. 73, no. 5, pp. 538–546, 2008.
- [2] S. Uchino, J. A. Kellum, R. Bellomo et al., “Acute renal failure in critically ill patients: a multinational, multicenter study,” *JAMA*, vol. 294, no. 7, pp. 813–818, 2005.
- [3] R. L. Mehta, M. T. Pascual, S. Soroko et al., “Spectrum of acute renal failure in the intensive care unit: the PICARD experience,” *Kidney International*, vol. 66, no. 4, pp. 1613–1621, 2004.
- [4] W. Silvester, R. Bellomo, and L. Cole, “Epidemiology, management, and outcome of severe acute renal failure of critical illness in Australia,” *Critical Care Medicine*, vol. 29, no. 10, pp. 1910–1915, 2001.
- [5] S. Kresse, H. Schlee, H. J. Deuber, W. Koall, and B. Osten, “Influence of renal replacement therapy on outcome of patients with acute renal failure,” *Kidney International Supplements*, vol. 72, pp. S75–S78, 1999.
- [6] R. Jacobs, P. M. Honore, O. Joannes-Boyau et al., “Septic acute kidney injury: the culprit is inflammatory apoptosis rather than ischemic necrosis,” *Blood Purification*, vol. 32, no. 4, pp. 262–265, 2011.
- [7] S. Y. Lee, Y. S. Lee, H. M. Choi et al., “Distinct pathophysiologic mechanisms of septic acute kidney injury: role of immune suppression and renal tubular cell apoptosis in murine model of septic acute kidney injury,” *Critical Care Medicine*, vol. 40, no. 11, pp. 2997–3006, 2012.
- [8] C. Hetz, “The unfolded protein response: controlling cell fate decisions under ER stress and beyond,” *Nature Reviews Molecular Cell Biology*, vol. 13, no. 2, pp. 89–102, 2012.
- [9] J. Teng, M. Liu, Y. Su et al., “Down-regulation of GRP78 alleviates lipopolysaccharide-induced acute kidney injury,” *International Urology and Nephrology*, vol. 50, no. 11, pp. 2099–2107, 2018.

- [10] V. Esposito, F. Grosjean, J. Tan et al., "CHOP deficiency results in elevated lipopolysaccharide-induced inflammation and kidney injury," *American Journal of Physiology-Renal Physiology*, vol. 304, no. 4, pp. F440–F450, 2013.
- [11] Y. Jia, Z. Li, C. Liu, and J. Zhang, "Methane medicine: a rising star gas with powerful anti-inflammation, antioxidant, and antiapoptosis properties," *Oxidative Medicine and Cellular Longevity*, vol. 2018, Article ID 1912746, 10 pages, 2018.
- [12] Y. Yao, L. Wang, P. Jin et al., "Methane alleviates carbon tetrachloride induced liver injury in mice: anti-inflammatory action demonstrated by increased PI3K/Akt/GSK-3 β -mediated IL-10 expression," *Journal of Molecular Histology*, vol. 48, no. 4, pp. 301–310, 2017.
- [13] A. Sun, W. Wang, X. Ye et al., "Protective effects of methane-rich saline on rats with lipopolysaccharide-induced acute lung injury," *Oxidative Medicine and Cellular Longevity*, vol. 2017, Article ID 7430193, 12 pages, 2017.
- [14] L. Wang, Y. Yao, R. He et al., "Methane ameliorates spinal cord ischemia-reperfusion injury in rats: antioxidant, anti-inflammatory and anti-apoptotic activity mediated by Nrf2 activation," *Free Radical Biology & Medicine*, vol. 103, pp. 69–86, 2017.
- [15] L. Liu, Q. Sun, R. Wang et al., "Methane attenuates retinal ischemia/reperfusion injury via anti-oxidative and anti-apoptotic pathways," *Brain Research*, vol. 1646, pp. 327–333, 2016.
- [16] R. He, L. Wang, J. Zhu et al., "Methane-rich saline protects against concanavalin A-induced autoimmune hepatitis in mice through anti-inflammatory and anti-oxidative pathways," *Biochemical and Biophysical Research Communications*, vol. 470, no. 1, pp. 22–28, 2016.
- [17] W. Wang, X. Huang, J. Li et al., "Methane suppresses microglial activation related to oxidative, inflammatory, and apoptotic injury during spinal cord injury in rats," *Oxidative Medicine and Cellular Longevity*, vol. 2017, Article ID 2190897, 11 pages, 2017.
- [18] J. Zhang, J. Bi, S. Liu et al., "5-HT drives mortality in sepsis induced by cecal ligation and puncture in mice," *Mediators of Inflammation*, vol. 2017, Article ID 6374283, 12 pages, 2017.
- [19] Z. Ye, O. Chen, R. Zhang et al., "Methane attenuates hepatic ischemia/reperfusion injury in rats through antiapoptotic, anti-inflammatory, and antioxidative actions," *Shock*, vol. 44, no. 2, pp. 181–187, 2015.
- [20] I. Ohsawa, M. Ishikawa, K. Takahashi et al., "Hydrogen acts as a therapeutic antioxidant by selectively reducing cytotoxic oxygen radicals," *Nature Medicine*, vol. 13, no. 6, pp. 688–694, 2007.
- [21] T. Miyaji, X. Hu, P. S. T. Yuen et al., "Ethyl pyruvate decreases sepsis-induced acute renal failure and multiple organ damage in aged mice," *Kidney International*, vol. 64, no. 5, pp. 1620–1631, 2003.
- [22] F. G. Brivet, D. J. Kleinknecht, P. Loirat, and P. J. M. Landais, "Acute renal failure in intensive care units—causes, outcome, and prognostic factors of hospital mortality; a prospective, multicenter study. French study group on acute renal failure," *Critical Care Medicine*, vol. 24, no. 2, pp. 192–198, 1996.
- [23] A. Zarbock, H. Gomez, and J. A. Kellum, "Sepsis-induced acute kidney injury revisited: pathophysiology, prevention and future therapies," *Current Opinion in Critical Care*, vol. 20, no. 6, pp. 588–595, 2014.
- [24] E. Szegezdi, S. E. Logue, A. M. Gorman, and A. Samali, "Mediators of endoplasmic reticulum stress-induced apoptosis," *EMBO Reports*, vol. 7, no. 9, pp. 880–885, 2006.
- [25] D. T. Rutkowski, S. M. Arnold, C. N. Miller et al., "Adaptation to ER stress is mediated by differential stabilities of pro-survival and pro-apoptotic mRNAs and proteins," *PLoS Biology*, vol. 4, no. 11, article e374, 2006.
- [26] M. Boros, M. Ghyczy, D. Érces et al., "The anti-inflammatory effects of methane*," *Critical Care Medicine*, vol. 40, no. 4, pp. 1269–1278, 2012.
- [27] T. Kai, K. A. Jones, and D. O. Warner, "Halothane attenuates calcium sensitization in airway smooth muscle by inhibiting G-proteins," *Anesthesiology*, vol. 89, no. 6, pp. 1543–1552, 1998.